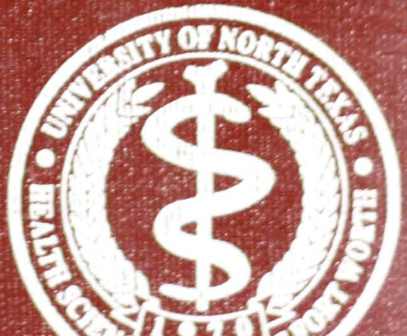
UNIVERSITY OF NORTH TEXAS
HEALTH SCIENCE CENTER AT FORT WORTH
1970

UNTHSC - FW
M02E0N

LEWIS LIBRARY
[illegible] Center
3500 Camp Bowie Blvd
Ft. Worth, Texas 76107-2699

Ra

Pacheco-Rodriguez, Gustavo, Distribution of Poly(ADP-ribose) Glycohydrolase in Different Functional Domains of the Cell Nucleus. Doctor of Philosophy (Biomedical Sciences), August, 1996, 147 pp, 3 tables, 44 illustrations, bibliography, 138 titles.

In this study, the distribution of poly(ADP-ribose) glycohydrolase (PARG) in different subdomains of the cell nucleus and the role of non-covalent interactions of poly(ADP-ribose) with nuclear proteins have been characterized. An assay that allows the simultaneous determination of specific non-covalent interactions of poly(ADP-ribose) with nuclear proteins as well as PARG activity by high resolution polyacrylamide gel electrophoresis was developed. This method was made possible by the enzymatic synthesis of $(\text{ADP-ribose})_{2\text{-}70}$ at 10 μM NAD^+ with purified poly(ADP-ribose) polymerase (PARP). Either purified or nuclear-associated PARG degraded poly(ADP-ribose) biphasically. Nuclei were fractionated into functional domains namely, chromatin, nuclear matrix and nuclear envelope. These domains were characterized biochemically by their protein composition and by electron microscopy. PARG activity was identified mainly with chromatin and the nuclear matrix. Interestingly, PARG activity was also associated with the nuclear envelope. Thus, the poly(ADP-ribosyl)ation pathway is regulated topologically. It was further determined that poly(ADP-ribose) interacts non-covalently with purified histone proteins or proteins in the nuclear environment. In addition, the nuclear matrix proteins also interacted non-covalently with poly(ADP-ribose). These non-covalent interactions appear to regulate the catabolism of poly(ADP-ribose) via a catabolite intermediate constituted of a [protein][poly(ADP-ribose)] complex. The affinity of the nuclear associated protein responsible for triggering the degradation of poly(ADP-ribose) correlates with the affinity of histone H4 for ADP-ribose chains of 20 residues or more.

The finding of this research stresses that : a) poly(ADP-ribose) is catabolized by

PARG *in vivo;* b) PARG is associated with chromatin, nuclear matrix and the nuclear envelope; c) the degradation of poly(ADP-ribose) is dependent on its non-covalent interactions with nuclear proteins; and d) histone H4 appears to be responsible for triggering the catabolism of poly(ADP-ribose).

DISTRIBUTION OF POLY(ADP-RIBOSE) GLYCOHYDROLASE IN DIFFERENT FUNCTIONAL DOMAINS OF THE CELL NUCLEUS

Gustavo Pacheco-Rodriguez, B.S., M.S.

APPROVED:

Rafael Alvarez

Major Professor

Committee Member

Committee Member

Committee Member

Ming-chi Wu

Committee Member

University Member

Ladislav

Acting Chair, Department of Biochemistry and Molecular Biology

Thomas Yorio

Dean, Graduate School of Biomedical Sciencies

DISTRIBUTION OF POLY(ADP-RIBOSE) GLYCOHYDROLASE IN DIFFERENT FUNCTIONAL DOMAINS OF THE CELL NUCLEUS

DISSERTATION

Presented to the Graduate Council of the
Graduate School of Biomedical Sciences
University of North Texas Health Science Center at Fort Worth
in Partial Fulfillment of the Requirements

For the Degree of

DOCTOR OF PHILOSOPHY

By

Gustavo Pacheco-Rodriguez, B.S., M.S.
Fort Worth, Texas
August, 1996

TABLE OF CONTENTS

LIST OF TABLES vii
LIST OF ABREVIATIONS viii
LIST OF ILLUSTRATIONS x

Chapter

I. INTRODUCTION 1

Chromatin 4
Nuclear matrix 10
Nuclear envelope 13
Nuclear pore complex 16
Nucleolus 16
Poly(ADP-ribosyl)ation pathway 17
Poly(ADP-ribose) polymerase 17
Protein targets for poly(ADP-ribosyl)ation 20
Catabolism of poly(ADP-ribose) 21
Poly(ADP-ribose) glycohydrolase 21
Properties of Nuclear Poly(ADP-ribose) glycohydrolase 22
Inhibitors of Poly(ADP-ribose) glycohydrolase 22
Subnuclear Distribution of Poly(ADP-ribose) polymerase

and Poly(ADP-ribose) glycohydrolase 27
Poly(ADP-ribosyl)ation of proteins and chromatin structure 27
General hypothesis 32
Purpose of the study 32

II. MATERIALS AND METHODS 33

Materials 33
Isolation of nuclei 34
Isolation of H1-depleted chromatin 34
Fractionation of nuclei 34
Preparation of samples for electron microscopy 35
Proteinase-treatment 35
Purification of PARP 36
Purification of PARG 36
Enzyme assay for PARP 36
Synthesis of poly(ADP-ribose) 36
Poly(ADP-ribose) purification 37
Size exclusion chromatography of protein-free poly(ADP-ribose) 37
High resolution polyacrylamide gel electrophoresis of protein-free ADP-ribose polymers 37
Enzyme assay for poly(ADP-ribose) glycohydrolase 38
Poly(ADP-ribose) mobility shift assays 38
HPLC identification of the products generated by either PARG of phosphodiesterase

digestion of [^{32}P]poly(ADP-ribose) 38

Determination of ADP-ribose chain lengths 39

III RESULTS 40

Characterization of isolated nuclei 43

Association of PARP with chromatin 43

Development of enzyme assay to measure poly(ADP-ribose) glycohydrolase activity 43

Enzyme assay for PARG activity 48

Subnuclear distribution of poly(ADP-ribose) glycohydrolase 63

Nuclear fractionation into distinct functional domains 63

Protein composition of each subnuclear domain 63

Electron microscopy of each subnuclear domain 70

Identification of PARG in different subnuclear domains 70

Kinetic characterization of nuclear matrix associated PARG activity 77

Non-covalent interactions of poly(ADP-ribose with nuclear proteins 82

Inhibition of PARG activity by histone and nuclear matrix proteins 83

Non-covalent interactions of free poly(ADP-ribose) with nuclear proteins 90

Protease treatment of isolated nuclei 90

The efficiency of ADP-ribose polymers to interact non-covalently with nuclear proteins is size-dependent 96

Complex formation as function of temperature 103

Non-covalent interactions of nuclear proteins with protein-free poly(ADP-ribose) by SDS-PAGE 114

Poly(ADP-ribose) ionic interactions with H1-depleted chromatin 114

Non-covalent interactions of histone proteins with poly(ADP-ribose) 117

PARG activity in the presence of histone H4 124

Role of PARP in the degradation of poly(ADP-ribose) by PARG activity 129

IV DISCUSSION 133

REFERENCES 140

LIST OF TABLES

Tables Page

1. Enzyme properties of pure poly(ADP-ribose) glycohydrolase 25
2. Comparison of poly(ADP-ribose) glycohydrolase from pig liver and human placenta 26
3. Percent yield and chain lengths of the poly(ADP-ribose) synthesized with different enzyme sources 49

LIST OF ABBREVIATIONS

ADP	Adenosine 5'diphosphate
ADPR	Adenosine 5'diphosphate ribose
AMP	Adenosine 5'monophosphate
APL	ADP-ribose Protein Lyase
BPB	Bromophenol Blue
BSA	Bovine Serum Albumin
CPM	Counts per minute
DHB-B	Dihhydroxyboronyl-Bio-Rex 70
DTT	Dithiothreitol
EDTA	Ethylene diamine tetracetic acid
ER	Endoplasmic Reticulum
HMG	High Mobility Group Proteins
HMG CoA	3-hydroxy-3-methylglutaryl coenzyme A
HPLC	High Performance Liquid Chromatography
LAP	Lamin Associated Proteins
MAR	Matrix Attachment Regions
NAD^+	Nicotinamide Adenine Dinucleotide
NE	Nuclear Envelope
NLS	Nuclear Localization Signal
NPC	Nuclear Pore Complex

NM	Nuclear Matrix
NTF	Nuclear Transport Factor
NuMa	Nuclear Mitotic Apparatus
PAGE	Polyacrylamide Gel Electrophoresis
PARG	Poly(ADP-ribose) Glycohydrolase
PARP	Poly(ADP-ribose) Polymerase
PMSF	Phenylmethyl-Sulfonyl Fluoride
PRAMP	phosphoribosyl-adenosine 5'monophosphate
PR_2AMP	Di-phosphoribosyl-adenosine 5'monophosphate
RLN	Rat Liver Nuclei
SDS	Sodium dodecylsulphate
SDS-PAGE	Sodium dodecylsulphate- polyacrylamide gel electrophoresis
TCA	Trichloroacetic acid
TLC	Thin Layer Chromatography
XC	Xylene Cyanol

LIST OF ILLUSTRATIONS

Figure Page

1. Nuclear Subdomains and structural changes of the cell nucleus during the cell cycle 2

2. Schematic drawing of histone proteins 5

3. Schematic representation of the nucleosome 7

4. Scheme for the fractionation of eukaryotic nuclei into separate functional domains 11

5. Enzymatic cycle of the poly(ADP-ribosyl)ation pathway 18

6. Mode of action of poly(ADP-ribose)glycohydrolase 23

7. Structural changes of chromatin are modulated by protein-poly(ADP-ribosyl)ation 28

8. Diagram of the experimental approach used to study the subnuclear distribution of PARG and the role of non-covalent interactions between poly(ADP-ribose) and proteins in enzyme activity 41

9. Electron micrograph of rat liver nuclei 44

10. Kinetics of Poly(ADP-ribose) synthesis with rat liver nuclear extracts at 20 μM NAD^+ 46

11 Size distribution of ADP-ribose polymers before and after affinity chromatography on a boronate resin 50

12. Kinetics of PARG activity associated with rat liver nuclei 52

13. Poly(ADP-ribose) glycohydrolase activity is protein concentration-dependent 54

14. Graphical representation of the kinetics of monomeric ADP-ribose formation with a crude extract of PARG 56
15. PARG degrades free poly(ADP-ribose) biphasically 59
16. Chromatographic identification of ADP-ribose as the main product generated by partially purified PARG 61
17. Experimental design used to identify PARG activity in functional subdomains of the nucleus 64
18. Experimental protocol for the isolation of nuclear functional domains 66
19. Protein composition of nuclei, nuclear matrix and nuclear envelope (Triton X-100 extract) as determined by Coomassie blue staining following SDS-PAGE 68
20 Electron micrographs of intact rat liver nuclei (panel A), nuclease digested nuclei (panel B), nuclear matrix II (with nuclear envelope) (panel C) and nuclear matrix III (without nuclear envelope) (panel D). 71
21. Poly(ADP-ribose) glycohydrolase activity is associated with intact nuclear chromatin, nuclear matrix III and the nuclear envelope 73
22. Specific activity of PARG associated with chromatin, nuclear matrix, and nuclear envelope 75
23. Formation of monomeric ADP-ribose by the nuclear matrix III extract 78
24 Formation of free ADP-ribose with increasing amounts of nuclear matrix protein 80
25 Non-covalent interactions of protein-free [^{32}P]poly(ADP-ribose) with histone and

non-histone proteins 84

26. Inhibition of purified PARG activity by histone proteins and nuclear matrix proteins 86

27. Size distribution of ADP-ribose polymers following incubation of poly(ADP-ribose) with 150 ng of PARG in the presence of increasing amounts of nuclear matrix proteins 88

28. Non-covalent interactions of poly(ADP-ribose) with nuclear proteins 91

29. Inhibition of endogenous PARG activity with 10 mM ADP-ribose 94

30. HPLC colecular sieving of protein-free [^{32}P]poly(ADP-ribose) on a BioSil TSK-125 column 97

31. Size distibution of [^{32}P]poly(ADP-ribose) following molecular sieve chromatography on a TSK-125 column 99

32. Non-covalent interactions of ADP-ribose polymers of various sizes with nuclear proteins 101

33. Formation of monomeric ADP-ribose and complex formation in interactions of RLN with different fractions of [^{32}P]poly(ADP-ribose) 104

34. Kinetics of complex formation and PARG activity with a crude nuclear extract 106

35. Graphical representation of Fig. 34 following densitometric scanning of the complex and free monomeric ADP-ribose 108

36. Kinetics of nuclear associated poly(ADP-ribose) glycohydrolase at 0, 37 and 60 °C 110

37. Kinetics of [protein][poly(ADP-ribose)] degradation at 0, 37 and 60 °C 112

38. Non-covalent interactions of poly(ADP-ribose) with total nuclear proteins 115

39. Coomassie blue staining of Histone H1-depleted chromatin 118

40. Non-covalent binding of poly(ADP-ribose) to H1-depleted chromatin 120

41. Binding of individual histone proteins to poly(ADP-ribose) at 1:8 and 1:16 molar ratios of poly(ADP-ribose):Histone 122

42. Non-covalent binding of histone H4 to free poly(ADP-ribose) 125

43. PARG activity in the presence of histone H4 127

44. Poly(ADP-ribose) glycohydrolase activity in the presence of different amounts of PARP 130

CHAPTER I

INTRODUCTION

The cell nucleus is the organelle that functions in maintaining a separation between cytoplasmic and nuclear components. It is also an organelle that suffers rapid structural changes during the cell cycle. For instance, the nucleus is disrupted at the onset of mitosis and is reformed prior to the G1 phase of the cell cycle (Fig. 1A). The nucleus may be subdivided into several functional domains such as chromatin (euchromatin and heterochromatin), nuclear matrix, nuclear envelope, nuclear pore complex and nucleolus (Fig. 1B).

These nuclear domains play different biological roles. For instance, while nucleocytoplasmic transport is mediated by the nuclear pore complex, ribosome biogenesis occurs in the nucleolus. Other domains allow for the organization of the genetic material. Therefore, while chromatin contains the genomic material, DNA replication appears to occur at the nuclear matrix. Not surprisingly, binding and processing of the DNA within each domain requires the recruitment of highly specialized molecules to specific sites. The positioning of these key molecules may be, at least in part, regulated by reversible post-translational modification (van Holde, 1988; Bradbury, 1992). These transfer reactions include for example poly(ADP-ribosyl)ation, acetylation, and phosphorylation. In general, these pathways require an "on" (transfer) and an "off"

Fig. 1. Nuclear subdomains and structural changes of the cell nucleus during the cell cycle. **A.** Functional sudomains of the nucleus include chromatin, nuclear matrix, nuclear envelope, nucleolus, and nuclear pores. **B.** The nuclear envelope is disassembled at the onset of mitosis and re-assembled prior to the G1 phase of the cell cycle.

A

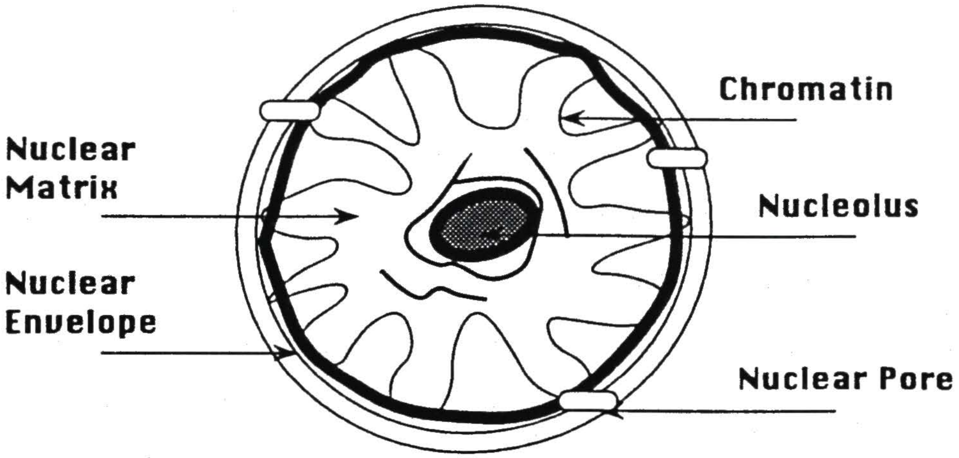
Chromatin
Nuclear Matrix
Nucleolus
Nuclear Envelope
Nuclear Pore

B

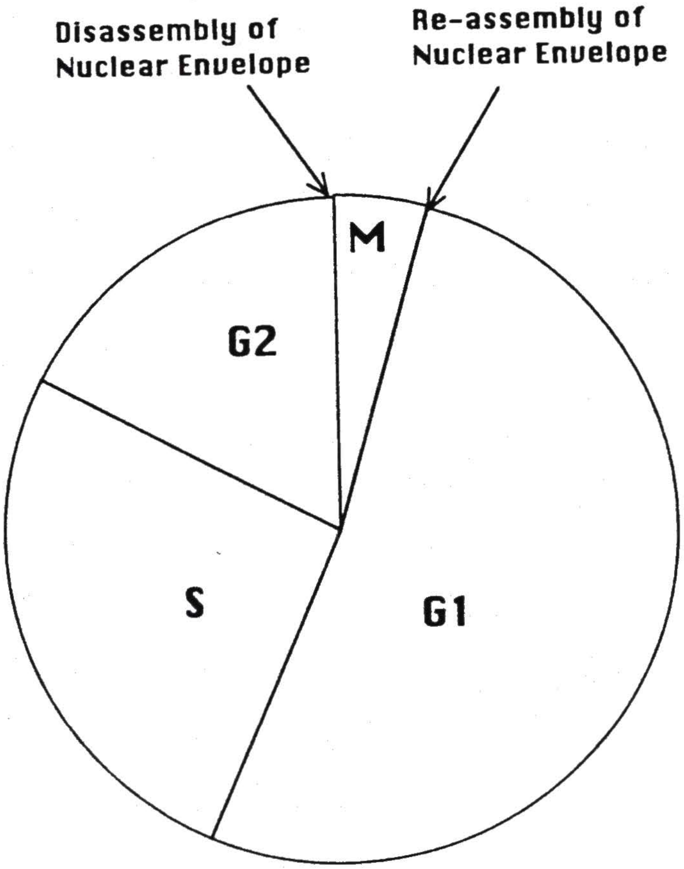
Disassembly of Nuclear Envelope
Re-assembly of Nuclear Envelope
M
G2
S
G1

reaction (cleavage). Therefore, at least two enzymatic activities are required.
For example in poly(ADP-ribosyl)ation reactions the on and off enzyme reactions are catalyzed by poly(ADP-ribose)polymerase [E.C.2.4.2.30] (PARP) and poly(ADP-ribose) glycohydrolase (PARG), respectively.

Chromatin. The DNA in eukaryotic cells is complexed with histone proteins although DNA may also be complexed with non-histone proteins to a large degree. Both types participate in the modulation of chromatin structure and function (van Holde, 1988). Histone proteins are the most abundant proteins in the cell nucleus and are present in a molar ratio of 1/1 with DNA. By contrast, non-histone proteins are found in a 0.5/1 molar protein:DNA ratio (Hyde, 1979). The five histone proteins are H1, H2A, H2B, H3 and H4. Structurally, histone proteins contain amino and carboxy terminal "tails" and a central globular domain. The histone tails are highly enriched in lysine and arginine residues (Fig. 2). Histone proteins are responsible for the DNA packaging in the nucleus. In the hierarchical organization of the genome, the DNA is first folded around a histone protein core forming the nucleosome *e. g.*, the repeating unit of chromatin (Kornberg, 1974). Nucleosomes are constituted of roughly 200 bp of DNA, an octamer of core histone proteins, and a linker histone (Fig. 3). The octamer of core histone proteins contains two molecules each of H2A, H2B, H3 and H4. This octamer is wrapped by usually 146 bp of nucleosomal DNA. Then, the nucleosome is sealed off by one molecule of histone H1, the linker histone, which binds both linker and nucleosomal DNA. The chemical interactions between DNA and histone proteins are non-covalent in nature, and the interactions that govern the core nucleosomes are heterotypic. Thus, there are strong interactions of H2A with H2B and H3 with H4 (Eickbush and Moudrianakis, 1978). A nucleosome could also be defined as a tetramer

Fig. 2. Schematic drawing of histone proteins. Histone proteins are mainly constituted of sequence terminal tail(s) and a globular region. The amino and carboxy terminal tails are indicated by lines and show the corresponding number of aminoacids in their primary sequence. The globular region is represented by an oval. The estimated net ionic charge of the histone proteins at physiological pH is also indicated (Data from van Holde, 1988).

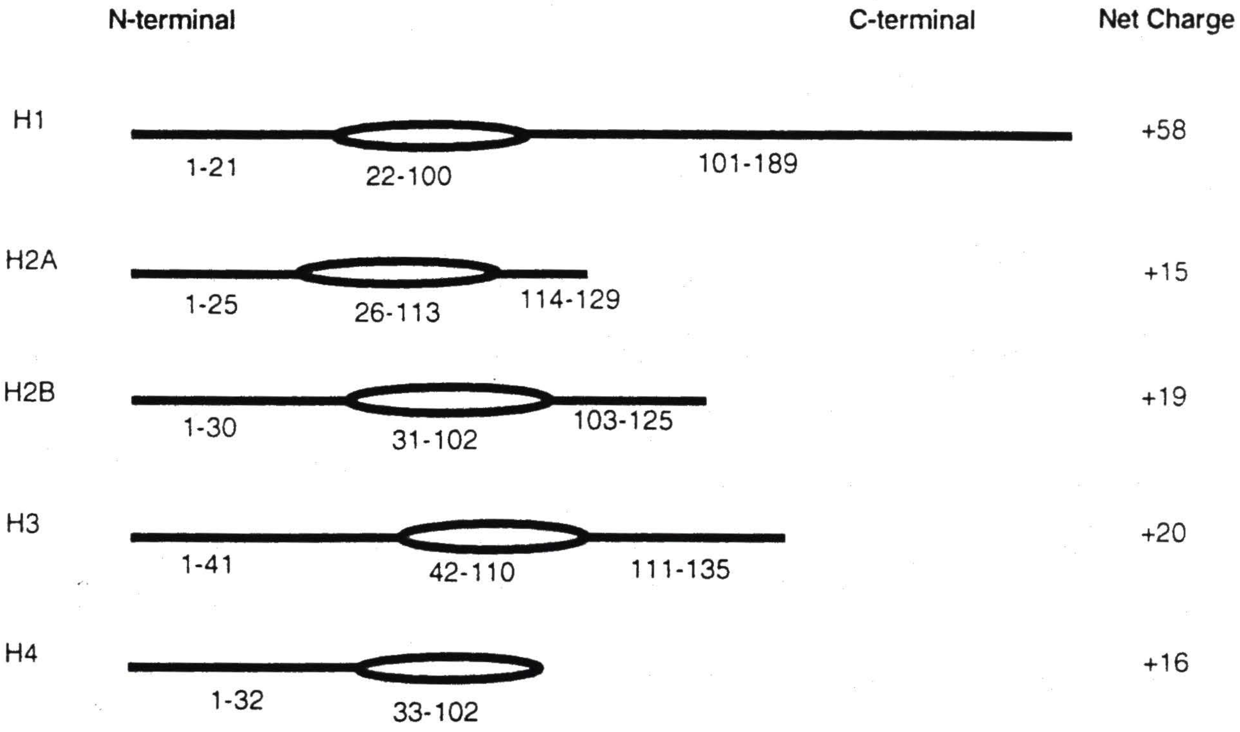
N-terminal
C-terminal
Net Charge
H1
1-21
22-100
101-189
+58
H2A
1-25
26-113
114-129
+15
H2B
1-30
31-102
103-125
+19
H3
1-41
42-110
111-135
+20
H4
1-32
33-102
+16

Fig. 3. Schematic representation of the nucleosome. A nucleosome is the basic unit of eukaryotic chromatin and is integrated of approximately 200 bp of DNA and nine histone polypeptides. The core nucleosome is formed by 2 molecules each of core histones-H2A, H2B, H3 and H4. Functionally, two dimers of H2A/H2B and a tetramer of H3/H4 conform the nucleosome (**A**). The DNA (146 bp) is wrapped around the tetramer (**B**); however, the binding of the two H2A/H2B dimers increase the folding of DNA (**C**). Histone H1 (linker histone) binds and seals off the nucleosome (**D**). H1 interacts with core and linker DNA.

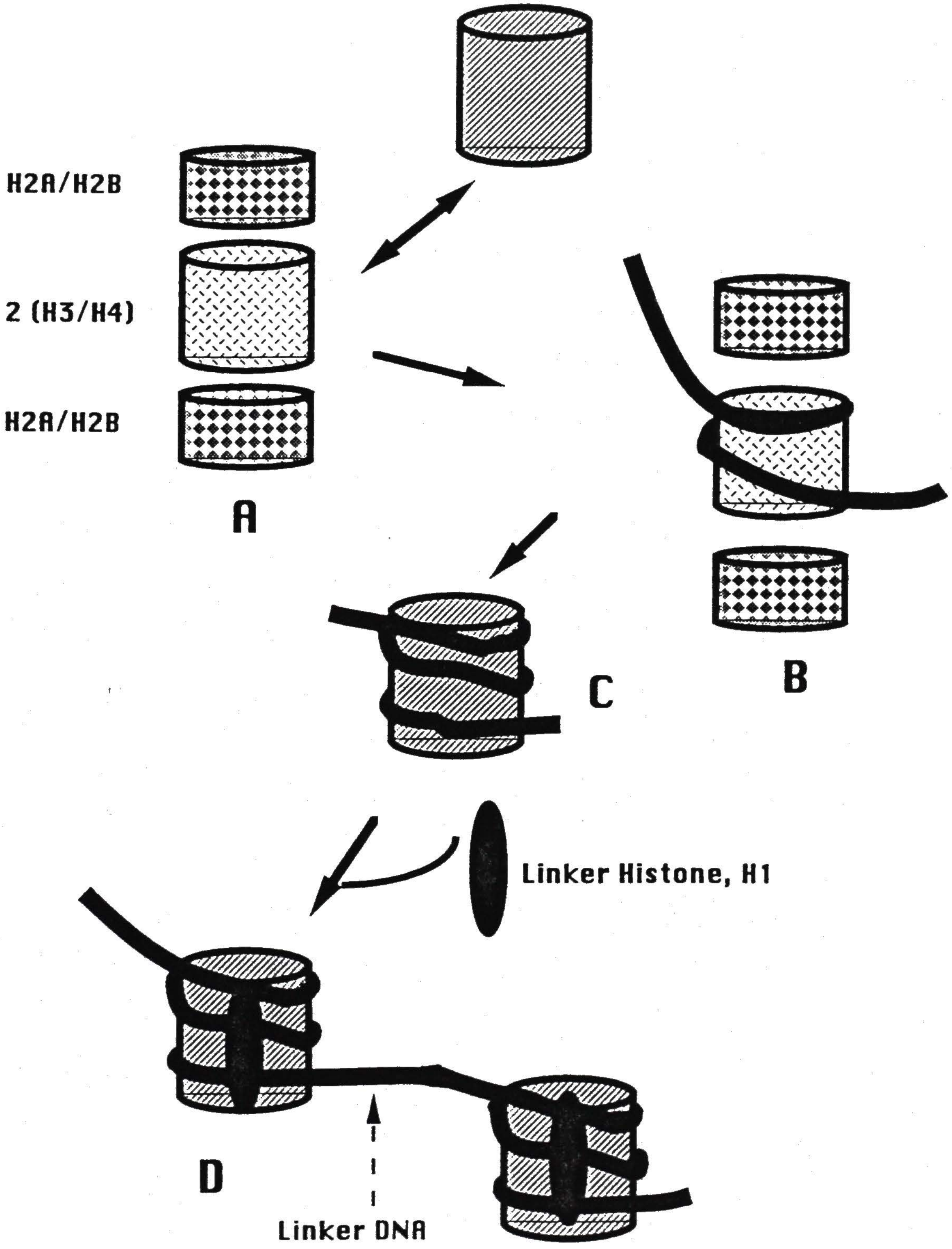
H2A/H2B
2 (H3/H4)
H2A/H2B
A
B
C
Linker Histone, H1
D
Linker DNA

of H3/H4 and two dimers of H2A/H2B (Arents, *et al.*, 1991). This is a definition based on structural (Arents, *et al.*, 1991) and functional studies (Hansen and Wolffe, 1994). The protein-protein interactions between histones are mediated by the recently described "histone fold motif" (Arents and Moudrianakis, 1995) which is made of a central long helix of 27 residues and is flanked by two loops which are also flanked by short helices.

The beads on a string arrangement of nucleosomes in DNA are coiled with the participation of histone H1 to generate the 30 nm fiber or the "condensed fiber" (Thoma, *et al.,* 1979). The 30 nm fiber structure is stabilized by protein-protein interactions between nucleosomes through the histone tails (Garcia-Ramirez, *et al.*, 1992). The supercoiled structure of chromatin seems to be the natural conformation of chromatin during interphase in the cell cycle. However, the actual DNA substrate for transcription, replication and repair is the "beads on a string" chromatin form. Therefore, these transitional changes must be finely regulated by other mechanisms. It appears that to obtain protein-free DNA which would be accessible to the enzyme machineries of DNA replication, transcription and repair, the following steps are required: i) dissociation of linker histone (H1) from chromatin to relax the 30 nm fiber; ii) dissociation of the H2A/H2B dimer from the tetramer composed of H3 and H4; and iii) the dissociation of the H3/H4 tetramer from DNA.

Interphase chromatin is not a disperse or amorphous structure. It is organized in loops with the participation of the nuclear matrix *via* the nuclear matrix attachment regions (MAR) (Cook, 1991). Therefore, in order to understand the organization of the genetic material *in situ*, the nucleus has been subdivided into different functional domains.

Numerous studies have been carried out to determine the composition and function(s) of subnuclear domains at the biochemical level. In general, current methods utilized for this purpose involve three steps (Fig. 4): **1)** cleavage of DNA; **2)** extraction of degraded DNA and chromosomal proteins with low and high salt concentration buffers; and 3) separation of the nuclear envelope with a non-ionic detergent (Triton X-100). In some cases steps 2 and 3 are inverted (Tubo and Berezney, 1987). Studies carried out with this general protocol have proven useful in the identification of proteins from each subnuclear functional domain. A general scheme of these studies is shown on figure 4.

Nuclear matrix. The nuclear matrix (NM) has been defined based on biochemical, morphological and functional properties (Berezney, *et al.,* 1995). Biochemically, the NM is the proteinaceous structure remaining following: i) nuclease digestion, ii) chromatin extraction with low and high salt concentration buffers, and iii) detergent extraction with Triton X-100 (Berezney and Coffey, 1974). A typical nuclear matrix contains 10% nuclear protein, 2% nuclear DNA, 29% nuclear RNA and 1.5% phospholipid (Berezney, *et al.*, 1995). Of particular interest is the fact that this subnuclear structure contains poly(ADP-ribose) (Cardenas-Corona, *et al.*, 1987). Two-dimensional gel electrophoresis shows that there are approximately 200 proteins (Fey and Penman, 1988); however, prominent proteins comprise no more than fifteen polypeptides. These include the lamins (A, B, and C), nucleolar protein B-23 and core hnRNP proteins. The remaining proteins are termed "matrin" proteins (Nakayasu and Berezney, 1991). This family of proteins vary in size from 42 to 190 kDa. Many of the prominent proteins of NM are DNA binding proteins (Hakes and Berezney, 1991). Other proteins such as AKAP 95 (Coghlan *et al.*, 1994) and NuMa (nuclear mitotic apparatus protein) have also been identified as important components of the nuclear matrix (Zeng *et al.,* 1994).

Morphologically, the NM is the framework of the cell nucleus (Berezney and Coffey, 1977). It is composed of a fibrogranular internal matrix, residual nuclear envelope and residual nucleoli. These structures are the basis for the functions in which

Fig. 4. Scheme for the fractionation of eukaryotic nuclei into separate functional domains. **1**) DNA degradation by either endonucleases or exonucleases. **2**) Chromatin proteins and nucleotides are extracted with buffers containing low (**2A**) and high (**2B**) salt concentration. **3**) the nuclear envelope is removed with non-ionic detergent.

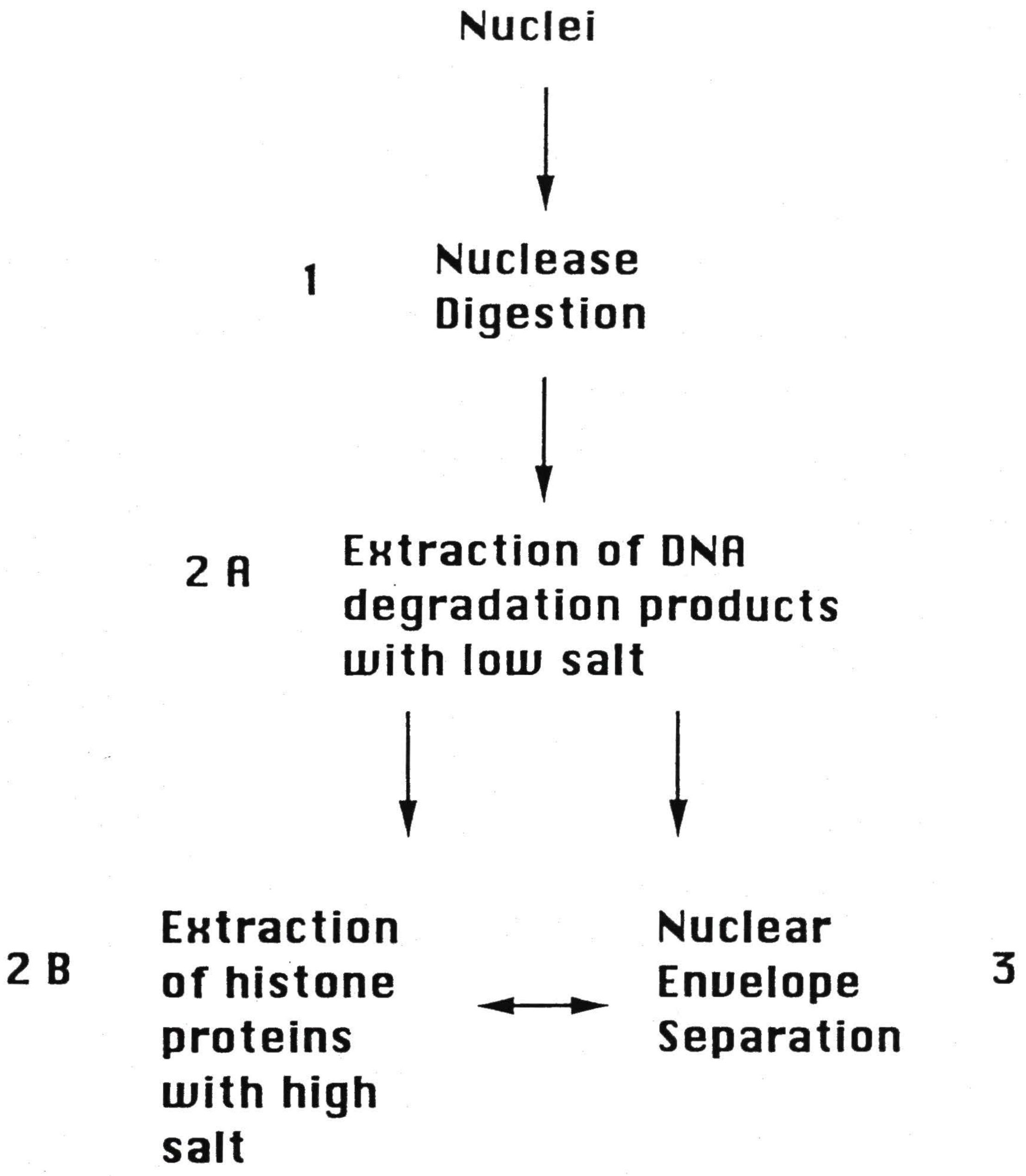
Nuclei
1
Nuclease Digestion
2 A
Extraction of DNA degradation products with low salt
2 B
Extraction of histone proteins with high salt
Nuclear Envelope Separation
3

the nuclear matrix is implicated. The nuclear matrix regulates structural and functional aspects of the genome through nuclear matrix attachment regions (Gasser and Laemmli, 1987).

Functionally, the NM includes sites for DNA replication (Berezney and Coffey, 1975), transcription (Jackson, *et al.,* 1985) and DNA repair (Jackson, *et al.,* 1994a,b). The NM also contains chromatin and ribonucleoprotein domains, and some of the proteins that are important for DNA replication such as DNA polymerase α and primase activity (Tubo and Berezney, 1987) as well as DNA topoisomerase II (Fernandez and Catapano, 1991). Not surprisingly, the sites for initiation of DNA replication (ORI) are also in close contact with the nuclear matrix (Pardoll, *et al.,* 1980; Razin, *et al.,* 1986). Similarly, the participation of the nuclear matrix in transcription is substantiated by the finding that a fraction of RNA polymerase II (Lewis, *et al.*, 1984), spliceosome-associated proteins (Blenkowe, *et al.*, 1994) and transcription factors (van Wijnen *et al.*, 1993) are associated with this structure.

The underlaying lamina of the cell nucleus is shared between the nuclear matrix and the nuclear envelope. In fact, it appears that the lamina plays a role in chromatin organization and also in the reassembly of the nuclear envelope following cell division.

Nuclear envelope. The nuclear envelope (NE) is made of an outer and an inner nuclear membrane, nuclear pore complexes and the lamina (Gerace and Foisner, 1994). The nuclear envelope is composed of 70% protein, 3% DNA, 5% RNA and 22% phospholipids (Harris, 1978). The perinuclear space is formed between the two nuclear membranes, and it is continuous with the endoplasmic reticulum. In fact, inhibition of 3-hydroxy-3-methylgutaryl coenzyme A (HMG CoA), an integral membrane protein, shows that the smooth endoplasmic reticulum gives origin to the nuclear envelope membranes (Pathak, *et al.,* 1986). The nuclear membrane is a double lipid bilayer which serves as boundary to separate the nucleus from the cytoplasm. In rat liver, the pool of phospholipids is a mixture of sphingomyelin, phosphatidylcholine, phosphatidylethanolamine, phosphatidylserine, phosphatidylinositol, phosphatidic acid, lysophosphatidylcholine, and lysophosphatidylethanolamine. These lipids appear to play a role in nuclear envelope signal transduction events (Raben *et al.,* 1994).

The outer nuclear membrane is coated with ribosomes (Gerace and Burke, 1988). Additionally, outer nuclear membrane and endoplasmic reticulum contain similar enzymatic activities (Amar-Costesex, *et al.,* 1974). Therefore, the nuclear envelope contain enzymes such as ATPase, glucose-6-phosphatase, glucose-1-phosphatase, alkaline phosphatase, acid phosphatase, cytochromes and other reductases (Harris, 1978). The similarity in protein composition between the ER and outer nuclear membrane represent the continuity of this membrane.

The nuclear envelope is maintained intact during interphase, but it is disrupted at the onset of mitosis. Disruption and re-formation of the nuclear envelope during mitosis commit the cell to a single event of DNA replication during the S phase of the cell cycle (Blow and Laskey, 1988). This appears to be mediated by a replication licensing factor(s) (Romanowski and Madine, 1996)

Proteins of the inner nuclear membrane include otefin, lamina associated proteins (LAP), and p58 (Gerace and Foisner, 1994). It is usually accepted that these proteins serve as linkages for interactions of nuclear membranes with the underlaying lamina. These interactions appear to be disrupted during mitosis. Otefin is a protein of 53 kDa localized in the nuclear envelope of *Drosophila*. Antibodies raised to the translation product of the otefin cDNA interact with mammalian nuclear envelope protein (Padan, *et al.*, 1990). Similarly, LAP proteins identified from rat liver are classified in LAPI and LAP2 according to specific recognition epitopes by monoclonal antibodies. LAPI includes the subtypes 1A, 1B and 1C. Whereas LAP 1 and 2 bind lamins *in vitro*, LAP 2 binds to mitotic chromosomes. Additionally, these proteins are substrates for phosphorylation (Foisner and Gerace, 1993).

The lamina is a meshwork of proteins composed of lamins A, B and C (Aebi, *et al.*, 1986). These proteins have molecular weights of 70, 68, and 60 kDa. Analysis of the cDNA from lamin proteins shows that they are composed of three distinct segments. The N-terminal fragment constituted of 30-40 residues which contains a site for phosphorylation. Similarly, the C-terminal fragment composed of 210-300 aminoacids also possesses phosphorylation sites which are in proximity to the nuclear localization signal. In addition, the C-terminal domain of lamins A and B includes sites for isoprenylation and carboxymethylation. The central rod like domain of lamin proteins is composed of approximately 350 residues. This polypeptide forms an α-helical protein structure which is characteristic of intermediary filaments (McKeon, *et al.*, 1986; Fisher *et al.*, 1986). Based on aminoacid sequence and patterns of expression, lamin proteins are classified as type A (lamins A and C) and type B (lamin B). While lamins B-type are expressed in all the tissues, A-type lamins are only expressed in differentiating tissues. Lamin proteins are implicated in chromatin organization and nuclear envelope reassembly. The isoprenylation of lamin proteins seems to be important for association with the nuclear envelope (Holtz, *et al.*, 1989). Recently, it has been shown that lamin proteins interact with the tails of core histone proteins (Taniura, *et al.*, 1995). These findings may represent a link between chromatin organization and nuclear envelope structures.

The sites of interaction between the outer and inner nuclear membrane are the nuclear pore complexes (NPC) which are different from the outer and inner membranes of the nucleus. Recent studies show that the pore membrane is in close contact with the NPC which mediates the specific nucleocytoplasmic transport of molecules (Pante and Aebi, 1995).

Nuclear pore complex (NPC). The nuclear pore complex is an assembly of proteins of approximately 10^8 Da that serves for nucleocytoplasmic transport (Davis, 1995). It is estimated that this complex is composed of approximately 100 different polypeptides (Reichelt, *et al.,* 1990). The component of the NPC are: i) basic framework, ii) central plug or channel complex, iii) cytoplasmic ring and the cytoplasmic filaments, iv) the nuclear ring and the nuclear basket. Whereas molecules of 9 nm are transported by diffusion, larger molecules are transported actively *via* a two steps process. The latter has been shown with proteins that contain nuclear location signals (NLS). The first step includes docking of the transported molecule with the participation of cytosolic factors such as importin α, importin β, Ran, and nuclear transport factor 2 (NTF 2). The second step is dependent on ATP hydrolysis and temperature (Pante and Aebi, 1996).

Nucleolus. The nucleolus is a subnuclear domain which is not protected by a membranous structure. Microscopical studies show at least three distinct regions termed fibrillar center, dense fibrillar component and granular component. The clustering of nucleolus components appears to be regulated by protein-protein interactions and by protein-nucleic acid interactions. Some of the components of the nucleolus are RNA polymerase I, transcription factor UBF, ribonucloprotein complexes, and ribosomal RNA. The main role of the nucleolus is in the biogenesis of ribosomes. The steps involved in this process include transcription of rDNA, processing of pre-rRNA transcript, assembling of the rRNA with ribosomal proteins, and transport of the pre-assembled ribosome to the cytoplasm. The transport of the ribosomes from the nucleus to the cytoplasm has been correlated to the association of the nuclear envelope with the nucleolus (Bourgeois and Hubert, 1988).

Separate functional sudomains are required in the cell nucleus to prevent undesired interactions of nuclear components. The assembly of each domain is mediated mainly by protein-protein interactions which appear to be modulated by postranslational modifications reactions. For instance, phosphorylation of lamin proteins is required for nuclear disruption (Ohaviano and Gerace, 1985). On the other hand, DNA damage that causes breaks on DNA trigger poly(ADP-ribosyl)ation of DNA binding proteins which affects the structure and function of chromatin (Boulikas, 1993).

Poly(ADP-ribosyl)ation pathway. Poly(ADP-ribosyl)ation is a reversible post-translational modification of DNA binding proteins in higher organisms. Figure 5 outlines the sequence of molecular events in this pathway. First, the poly(ADP-ribosyl)ation of proteins is initiated by the binding of PARP to DNA nicks or breaks (Benjamin and Gill, 1980). DNA binding promotes homodimerization (Mendoza-Alvarez and Alvarez-Gonzalez, 1993; Panzeter and Althaus, 1994) and/or heterodimerization of PARP with other DNA binding proteins. The activation of PARP leads to the utilization of NAD^+ as an ADP-ribosylating substrate for the synthesis of poly(ADP-ribose). ADP-ribose polymers are primarily linked to PARP and histone proteins *in vivo* and *in vitro* (Ogata, *et al.*, 1981; Adamietz and Rudolph, 1984; Adamietz, 1987). On the other hand, poly(ADP-ribose) glycohydrolase (PARG) catalyzes the de-poly(ADP-ribosyl)ation reaction (Miwa and Sugimura, 1971). Finally, ADP-ribose protein lyase (APL), the third enzyme involved in this pathway, cleaves the ADP-ribose residue directly attached to protein acceptors (Okayama, *et al.*, 1978).

Poly(ADP-ribose) Polymerase (PARP). Poly(ADP-ribose)polymerase is a ubiquitous enzyme in eukaryotic cells. The gene for PARP is localized in chromosome 1 of human cells (Cherney, *et al.*, 1987). The gene is constituted of 23 exons and is 43 kb

Fig. 5. Enzymatic cycle of the poly(ADP-ribosyl)ation pathway. DNA-strand breaks activate poly(ADP-ribose) polymerase (PARP) by facilitating enzyme dimerization. The enzyme dimer utilizes NAD^+ as an ADP-ribosylation substrate to synthesize (protein-bound) homopolymers of ADP-ribose. The degradation of poly(ADP-ribose) is carried out by poly(ADP-ribose) glycohydrolase (PARG) which generates free monomeric ADP-ribose, and ADP-ribose protein lyase (APL) which cleaves the ADP-ribose residue directly linked to protein.

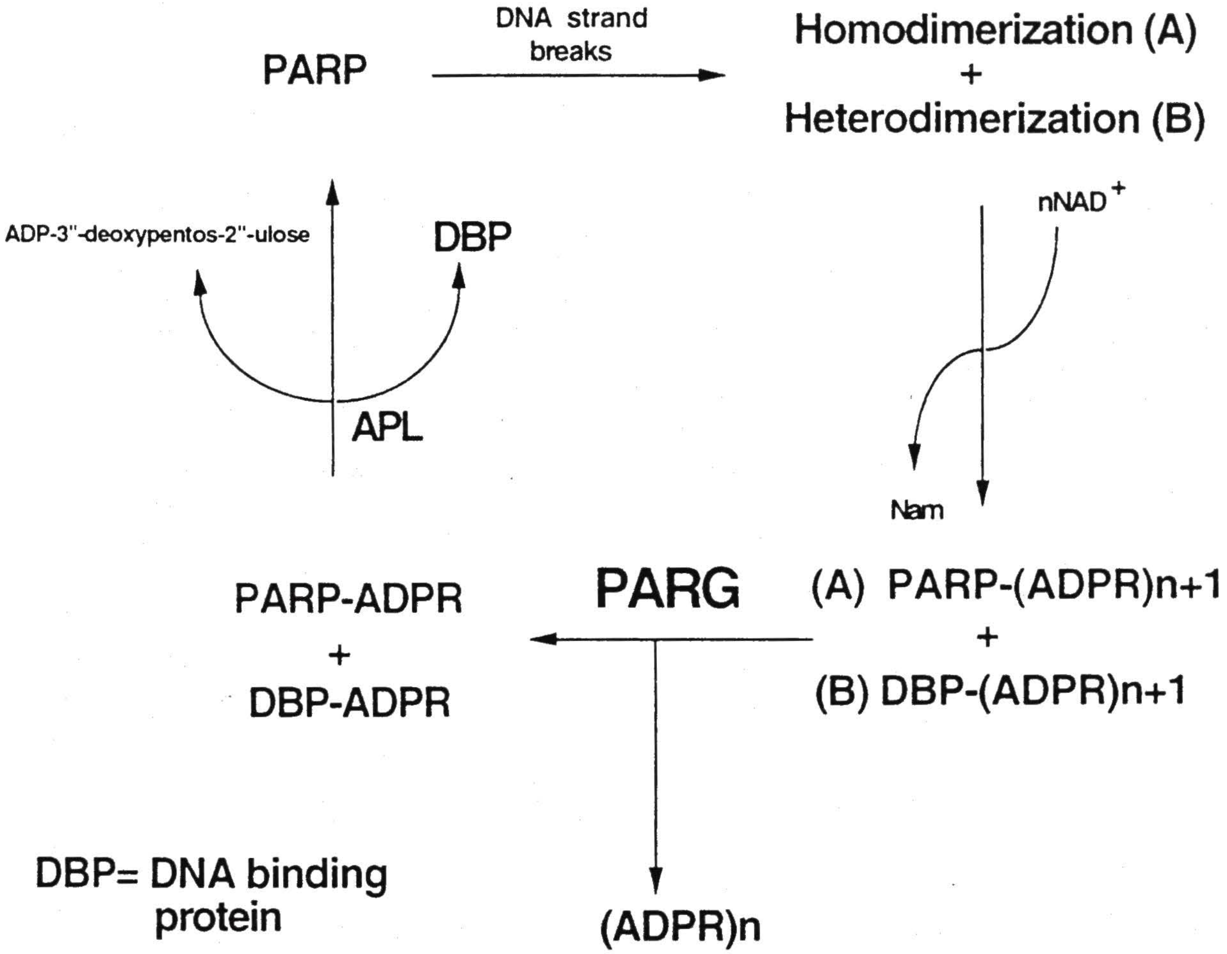
PARP
DNA strand breaks
Homodimerization (A)
+
Heterodimerization (B)
nNAD$^+$
Nam
ADP-3"-deoxypentos-2"-ulose
DBP
APL
PARP-ADPR
+
DBP-ADPR
PARG
(A) PARP-(ADPR)n+1
+
(B) DBP-(ADPR)n+1
(ADPR)n

DBP= DNA binding protein

in size (Auer, *et al.*, 1989). The cDNA of human PARP codes for a protein of 1,014 aminoacid residues with an estimated molecular mass of 113,153 Da (Kurosaki, *et al.*, 1987).

Three distinct peptide fragments are generated upon partial proteolytic digestion of PARP with papain and α-chymotrypsin (Kameshita, *et al.*, 1986). The 46 kDa amino-terminal domain contains zinc fingers I and II. Zinc fingers I (residues 2-97) and II (residues 106-207) allow for recognition of double (Ikejima, *et al.*, 1990) and single (Gradwohl, *et al.*, 1990) DNA strand breaks, respectively. These DNA-binding motifs belong to the class $C\text{-}Xaa_2\text{-}CX_{28\text{-}30}\text{-}H\text{-}Xaa_2\text{-}C$. The N-terminal domain also contains the bipartite nuclear localization signal (Schreiber, *et al.*, 1992) and a putative protein-protein recognition peptide (Buki, *et al.*, 1995). The 22 kDa central domain contains several of the substrate acceptor sites for auto-poly(ADP-ribosyl)ation. Furthermore, this domain includes a putative "leucine zipper" in *Drosophila* that may allow for protein-protein interactions (Uchida, *et al.*, 1993a). The 54 kDa C-terminal fragment contains the catalytic or NAD^+-binding site. This site possesses the critical glutamate residue for catalysis equivalent to the catalytic glutamate found in prokaryotic mono(ADP-ribosyl)transferases (Marsischky, *et al.*, 1995).

Protein targets for poly(ADP-ribosyl)ation. The protein targets for poly(ADP-ribosyl)ation are DNA-binding proteins. *In vivo* and *in vitro* studies have shown that the main targets for poly(ADP-ribosyl)ation include first PARP itself and histone H1 (Ogata, *et al.*, 1981; Adamietz, 1987). In addition, histone H2B (Adamietz, and Rudolph, 1984), high mobility group proteins (HMG) 14/17 (Tanuma, *et al.*, 1986a), nuclear matrix lamins (Adolph and Song, 1985), nuclear matrix proteins (Wesierska-Gadek and Sauermann, 1985), topoisomerases I and II (Ferro, *et al.*, 1984; Kasid, *et al.*, 1989; Schroder, *et al.*, 1989), DNA polymerases α and β (Yoshihara, *et al.*, 1985), DNA ligase II (Yoshihara, *et al.,* 1985), and both subunits of transcription factor TFIIF (Rawling and Alvarez-Gonzalez, 1996) are poly(ADP-ribosyl)ated.

Catabolism of poly(ADP-ribose). The half life of poly(ADP-ribose) is less than one minute in cells treated with alkylating agents. However, the half life of constitutive basal poly(ADP-ribose) is approximately seven hours (Alvarez-Gonzalez and Althaus, 1989). Therefore, the degradation of poly(ADP-ribose) appears to be dependent on the intracellular concentration of poly(ADP-ribose). This observation with cultured cells has been correlated with the higher affinity of PARG for ADP-ribose chains larger than 20 residues (Hatakeyama, *et al.*, 1986). Interestingly, in cultured cells exposed to hyperthermia, the turnover of poly(ADP-ribose) decreased because of the heat inactivation of PARG (Jonsson, *et al.,* 1988b); however, the poly(ADP-ribose) turnover was restored in a time-dependent manner when cells were returned to 37 °C (Jonsson, *et al.,* 1988a). *In vitro* studies with the 34I cell line derived from mouse mammary carcinomas showed that treatment with glucocorticoids decrease poly(ADP-ribosyl)ation on HMG 14 and 17 proteins (Tanuma, *et al.,* 1983). In subsequent studies performed with potent and specific inhibitors of PARG, it has been shown that de-poly(ADP-ribosyl)ation of HMG 14/17 is a crucial event in gene expression mechanisms (Tsai, *et al.,* 1992). Thus, poly(ADP-ribose) catabolism appears to be linked to regulation of gene expression.

Poly(ADP-ribose)glycohydrolase (PARG). The catabolism of poly(ADP-ribose) is catalyzed by poly(ADP-ribose) glycohydrolase (PARG) which is an enzyme widely distributed in higher organisms. This enzyme breaks the 1"-2' glycosidic linkages of poly(ADP-ribose) generating mainly monomeric ADP-ribose (Miwa *et al.,* 1974) (Fig.6A). The mode of hydrolysis appears to be both endo (Ikejima and Gill, 1988) and exoglycosidic (Miwa, *et al.,* 1974) (Fig. 6B) depending on the conditions used. The modes of poly(ADP-ribose) hydrolysis have been substantiated by Brochu *et al.* (1994).

PARG has been purified from different sources including human placenta, pig liver, and erythrocytes (table 1). It has been estimated that there are from 2,000 (Hatakeyama, *et al.*, 1986) to 50,000 molecules of PARG per nucleus (Tanuma, *et al.*, 1986b). At least two forms of PARG have been identified: i) one in the cytosol; and ii) one in the nucleus (Maruta, *et al.*, 1991). Both enzyme forms have been partially characterized in guinea pig liver (Maruta, *et al.*, 1991). The nuclear enzyme, 75.5 kDa, and the cytosolic enzyme, 57 kDA were named PARG I and PARG II, respectively. Their acidic/basic ratios are 1.26 and 2.88, respectively. Tanuma and Endo (1990) reported the purification and characterization of PARG from human erythrocytes. This observation supports the finding of a cytosolic PARG since erythrocytes are enucleated cells. PARG activity has also been detected in metaphase chromosomes of HeLa S3 cells (Tanuma, *et al.*, 1982).

Properties of nuclear PARG. Nuclear PARG was first purified to homogeneity from guinea pig liver (Tanuma, *et al.*, 1986b) and later from human placenta (Uchida, *et al.*, 1993b). The enzymatic properties of pure PARG are shown in table 2. PARG possesses high affinity for ADP-ribose chains of 20 residues or more (Hatakeyama, *et al.*, 1986). Experiments with PARG isolated from human placenta show that the kinetic parameters depend on the length and complexity of poly(ADP-ribose) (Uchida, *et al.*, 1993b). In the same study, it was shown that protein-bound poly(ADP-ribose) is a better substrate for PARG than protein-free poly(ADP-ribose). At present the role of the protein acceptor in poly(ADP-ribose) degradation is unknown.

Inhibitors of PARG. Currently, there is a relative lack of potent and specific inhibitors of PARG; however, several studies have shown that PARG is inhibited by

Fig. 6. Mode of action of poly(ADP-ribose) glycohydrolase. Poly(ADP-ribose) glycohydrolase cleaves the glycosidic linkage 1''-2' of poly(ADP-ribose) (**A**). This bond may be hydrolyzed either at internal ribose-ribose bonds (endoglycosidic cleavage) or from the non-reducing end of the polymer (exoglycosidic cleavage) (**B**). Note that, endoglycosidic cleavage generates protein-free ADP-ribose oligomers. By contrast, monomeric ADP-ribose is the only enzyme product of exoglycosidic cleavage.

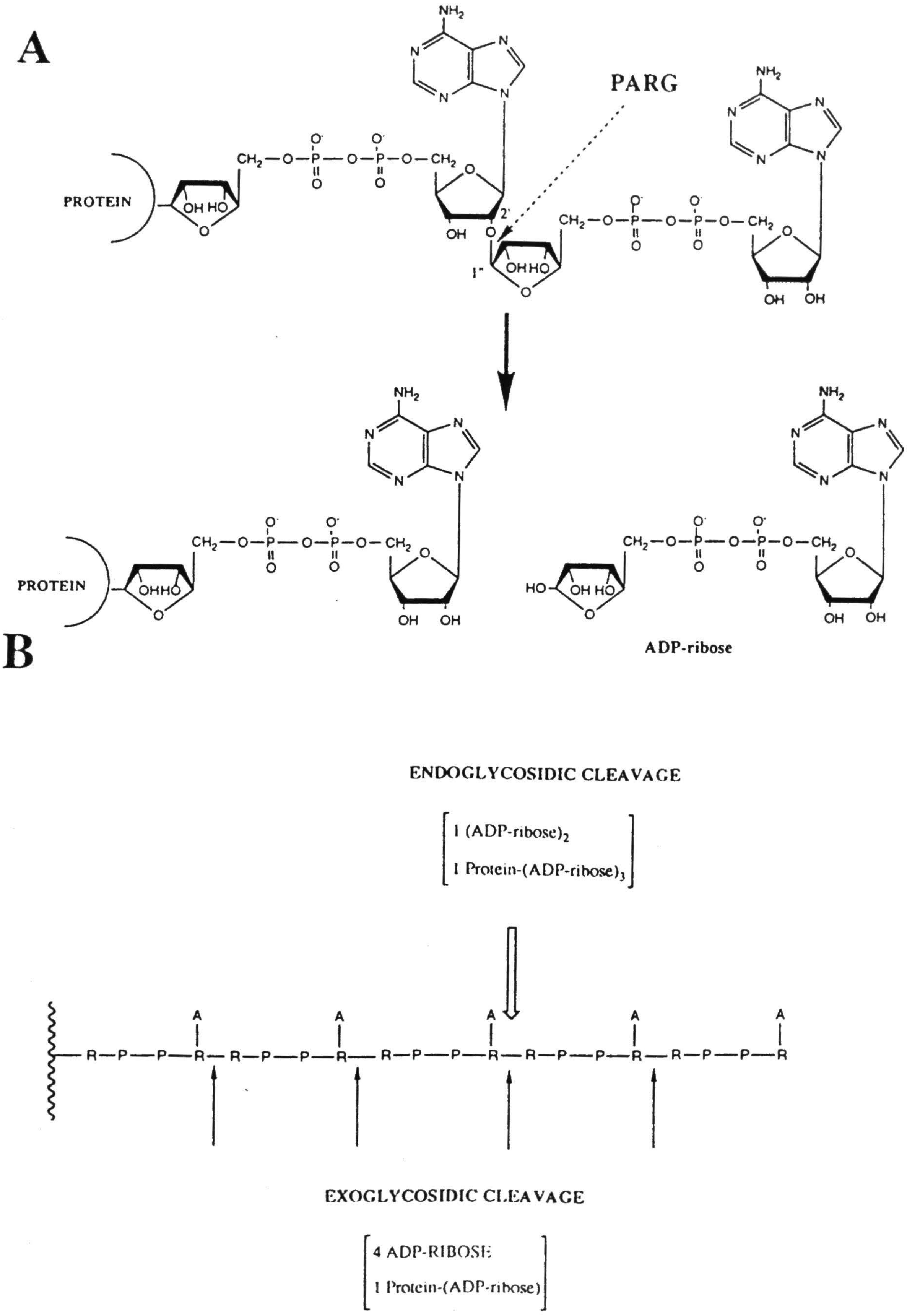
A
PARG
PROTEIN
NH2
N
OH HO
OH
2'
1"
CH2—O—P—O—P—O—CH2
O⁻
O
PROTEIN
ADP-ribose
HO
B
ENDOGLYCOSIDIC CLEAVAGE
1 (ADP-ribose)2
1 Protein-(ADP-ribose)3
A
R—P—P—R
EXOGLYCOSIDIC CLEAVAGE
4 ADP-RIBOSE
1 Protein-(ADP-ribose)

Table 1. Enzyme properties of pure poly(ADP-ribose) glycohydrolase.

Tissue Source	Nuclear form	Molecular weight on SDS-polyacrylamide gels	Reference
Calf thymus	No	G.F. 48*	Miwa *et al.*, 1974
Pig thymus	No	61.5 and 67.5	Tavassoli, *et al.*, 1983
Guinea Pig liver	No	75.5	Tanuma *et al.*, 1986b
HeLa S3 cells	Yes	72	Tanuma *et al.*, 1986c
HeLa S3 cells	Yes	53	Tanuma *et al.*, 1986c
Calf thymus	No	59	Hatakeyama, *et al.*, 1986
Bull testis	No	N.R.	Menard and Poirier 1987
Human erythrocytes	No	59	Tanuma and Endo 1990
Calf thymus	No	59 and 60	Thomassin, *et al.*, 1990
Guinea pig liver	No	59.5	Maruta, *et al.*, 1991
34I cells	Yes	N.R.	Tsai, *et al.*, 1992
Human placenta	Yes	71	Uchida, *et al.*, 1993b
Calf thymus	No	60 and 66,74	Brochu, *et al.*, 1994

N.R., not reported
* Gel filtration

Table 2. Comparison of poly(ADP-ribose) glycohydrolase from pig liver and human placenta.

	Pig liver	Human Placenta
Molecular weight (kDa)(SDS-PAGE)	75.5	71.0
Kinetic constants		
$K_{(ADPR)_n}$ (μM)	2.3	1.8
Vmax (μmol min^{-1}mg $protein^{-1}$)	36.0	67.0
pI	6.6[b]	6.73
Acidic/Basic aminoacids	1.26[b]	1.27
Time course (30-40% hydrolysis)	linear	linear
Mode of hydrolysis	Exoglycosidic	Exoglycosidic
Optimum pH	6.8-7.0	6.0-7.5
Thiol requirement	Yes	Yes
Effect of mono- and divalent cations	Concentration-dependendent	Concentration-dependent
Effect of nucleotides		
ADP-ribose	Inhibits	Inhibits
cAMP	Inhibits	Inhibits
β-NAD^+	No effect	No effect

[a] The measurement was correlated to the same average polymer size of the substrate

[b] Data from (Maruta, *et al.*, 1991).

ADP-ribose (Miwa, *et al.*, 1974), cAMP (Ueda, *et al.*, 1972), DNA intercalators (ethacridine, proflavine, ellipticine, daunomycin and Tilorone R10,556 DA) (Tavassoli, *et al.*, 1985), Ap4A (Tanuma, *et al.*, 1986b), histone proteins (Miwa, *et al.*, 1974; Tavassoli, *et al.*, 1985), denatured DNA (Tanuma, *et al.*, 1986b), lignin (Tanuma, *et al.*, 1989), nobotanins B, E, and K (Tsai, *et al.*, 1992). Interestingly, nobotanins B is an inhibitor of PARG both *in vivo* and *in vitro* (Tsai, *et al.*, 1992). By contrast, histones complexed with DNA in ratios 1:1 are ineffective inhibitors (Tanuma, *et al.*, 1986b). Recently, adenosine diphosphate (hydroxymethyl)pyrrolidinediol has been identified as novel inhibitor of PARG (Slama, *et al.*, 1995).

Subnuclear distribution of PARP and PARG. Both PARP and PARG are enzymes typically recognized as associated with chromatin (Ueda, *et al.*, 1975; Miyakawa, *et al.*, 1972). On the other hand, the polymers of ADP-ribose are tightly associated with the nuclear matrix (Cardenas-Corona *et al.*, 1987). A significant portion of PARP is also associated with the nuclear matrix (Alvarez-Gonzalez and Ringer, 1988), and some of proteins targeted for poly(ADP-ribosyl)ation are components of this fraction as well. More recently, electron microscopic observations suggest that PARP may be in close contact with the nuclear envelope (Mosgoeller, *et al.*, 1996). Also, the release of PARG from isolated nuclei requires buffers containing high salt concentration (Uchida, *et al.*, 1993b). Thus, PARG may also be tightly associated with nuclear structures such as the nuclear matrix and/or the nuclear envelope. Thus, one objective of this study is to investigate the subnuclear distribution of PARG.

Poly(ADP-ribosyl)ation of proteins and chromatin structure. PARP and PARG are chromatin-bound enzymes (Ueda, *et al.*, 1975; Miyakawa, *et al.*, 1972). The molecular role of poly(ADP-ribosyl)ation in the modulation of chromatin structure and

Fig. 7. Structural changes of chromatin are modulated by protein-poly(ADP-ribosyl)ation. The microscopic appearance of isolated oligonucleosomes is similar to that of the 30 nm fiber (**A**). Introduction of DNA strand breaks leads to the activation of PARP which poly(ADP-ribosyl)ates chromatin proteins. As a result, the "30 nm fiber" is decondensed to a "beads on a string" form (10 nm fiber) (**B**). Furthermore, the poly(ADP-ribosyl)ation of proteins leads to release of nucleosmal DNA either by the covalent modification of proteins or by non-covalent interactions of poly(ADP-ribose) with histone proteins (**C**). This process is made reversible by the action of PARG. Thus, degradation of poly(ADP-ribose) leads to the re-association of histones with DNA (**C** to **B**).

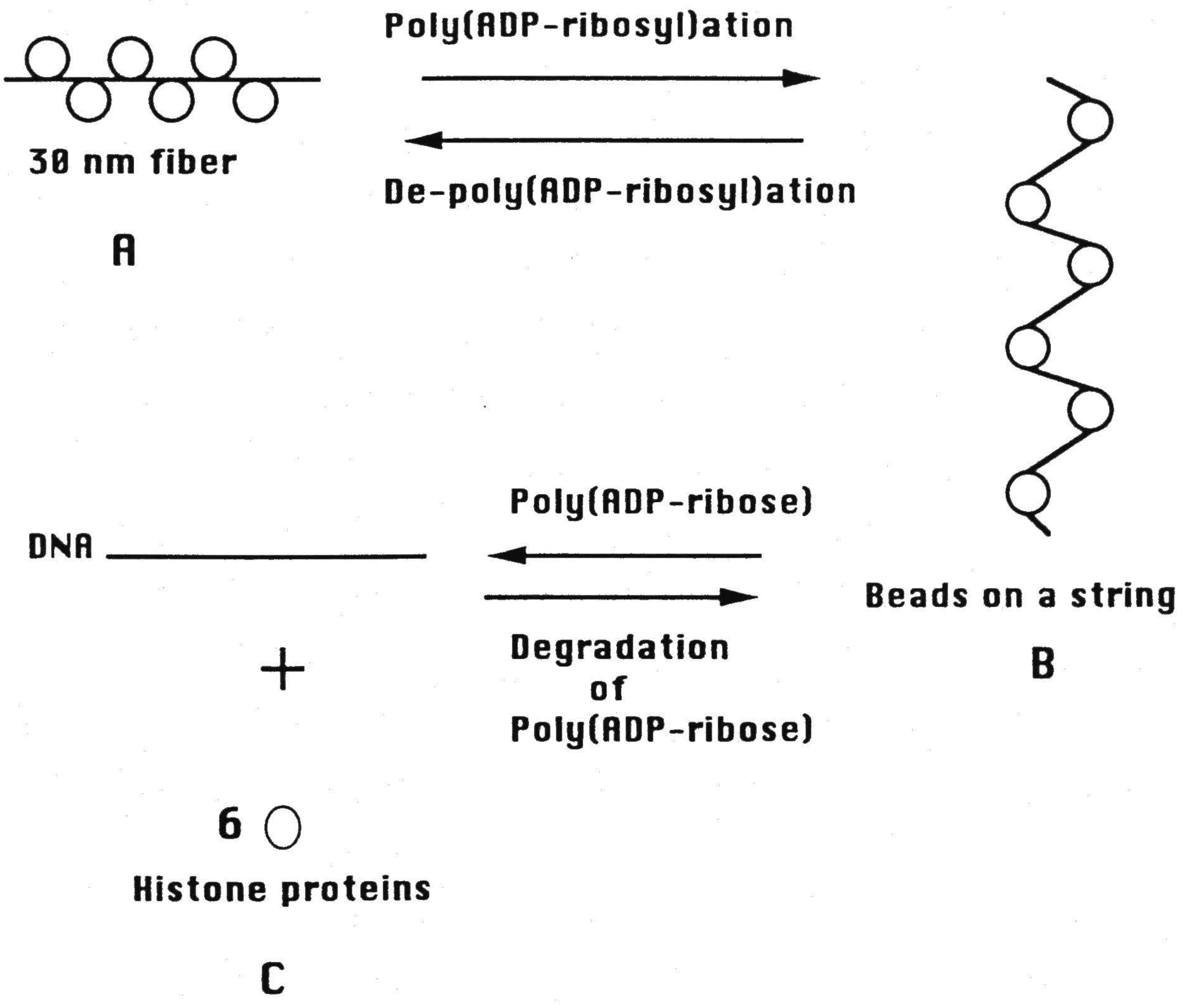
Poly(ADP-ribosyl)ation
De-poly(ADP-ribosyl)ation
30 nm fiber
A
Beads on a string
B
Poly(ADP-ribose)
Degradation of Poly(ADP-ribose)
DNA
+
6
Histone proteins
C

function is well documented (De Murcia, *et al.*, 1988). Figure 7 shows the chromatin structural changes that occur during poly(ADP-ribosyl)ation. First, covalent poly(ADP-ribosyl)ation of chromatin proteins results in the time dependent relaxation of the 30 nm fiber as determined by electron microscopy (Poirier, *et al.*, 1982). Interestingly, histone H1 is extensibly poly(ADP-ribosyl)ated as the 30 nm fiber is relaxed (Aubin, *et al*, 1983). Recondensation of the 30 nm fiber is also a time dependent process catalyzed by PARG which degrades the poly(ADP-ribose) covalently linked to PARP and histone H1 (De Murcia, *et al.*, 1986). Thus, the role of PARG appears to be to restore the structure of highly condensed chromatin (Fig. 7) (De Murcia,*et al.*, 1986). Not surprisingly, this post-translational modification disrupts the interactions between nucleosomal DNA and core histones (Mathis and Althaus, 1987). It has also been determined that poly(ADP-ribosyl)ation of DNA-metabolizing enzymes results in inhibition of the activity of the targeted protein. Therefore, protein-poly(ADP-ribosyl)ation affects not only chromatin compaction but also genomic functions.

In conclusion, it appears that the role of protein-poly(ADP-ribosyl)ation is double. One is mediated by the covalent poly(ADP-ribosyl)ation of DNA-binding polypeptides which modifies the function of the protein modified. Second, poly(ADP-ribose) molecules which are polyanionic in nature may interact non-covalently with some of the abundant chromatin proteins *i. e.* histones, leading to changes in the higher order structure of chromatin. Indeed, poly(ADP-ribose) interacts non-covalently with histone proteins (Panzeter, *et al.*, 1992). Based on this observation, a "histone shuttle" mechanism has been proposed (Realini and Althaus, 1993). In this model, a histone-DNA-PARP complex is formed following DNA strand breaks formation. Then, poly(ADP-ribosyl)ation of PARP causes the release of DNA from the histone-DNA-PARP complex, and histone proteins interact non-covalently with poly(ADP-ribose) preventing the binding of histone proteins to DNA. Finally, to restore the binding of histones to DNA, degradation of poly(ADP-ribose) by PARG activity is required.

The histone shuttle mechanism is based on experiments that were carried out *in vitro* with individual histone proteins. The role of poly(ADP-ribose) in nucleosome remodelling remains to be shown. Furthermore, it is yet to be shown that these non-covalent interactions occur *in vivo*. In this regard, it has been shown that poly(ADP-ribose) competes with DNA for binding to histone H4 (Sauermann and Wesierska-Gadek, 1986; Wesierska-Gadek, and Sauerman, 1988). Additionally, Thibault, *et al.*, (1992) performed experiments with isolated nucleosomes and protein-free poly(ADP-ribose). They showed that histone epitopes hidden in the native nucleosome structure were accessible in the presence of poly(ADP-ribose). Thus, these results suggest that poly(ADP-ribose) in fact remodels nucleosome structure. Furthermore, the terminal tails of histone proteins are targets for non-covalent binding to poly(ADP-ribose) (Panzeter, *et al.*, 1993), and these are responsible for providing contact sites to nuclear matrix lamins (Taniura *et al.*, 1995), nucleosome-nucleosome interactions (Garcia-Ramirez, *et al.*, 1992) and histone-DNA interactions (Arents, *et al.*, 1991).

The histone shuttle mechanism implies that poly(ADP-ribose) interacts non-covalently with histone proteins disrupting the interactions of DNA with histone proteins in nucleosomes (Althaus, 1992). However, signals that trigger degradation of poly(ADP-ribosyl)ation to allow formation of native nucleosomes have not been identified. The non-covalent interactions of poly(ADP-ribose) with nuclear proteins appear to be mediated not only by ionic contacts but also by specific structural features of the protein and ADP-ribose polymers. In this respect, poly(ADP-ribose) molecules longer than 20 ADP-ribose residues seem to be the most likely candidates for non-covalent interactions (Panzeter, *et al.*, 1992; Nozaki, *et al.*, 1994).

General Hypothesis. The chemical nature of the poly(ADP-ribose) molecule and its chromatin environment imply that non-covalent interactions of poly(ADP-ribose) with chromatin-associated proteins may be important in the catabolism of this polymer. In particular, "charge to charge" or ionic interactions seem feasible between this polyanionic molecule and cationic proteins such as histones. These interactions may lead to the formation of poly(ADP-ribose) degradation intermediates. Therefore, It is proposed that the half-life of poly(ADP-ribose) in vivo is determined by the subnuclear localization of PARG as well as by non-covalent interactions of poly(ADP-ribose) with nuclear proteins in each subnuclear domain.

Purpose of the study. In this study we intend to show that: *i*) the degradation of poly(ADP-ribose) is modulated by non-covalent interactions of poly(ADP-ribose) with chromatin proteins; *ii*) the catabolism of protein-bound polymers of ADP-ribose is topologically regulated.

CHAPTER II

MATERIALS AND METHODS

Materials. β-NAD$^+$, ADP-ribose, core histones, enriched histone H1, DNA and phenylmethyl-sulfonyl fluoride (PMSF) were purchased from Sigma Chemical Co. (St. Louis, MO). Pure histone H1, H2A, H2B, H3 & H4 and proteinase K were obtained from Boehringer, Mannheim (Indianapolis, IN). [Adenylate-^{32}P]NAD$^+$ (250 Ci/mmol) was from ICN Biomedicals (Irvine, CA). Bio Sil Sec 125 (300 mm x 7.8 mm i.d.), BIO-REX 70, and electrophoresis reagents were purchased from Bio-Rad (Richmond, CA). Phosphodiesterase from *Crotalus adamanteus* and NAD glycohydrolase from *Neurospora crassa* were obtained from Worthington Biochem. Corp (Freehold,NJ). [^{32}P]ADP-ribose and [^{32}P]AMP were synthesized with [^{32}P]NAD$^+$ as a substrate for NAD glycohydrolase and phosphodiesterase, respectively. Similarly, [^{32}P]PRAMP was obtained by phosphodiesterase treatment of [^{32}P]poly(ADP-ribose). Pipes (Piperazine-N,N-bis-(2-ethane-sulfonic acid), 1.5 sodium salt) was acquired from Electron Microscopy Sciences (Ft. Washington, PA). IS-1000 version 2.00 digital imaging system was from Alpha Innotech Corp.(CA)

Isolation of nuclei. Rat liver nuclei (RLN) were obtained by the method of Blobel and Potter (1969). Briefly, livers were obtained from healthy Sprague-Dawley rats and homogenized in a 250 mM sucrose solution containing TKM buffer (50 mM Tris-HCl, pH 7.5 at 4 °C; 25 mM KCl; and 5 mM $MgCl_2$). The homogenate was filtered through four layers of cheese cloth. The eluate obtained was diluted 1:3 (v/v) with 2.3 M sucrose in TKM. Then, the mixture was underlaid with 2.3 M sucrose in TKM. Next, the mixture was centrifuged at 39,000 rpm at 0-4 °C. The nuclei obtained in the pellet was further used as a source of PARP and PARG activities. Protein content was determined by the method of Smith, *et al.*, (1985).

Isolation of H1-depleted chromatin. The resin AG 50W-X2 (Bio-Rad) which is in sulphonic form was transformed to the sodium form as described by Bolund and Johns (1973). This was carried out by washing 1 ml resin with 10 ml of 1 M HCl. Then, the resin was treated with 15 ml of 1M NaOH. The resin in the sodium form was equilibrated with 50 mM Na_2HPO_4, pH 7.0 containing 0.2 mM EDTA and 500 mM NaCl. Depletion of H1 was carried out by the method of Thoma *et al.*, (1981). Nuclei isolated by the method of Blobel and Potter (1966) was adjusted to 50 mM Na_2HPO_4, pH 7.0, 0.2 mM EDTA and 500 mM NaCl. The nuclei/resin solution was stirred on ice for 90 min. The amount of resin added was 1/4 of the nuclei volume. The resin was pelleted at 500 g for 5 min. The supernatant contained the H1-depleted chromatin. The extraction of H1 was monitored by SDS-PAGE as described by Laemmli (1970).

Fractionation of nuclei. Rat liver nuclei were fractionated as previously described (Alvarez-Gonzalez and Ringer, 1988). Briefly, nuclei were incubated at 37 °C for 45 minutes to digest the DNA with endogenous nucleases (Berezney, and Bucholtz, 1981). Nuclei were subsequently centrifuged (780 g) for 15 minutes at 4 °C. The pellet was diluted in 10 mM Tris-HCl, pH 7.4 (Buffer A) containing 200 µM $MgCl_2$. Three extractions were carried out with buffer A, 200 µM $MgCl_2$ to remove chromatin. The bulk amount of chromatin was extracted with Buffer A, 200 µM $MgCl_2$, 2 M NaCl. Afterwards, the nuclear matrix was obtained by treatment of the remaining subnuclear structure with 1% Triton X-100, 5 mM $MgCl_2$. After washing the pellet twice in buffer A, 5 mM $MgCl_2$, to remove Triton X-100, nuclear matrices were resuspended in buffer A, 5 mM $MgCl_2$. The different fractions were kept at -70 °C until used. The protein composition of the each fraction was analyzed by SDS-polyacrylamide gel electrophoresis as described by Laemmli (1970) with 0.1 % SDS and 12 % polyacrylamide and 4 M urea.

Preparation of samples for electron microscopy. A standard protocol for electron microscopy was followed. First, the samples were fixed overnight with a solution composed of 2.5% glutaraldehyde in 125 mM Pipes buffer (pH 7.3), in the appropriate buffer for each fraction. For instance, nuclei, nuclear matrices/nuclear envelopes and nuclear matrices preparations contained Buffer A, 200 µM $MgCl_2$, Buffer A, 5 mM $MgCl_2$, 1% Triton, and Buffer A, 5 mM $MgCl_2$, respectively. Subsequently, samples were post-fixed in 1% aqueous OsO_4. Dehydration of the samples was achieved by series of graded ethanol solutions. The fixed material was infiltrated with different ratio mixtures of propylene oxide/epon 812. The samples were sectioned on a Leica ultracuts with a diamond knife. 10 and 300 nm sections in thickness of the samples were stained with orange acetate and Sato's lead (Sato, 1968). The different subnuclear fractions were viewed with a Zeizz EM 910 electron microscope.

Proteinase-treatment. A reaction mixture of 40 µl containing 125 mM Tris-HCl pH 8.0, 12.5 mM DTT, 625 µg/ml of protein and 1 mg/ml of freshly prepared proteinase K. The reaction mixture was incubated for 60 minutes at 37 °C. Next, the reactions were stopped with PMSF (1 mM).

Purification of poly(ADP-ribose) polymerase (PARP). PARP was purified by the method of Zahradka and Ebisuzaki (1984).

Purification of PARG. Poly(ADP-ribose) glycohydrolase was partially purified from calf thymus by a 30-60% ammonium sulfate cut. Next, the precipitated material was passed through Sephadex G-25 and the protein eluate was applied to a DNA-cellulose column. Fractions containing PARG activity were pooled and used in this study as partially purified PARG.

Enzyme assays for PARP. A typical reaction mixture (50 µl) contain 100 mM Tris-HCl, pH 8.0, 10 mM DTT, 10 mM $MgCl_2$, 20 µM [^{32}P]NAD$^+$ [6 µCi/nmol], and either rat liver nuclei [1 mg/ml] or 75 nM PARP. The synthesis was carried out for 30 minutes at 37 °C with either rat liver nuclei or purified PARP for 10 minutes. The incorporation of [^{32}P]ADP-ribose was determined by Cerenkov counting of the 20% TCA precipitable material

Synthesis of poly(ADP-ribose). Poly(ADP-ribose) was synthesized in a 500 µl reaction mixture containing 100 mM Tris-HCl, pH 8.0, 10 mM DTT, 10 mM $MgCl_2$, 10 µM [^{32}P]NAD$^+$ [6 µCi/nmol], and either rat liver nuclei [1 mg/ml] of purified PARP (75 nM). The synthesis of the polymer was carried out at for 30 minutes with rat liver nuclei or 10 minutes with purified PARP at 37 °C. The reaction was stopped with an equal volume of ice-cold 40% trichloroacetic acid (TCA). Samples were placed on ice for 1 hr. Then, the protein-polymer conjugates were washed three times with ice-cold 20 % TCA. Pellet containing the reaction products was rinsed with diethyl-ether to remove residual TCA. Subsequently, poly(ADP-ribose) was released from protein acceptors by alkaline treatment with 0.2 N KOH/20 mM EDTA for 2 hours at 60 °C and the samples were neutralized to pH 7.0 with 0.2 N HCl.

Poly(ADP-ribose) purification. Poly(ADP-ribose) was purified by affinity chromatography on dihydroxyboronyl-Bio-Rex 70 (DHB-B) as described by Alvarez-Gonzalez, *et al.* (1983). Briefly, samples containing radiolabed poly(ADP-ribose) were dissolved in 250 mM ammonium formate, pH 9.0 containing 6 M guanidine-HCl (10 ml). The samples were loaded onto 1 ml of DHB-B previously equilibrated with 250 mM ammonium formate pH 9.0 at 4 °C. Then, the column was washed with 10 ml of ice-cold 250 mM ammonium formate, pH 9.0, and elution of bound material carried out with water at 40 °C. The eluate was lyophilized and used as protein-free poly(ADP-ribose).

Size exclusion chromatography of protein-free Poly(ADP-ribose). Molecular sieve chromatography of poly(ADP-ribose) was performed by HPLC using a Bio-Sil SEC-125 column (300 mm x 7.8 mm i.d.) as described by Alvarez-Gonzalez and Jacobson (1987). The elution buffer was 100 mM potassium phosphate, pH 6.8 at a flow rate of 1 ml/min. Fractions were collected every 0.5 minutes. The amount of radioactivity in each fraction was determined by Cerenkov counting.

High resolution polyacrylamide gel electrophoresis of protein-free ADP-ribose polymers. Poly(ADP-ribose) size distribution was analyzed on 20% polyacrylamide gels by electrophoresis as described Alvarez-Gonzalez and Jacobson (1987). In brief, gels were pre-electrophoresed for 30 minutes at 10 mA using 50 mM Tris/borate, pH 8.3 containing 1.0 mM EDTA as the running buffer. Electrophoresis was carried out for 4-6 hours at 15 mA, and it was stopped after the marker BPB migrated 6 cm from the origin. Finally, the gel was covered with a plastic wrap and exposed to X-ray film at -80 °C.

Enzyme assay for poly(ADP-ribose) glycohydrolase. Assays for nuclear associated PARG consisted of either a 25 or 50 µl reaction mixtures containing 100 mM Tris-HCl, pH 8.0, 10 mM DTT, 30 nM [^{32}P]poly(ADP-ribose) in monomeric ADP-ribose residues, and 0.5 µg/ml of rat liver nuclei. The reaction mixture was incubated at 37 °C for the indicated times. Assays were also carried out in the presence of 10 mM ADP-ribose. The reactions were stopped by the addition of electrophoresis loading buffer and placed on ice. Samples were run on 20% polyacrylamide gels as described above. The relative amount of ADP-ribose was quantified by scanning analysis using the IS-1000 version 2.00 digital image system from Alpha Innotech Corp (CA).

Poly(ADP-ribose) mobility shift assays. A total volume of either 25 or 50 µL containing 100 mM Tris-HCl, pH 8.0, 10 mM DTT, 30 nM [^{32}P]poly(ADP-ribose) and the indicated protein(s) were incubated at 37 °C for the specified times. Afterwards, the mixture was resolved on 20% polyacrylamide gels by electrophoresis. The interaction of poly(ADP-ribose) with protein(s) was determined by the formation of a macromolecular complex at the origin. Finally, the analysis of the products generated (new radiolabeled bands formed after incubation) was carried out by densytometry as described above.

HPLC identification of the products generated by either PARG or phosphodiesterase activity digestion of [^{32}P]poly(ADP-ribose). Pure [^{32}P]Poly(ADP-ribose) was incubated with either PARG or phosphodiesterase. Incubation with PARG (6 µg/ml) was carried out for 60 minutes at 37 °C in a 50 µl reaction volume containing 10 mM Tris-HCl, pH 8.0, 10 mM DTT, and 30 nM [^{32}P]poly(ADP-ribose). [^{32}P]poly(ADP-ribose) (30 nM) was also treated for 120 minutes at 37 °C with phosphodiesterase (2 U) in a 50 µl mixture composed of 50 mM KH_2PO_4, and 10 mM $MgCl_2$. The hydrolytic products of either reaction were analyzed by HPLC on a Partisil 10-SAX column (250 mm x 4.6 mm i.d.) preceded by a guard column (50 mm X 1.5 mm i.d.) pre-equilibrated with 125 mM KH_2PO_4 , pH 4.7. The chromatographic run was started with 15 minutes of 100% 125 mM KH_2PO_4 , pH 4.7; then, a linear gradient was initiated. The gradient was run for 5 minutes ending with 100% 125 mM KH_2PO_4, pH 4.7 containing 0.5 KCl. The latter buffer was maintened for 25 minutes. Finally, inital HPLC conditions were re-established in two minutes for analysis of the next sample.

Determination of ADP-ribose chain lengths. Average size of ADP-ribose polymers was carried out by treating ADP-ribose polymers with 0.1 N KOH and 10 mM $MgCl_2$ for 2 hours at 37 °C. The pH of the mixture was brought to pH 7.0 with 0.1 N HCl. Following neutralization, the mixture was incubated with 3 U of snake venom phosphodiesterase in a solution of 100 µl containing 50 mM K_2HPO_4, pH 7.5, and 10 mM $MgCl_2$ (Alvarez-Gonzalez and Jacobson, 1987). The enzymatic reaction was carried out for 2 hours at 37 °C and was quenched by the addition of 300 µl of 50 mM KH_2PO_4, pH 4.7. The nucleotides obtained following hydrolysis were separated by HPLC on a partisil 10-SAX column (250 mm x 4.6 mm i.d.) preceded by a guard column containing the same material (50 mm x 1.5 mm i.d.) under isocratic conditions. The flow rate was 1 ml/min with buffer 125 mM KH_2PO_4 containing 0.5 M KCl. Fractions were collected every 0.5 minutes. The total amount of radiolabeled AMP, PRAMP and PR_2AMP were determined by scintillation counting and the average polymer size was calculated according to the formula $[AMP] + [PRAMP] + [PR_2AMP]/[AMP] - [PR_2AMP]$ (Miwa and Sugimura, 1982).

CHAPTER III

RESULTS

Poly(ADP-ribose) polymerase poly(ADP-ribosyl)ates DNA binding proteins. Acceptor proteins are components of specific subnuclear domains including chromatin, nuclear matrix and nuclear envelope. The reversibility of this process is insured by the action of poly(ADP-ribose) glycohydrolase. The polyanionic nature of poly(ADP-ribose) strongly suggests that non-covalent interactions of this polymer with cationic proteins are physiologically significant. In this dissertation, the identification of PARG activity in different subnuclear domains has been established. The role of non-covalent interactions in poly(ADP-ribose) catabolism has also been evaluated. In order to achieve this, an assay that simultaneously monitors PARG activity and non-covalent interactions of ADP-ribose polymers with cationic proteins was first developed. Secondly, nuclei were dissected out into chromatin, nuclear matrix and nuclear envelope, and the activity of PARG was determined in each of these domains. The experimental design of this research project is outlined in figure 8.

As a first step in this project, nuclei were characterized by electron microscopy and the protein composition of this organelle was determined by SDS-PAGE. Afterwards, the activities of PARP and PARG were determined as indicated in materials

Fig. 8. Diagram of the experimental approach used to study the subnuclear distribution of PARG and the role of non-covalent interactions between poly(ADP-ribose) and proteins in enzyme activity. **1.** This step involves the enzymatic synthesis and purification of $(\text{ADP-ribose})_{2\text{-}70}$, the substrate for PARG. **2.** Partial purification of PARG. **3.** Assay for PARG activity with the simultaneous observation of non-covalent interactions between poly(ADP-ribose) and nuclear proteins. **4.** Nuclei were isolated and characterized by electron microscopy and SDS-PAGE. **5.** Isolated nuclei were fractionated into chromatin, nuclear matrix and nuclear envelope. **6.** Identification of PARG activity in these fractions. **7.** Study of the roles played by non-covalent interactions of poly(ADP-ribose) with nuclear proteins in the activity of PARG.

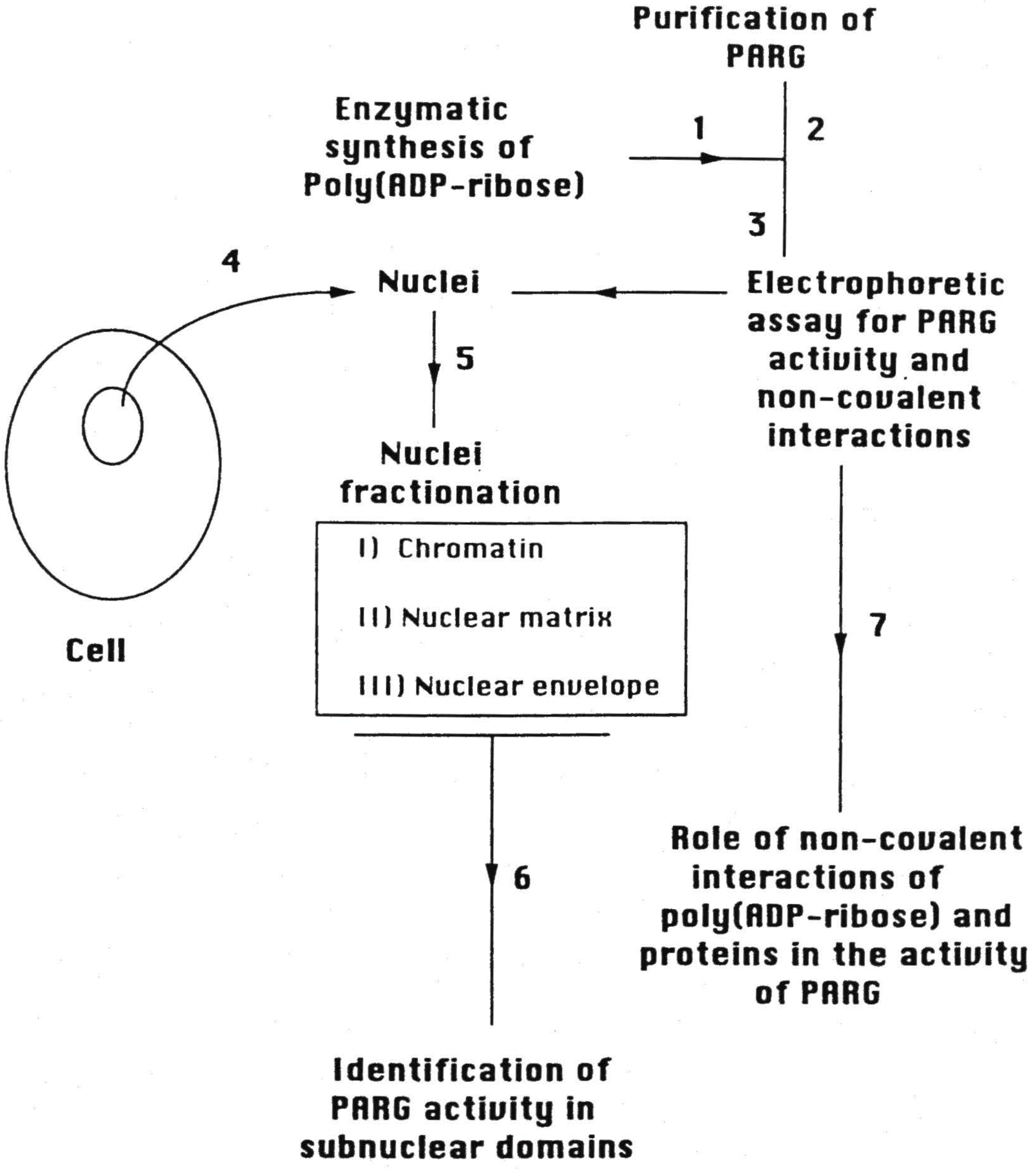
Purification of PARG
Enzymatic synthesis of Poly(ADP-ribose)
1
2
3
4
Nuclei
Electrophoretic assay for PARG activity and non-covalent interactions
5
Cell
Nuclei fractionation
I) Chromatin
II) Nuclear matrix
III) Nuclear envelope
7
6
Role of non-covalent interactions of poly(ADP-ribose) and proteins in the activity of PARG
Identification of PARG activity in subnuclear domains

and methods.

Characterization of isolated nuclei. Isolated rat liver nuclei were 90% intact as estimated by electron microscopy. In these preparations, the nuclear membranes, the nucleolus and disperse chromatin were easily visualized (Fig. 9). Analysis of the extract by SDS-PAGE confirmed the presence of histone H1 and core histones, as the most abundant proteins (see Fig(s). 19, 38 and39). The extract also showed the characteristic profile of non-histone proteins.

Association of PARP with chromatin. As expected, PARP was present in the cell nucleus. This was determined by incubations of disrupted nuclei with [^{32}P]NAD$^+$ that resulted in the incorporation of ADP-ribose into protein bound poly(ADP-ribose). The polymeric nature of the product was confirmed by electrophoretic analysis of the ADP-ribose chains synthesized following chemical release from proteins with alkali. The incorporation of ADP-ribose into polymeric form was both time- (Fig. 10) and substrate-concentration dependent. The peak of ADP-ribose incorporation was obtained at 20 minutes of incubation. Afterwards, the amount of ADP-ribose accumulated decreased beyond 20 min of incubation. These observations suggest that the total amount of poly(ADP-ribose) synthesized may be affected by the presence of PARG.

Development of enzyme assay to measure poly(ADP-ribose) glycohydrolase activity As a first step towards the determination of PARG activity, ADP-ribose polymers of 2-70 residues in size were synthesized. Three different sources of PARP were utilized for this purpose. Enzyme preparations included crude rat liver chromatin, calf thymus PARP and human PARP. ADP-ribose polymers synthesized with each preparation were characterized as shown on table 3. The ADP-ribose chains obtained with these preparations of PARP and 10 μM NAD$^+$ varied in size between 2-70 residues.

Fig. 9. Electron micrograph of rat liver nuclei. Isolated nuclei were prepared for electron microscopy as described in materials and methods. C, chromatin; NE, nuclear envelope; NU, nucleolus; Bar 1.92 µm.

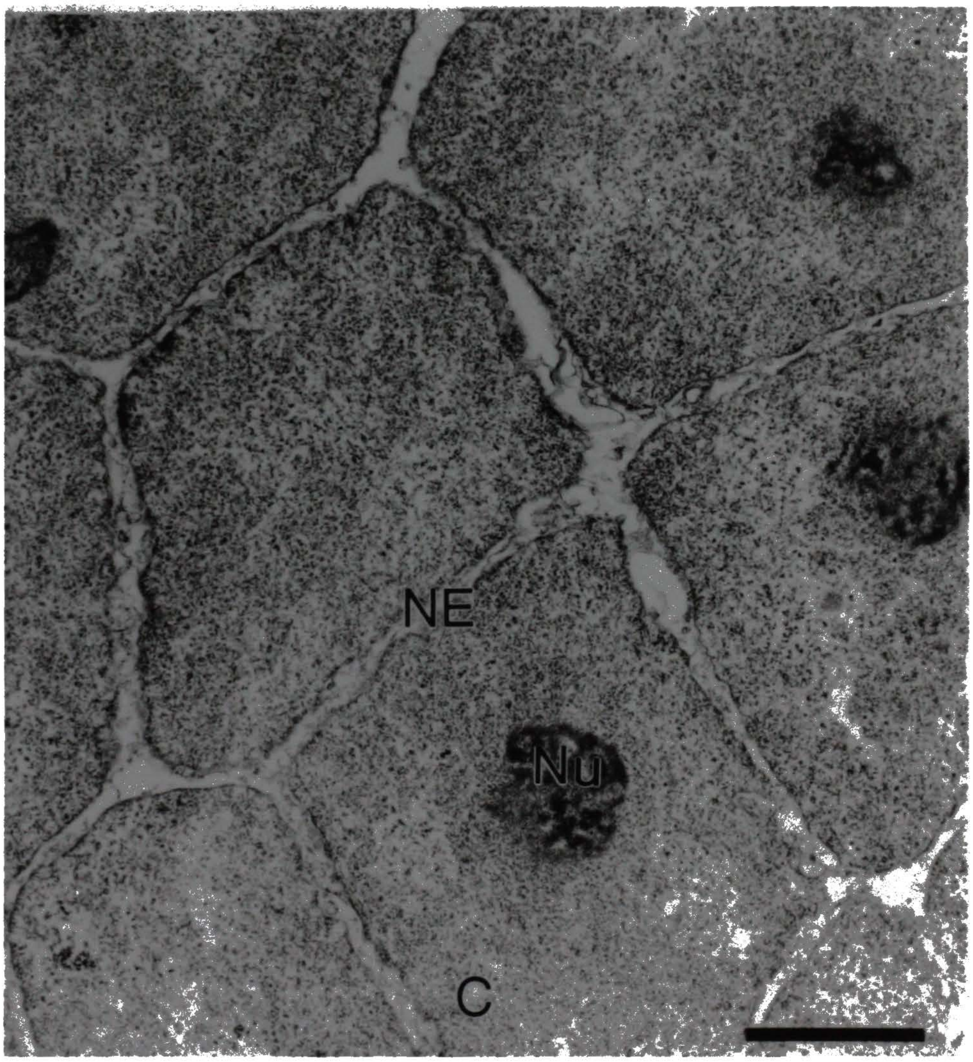
NE
Nu
C

Fig. 10. Kinetics of Poly(ADP-ribose) synthesis with a rat liver nuclear extract at 20 μM NAD^+. The enzyme activity is measured as fmoles of ADP-ribose incorporated/μg of protein at 37 °C. The assay was carried out as described in materials and methods. A 50 μl reaction mixture contained 100 mM Tris-HCl, pH 8.0, 10 mM DTT, 10 mM $MgCl_2$ and 20 μM NAD^+ and 1 mg of protein/ml.

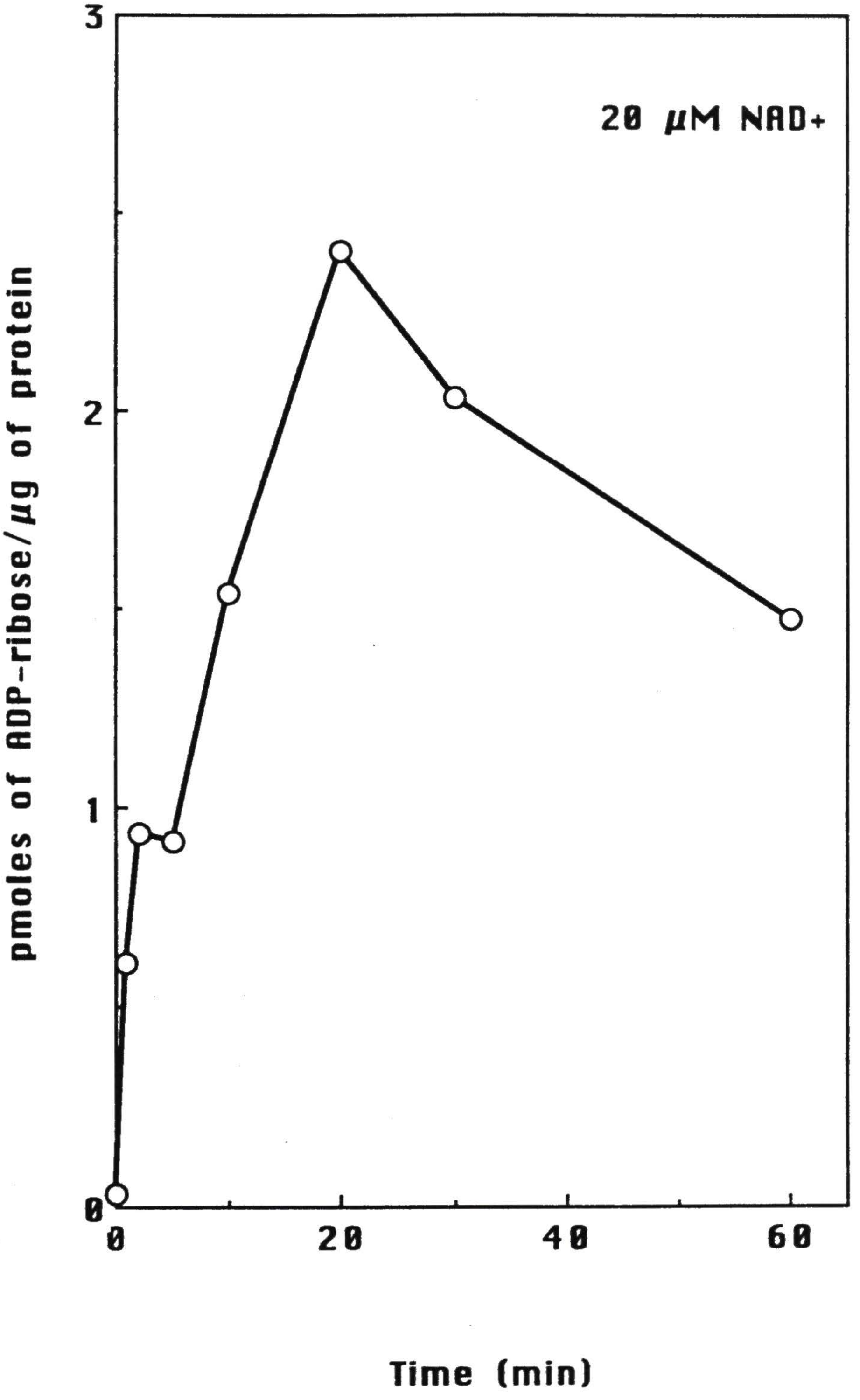
20 μM NAD+
pmoles of ADP-ribose/μg of protein
0
1
2
3
0
20
40
60
Time (min)

Despite the similarity of products generated with these enzyme preparations, purified PARP at 75 nM resulted in the most reproducible method to generate high yields of ADP-ribose polymers.

Figure 11 shows that the purified poly(ADP-ribose) did not contain monomeric ADP-ribose. This is an important point since monomeric ADP-ribose is the breakdown product of poly(ADP-ribose) as the result of PARG action. Purified ADP-ribose polymers of 2-70 residues in size were utilized as substrate to monitor PARG activity. The conditions of poly(ADP-ribose) synthesis permitted us to obtain preparations with low amounts of highly branched ADP-ribose chains as well.

Enzyme assay for PARG activity. The activity of PARG associated with rat liver nuclei was both time- and protein concentration-dependent . The enzyme activity was measured by following the formation of monomeric ADP-ribose in incubations of protein-free poly(ADP-ribose) with rat liver nuclei (Fig. 12, lanes 3-7). As expected, the enzyme product co-migrated with HPLC-pure monomeric ADP-ribose (Fig. 12, compare lanes 3-7 with 9). Interestingly, ADP-ribose chains of 20 residues or more were degraded first. This suggested that PARG possesses higher affinity for longer polymers of ADP-ribose. The AMP observed (Fig. 12, lanes 3-7) was generated from the hydrolysis of the phosphoanhydride bond of ADP-ribose in mild alkali. It is also important to note that the main degradation product of phosphodiesterase activity on poly(ADP-ribose), phosphoribosyl adenosine 5'-monophosphate (PRAMP), was not observed (Fig. 12, compare lanes 3-7 with lane 8). Therefore, this assay is not affected by contaminating phosphodiesterase(s).

Formation of monomeric ADP-ribose was also dependent on the total amount of nuclear protein (Fig. 13). In a similar type of assay, it was also observed that the degradation of poly(ADP-ribose) was linear up to 40% (Fig. 14). Nuclear-associated

Table 3. Percent yield and chain lengths of the poly(ADP-ribose) synthesized with different enzyme sources.

Enzyme Source	% of [^{32}P] NAD$^+$ incorporated	Chain length(s) (ADP-ribose)n
Human PARP	12.2	2-70
Calf thymus PARP	13.9	2-70 (variable)
Rat Liver Chromatin	4.6	2-70 (variable)

Fig. 11. Size distribution of ADP-ribose polymers before and after affinity chromatography on a boronate resin. Equal Cerenkov counts (5,000) of [^{32}P]poly(ADP-ribose) were applied on each lane. Lane 1 shows the distribution of ADP-ribose chains following alkaline release (0.2 N KOH/20 mM EDTA) from protein. Lane 2 shows the ADP-ribose chains following affinity chromatography. O, origin; XC, xylene cyanol (ADP-ribose)$_{20}$; BPB, bromophenol blue (ADP-ribose)$_8$.

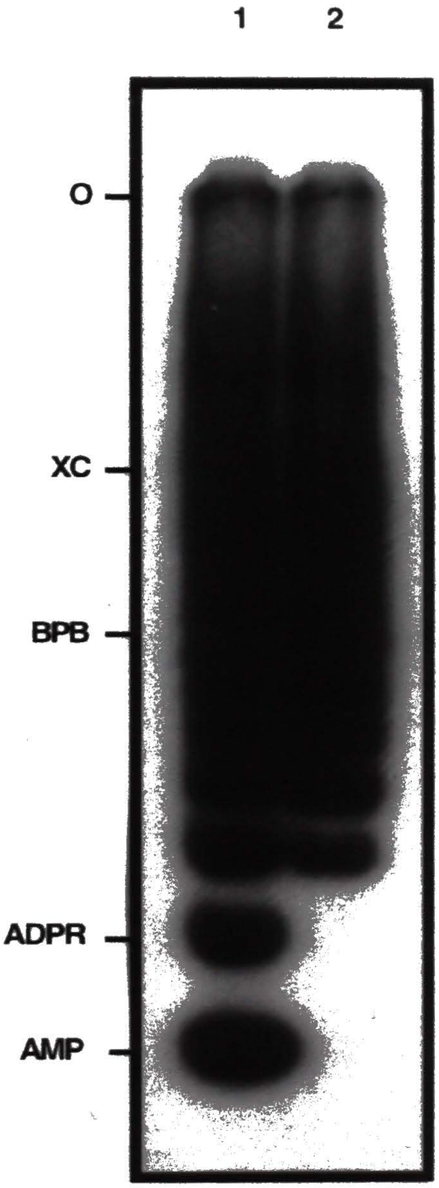
1
2
O
XC
BPB
ADPR
AMP

Fig. 12. Kinetics of PARG activity associated with rat liver nuclei. Autoradiography of the degradation products obtained following incubation of protein-free [^{32}P]poly(ADP-ribose) with rat liver nuclei. A 50 µl reaction mixture contained 69.5 nM [^{32}P]poly(ADP-ribose) and 500 µg of nuclear protein/ml and was incubated at 37 °C for the indicated times. Other components of this reaction are indicated in the materials and methods section. Lane 1, substrate control, size distribution of [^{32}P]poly(ADP-ribose) molecules. Lane 2, minus enzyme control, [^{32}P]poly(ADP-ribose) incubated 180 minutes in the absence of nuclei. Lanes 3-7 show degradation intermediates and products generated after 15, 30, 60, 120, and 180 minutes of incubation, respectively. Lane 8, [^{32}P]PRAMP; lane 9, [^{32}P]ADP-ribose; lane 10, [^{32}P]NAD$^+$.

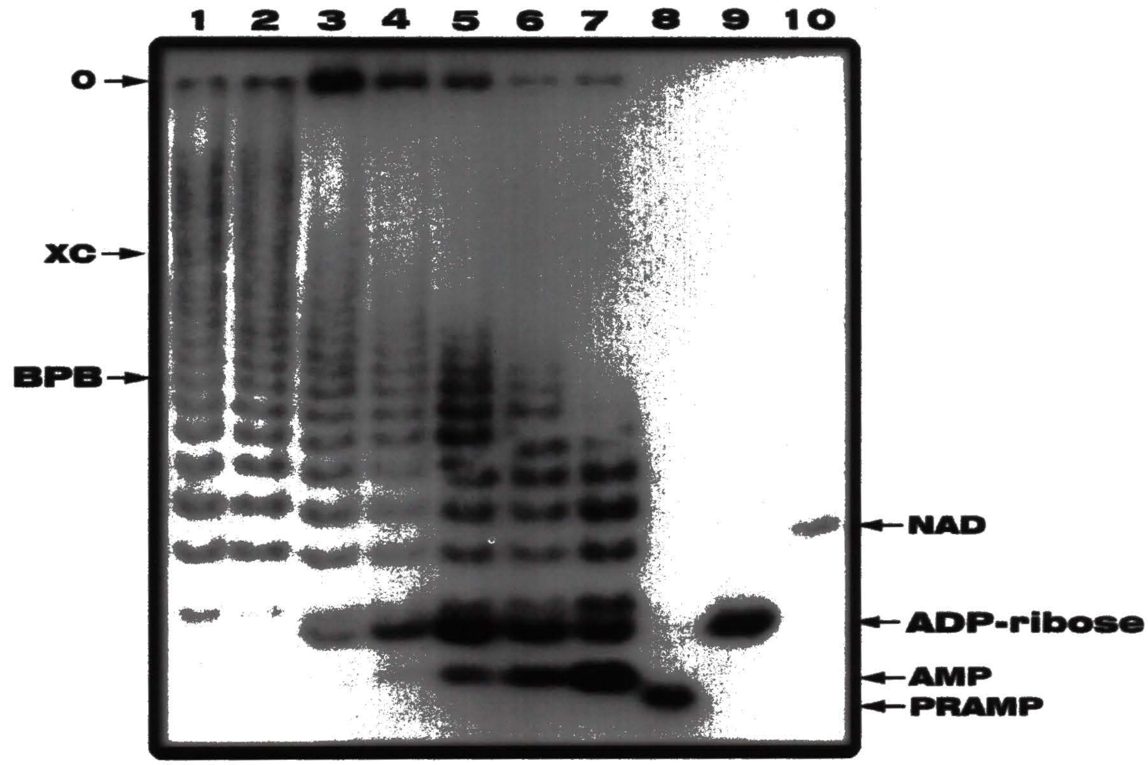
1
2
3
4
5
6
7
8
9
10
O
XC
BPB
NAD
ADP-ribose
AMP
PRAMP

Fig. 13. Poly(ADP-ribose) glycohydrolase activity is protein concentration-dependent. Increasing amounts of rat liver nuclear protein were incubated with 69.5 nM [^{32}P]poly(ADP-ribose) for 10 minutes at 37 °C. The percent of monomeric ADP-ribose generated was calculated by densitometric analysis.

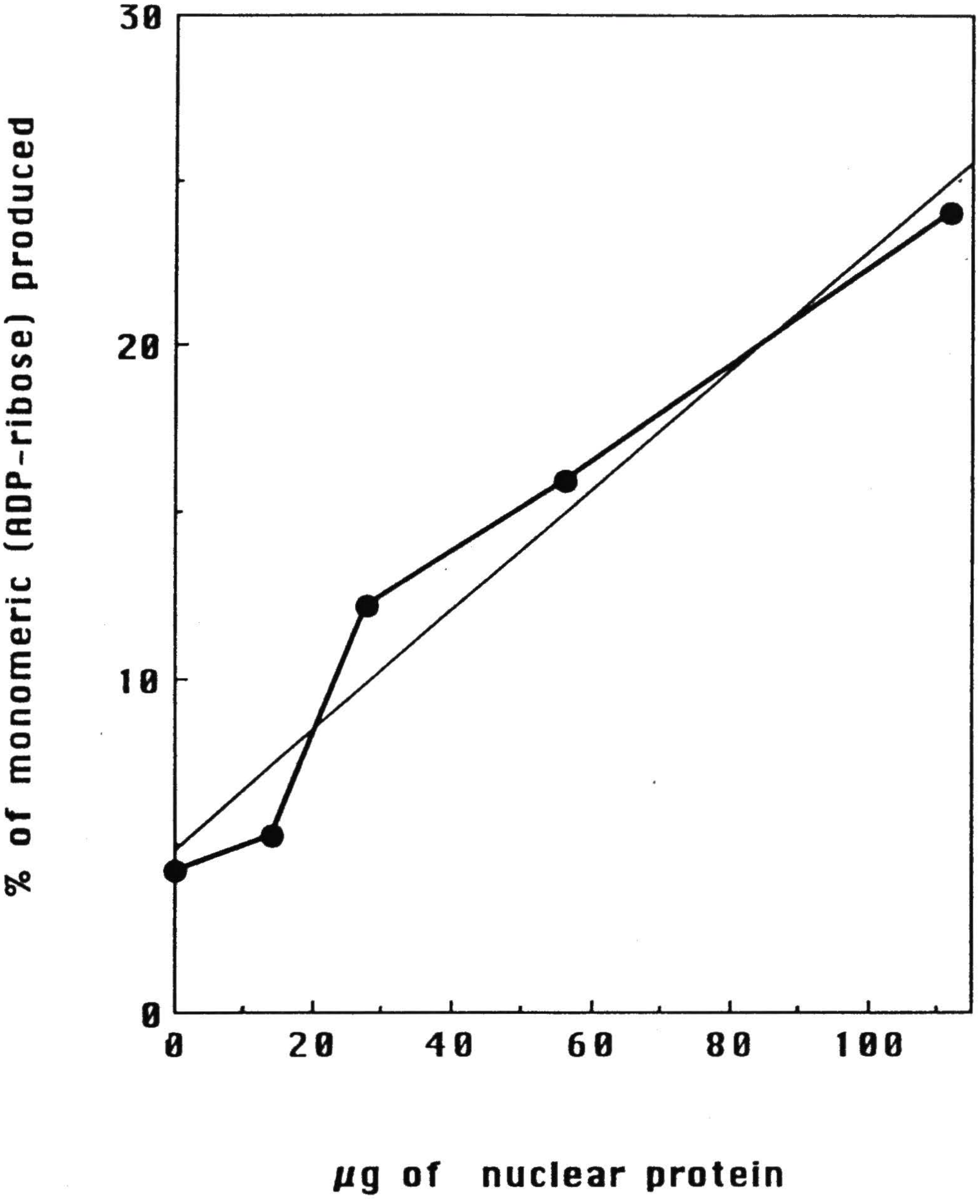
30
20
10
0
0
20
40
60
80
100
% of monomeric (ADP-ribose) produced
μg of nuclear protein

Fig. 14. Graphical representation of the kinetics of monomeric ADP-ribose formation with a crude extract of PARG activity. The percent of enzyme product formed were determined by spot densitometry of Figure 12.

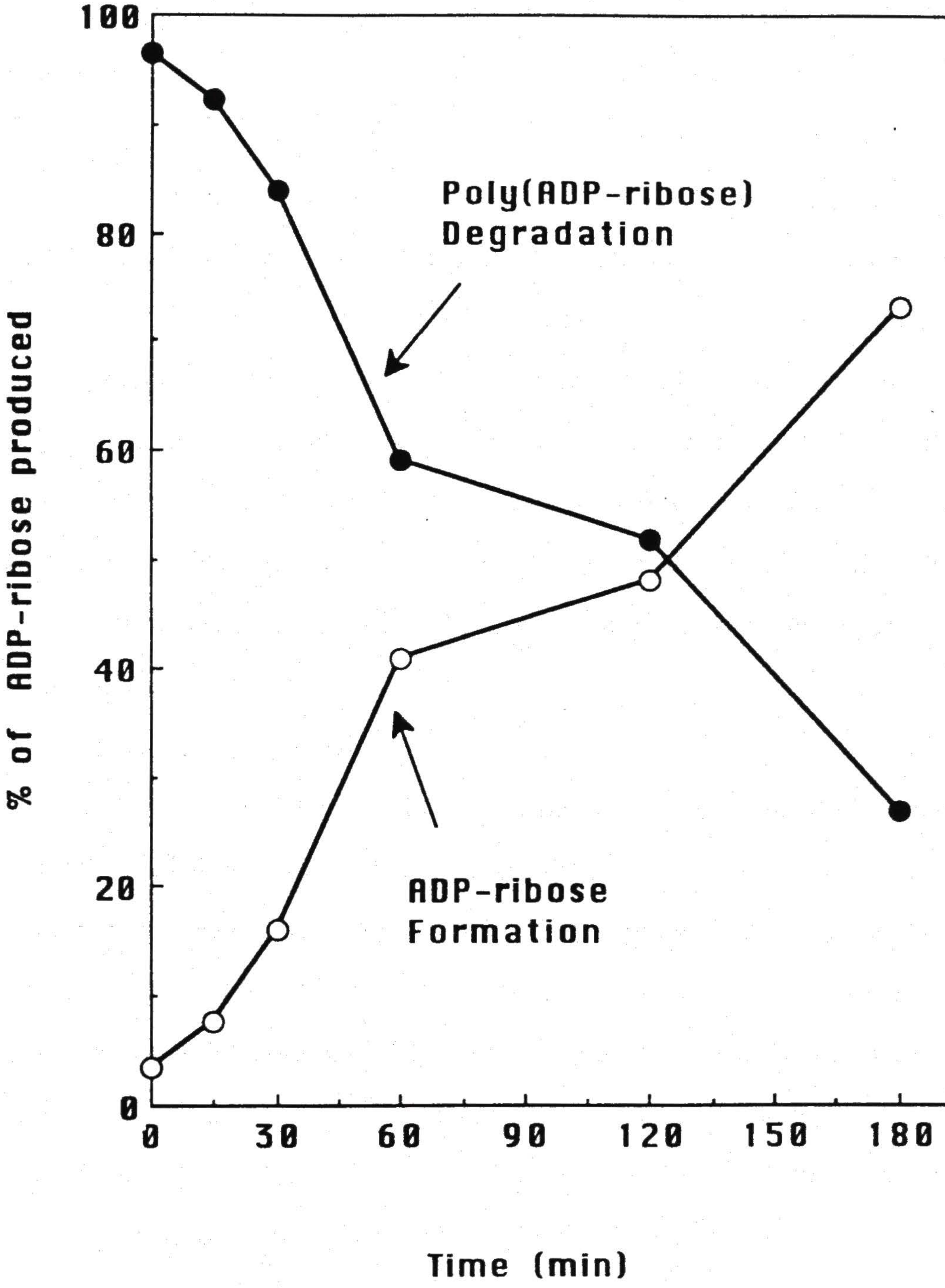
100
80
60
40
20
0
0
30
60
90
120
150
180
% of ADP-ribose produced
Time (min)
Poly(ADP-ribose)
Degradation
ADP-ribose
Formation

PARG generated free ADP-ribose biphasically (Fig. 15). The biphasic mode of poly(ADP-ribose) hydrolysis has been interpreted as the affinity of PARG for ADP-ribose chains larger than 20 residues in size (Hatakeyama, *et al.*, 1986). In our assays, PARG was quantitatively inhibited with 10 mM ADP-ribose (see below). These observations are in agreement with activity of purified PARG.

We next proceeded to establish the same enzyme assay with partially purified PARG. PARG was partially purified from calf thymus as indicated in materials and methods. This enzyme preparation also hydrolyzed poly(ADP-ribose) in a biphasic mode, and the activity was quantitatively inhibited with 10 mM ADP-ribose. The degradation product(s) generated in this assay were identified by SAX-HPLC (Fig. 16). Under these chromatographic conditions, the first peak observed was AMP and the second nucleotide eluted with ADP-ribose and showed a retention time of 9 minutes. The identity of the main peak as ADP-ribose was confirmed by running a sample spiked with authentic ADP-ribose.

PARG is present mainly in the cell nucleus; however, the distribution of PARG in different nuclear domains is unknown. Interestingly, it should be mentioned that this enzyme is resistant to extractions with high ionic strength buffers (Uchida *et al.*, 1993b). Thus, a fraction of PARG activity is not associated with chromatin. On the other hand, most protein targets for poly(ADP-ribosyl)ation include polypeptides associated with chromatin, the nuclear matrix, and the nuclear envelope. As a result, one could speculate that enzyme cycles of poly(ADP-ribosyl)ation occur in each of these domains. Therefore, We proceeded to evaluate the possibility that PARG activity is associated with the nuclear matrix and the nuclear envelope.

Fig 15. PARG degrades free poly(ADP-ribose) biphasically. Each data point corresponds to the ADP-ribose determined by densitometric analysis of figure 12.

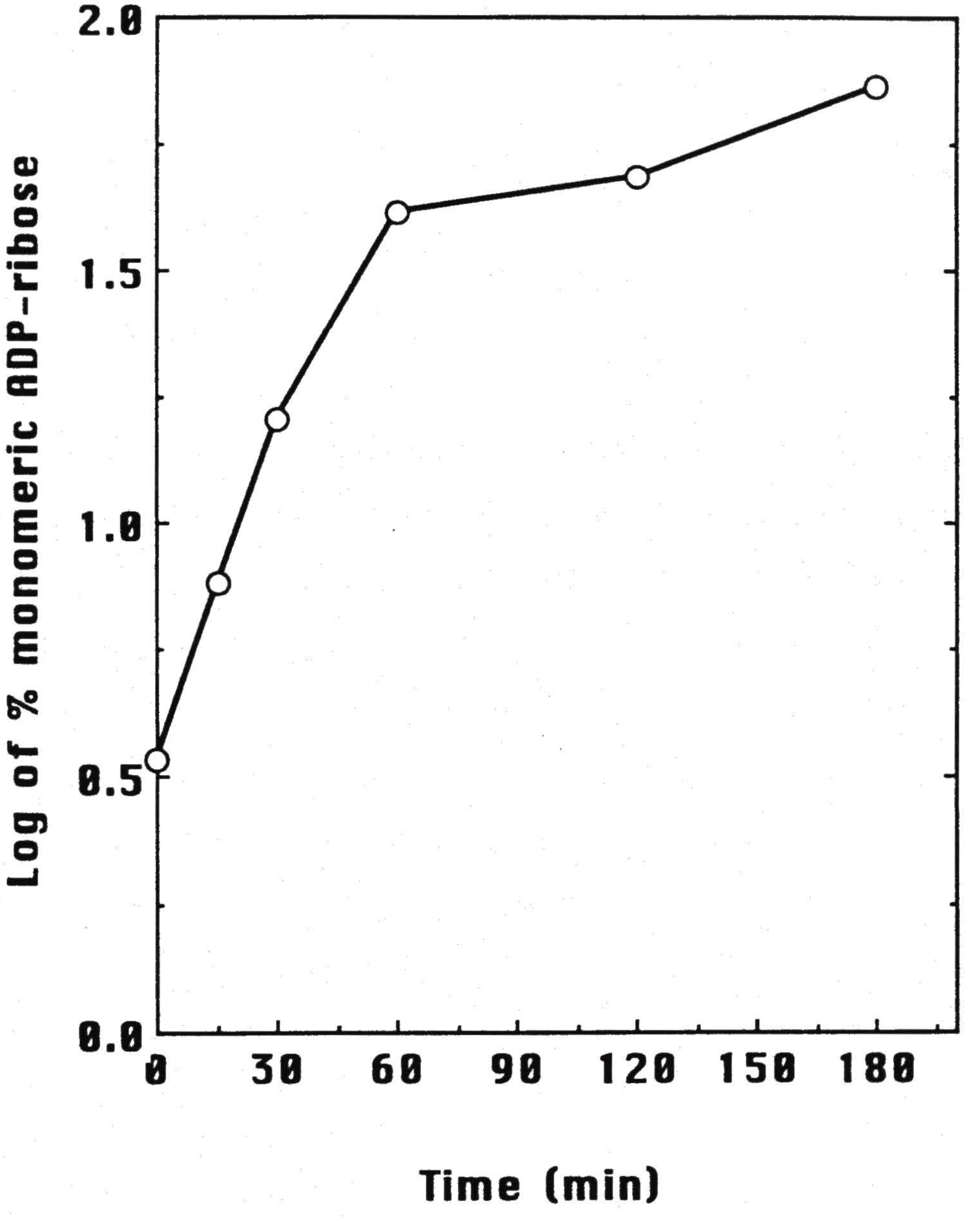
2.0
1.5
1.0
0.5
0.0
0
30
60
90
120
150
180
Log of % monomeric ADP-ribose
Time (min)

Fig. 16. Chromatographic identification of ADP-ribose as the main product generated by partially purified PARG. HPLC separation was carried out as described in materials and methods. The retention times for AMP and ADP-ribose are indicated with arrows.

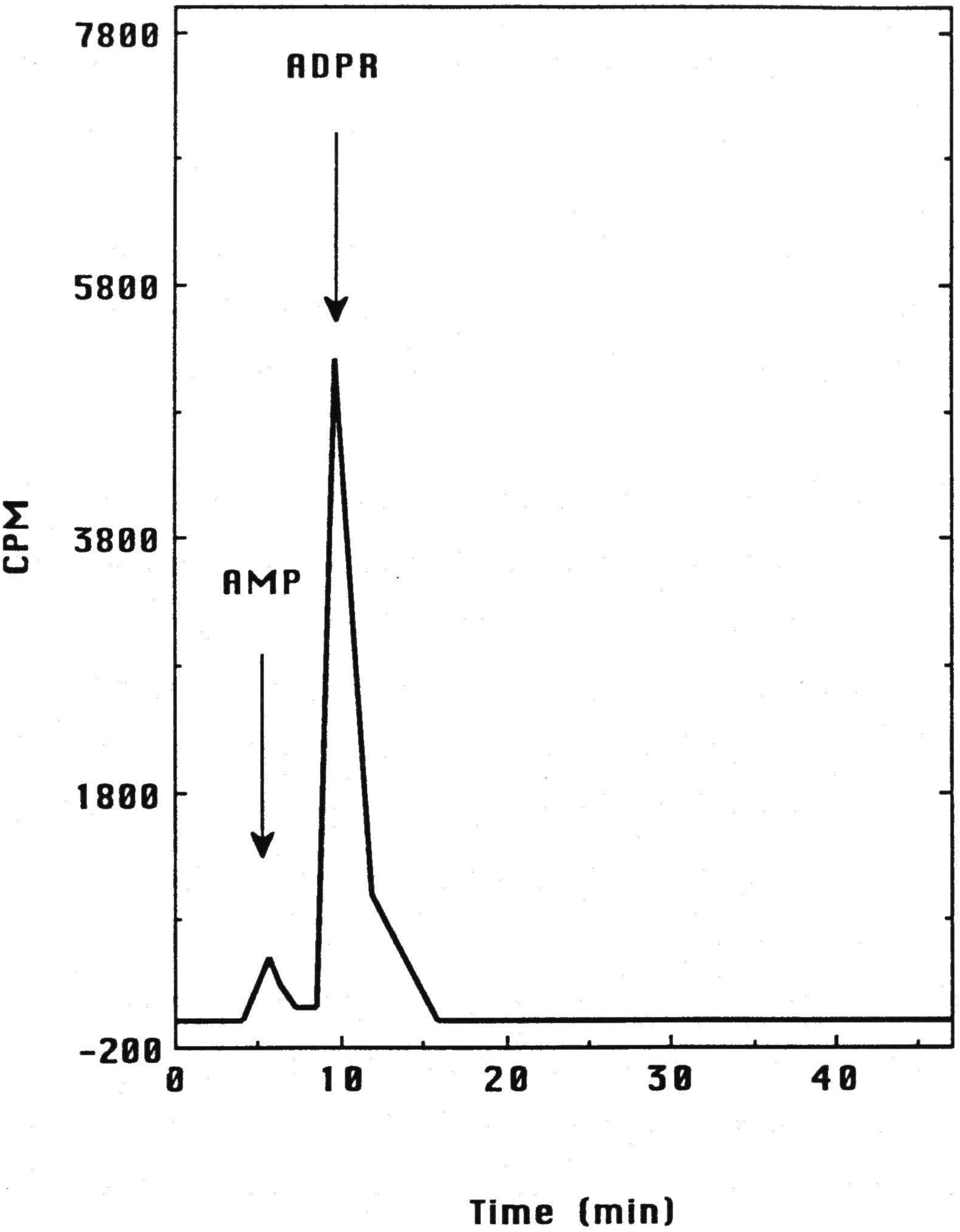
7800
5800
3800
1800
-200
ADPR
AMP
CPM
0
10
20
30
40
Time (min)

Subnuclear distribution of poly(ADP-ribose) glycohydrolase. The experimental approach followed to identify PARG in subnuclear domains is shown on figure 17. Isolated rat liver nuclei were fractionated into chromatin, nuclear matrix and nuclear envelope. Next, each domain was biochemically characterized by SDS-PAGE and electron microscopy.

Nuclear fractionation into distinc functional domains. The experimental protocol to obtain subnuclear fractions is outlined on figure 18. The procedure shown facilitated the isolation of chromatin, nuclear matrix and nuclear envelope (Berezney, 1984).

Protein composition of each subnuclear domain. Isolated nuclei contains both histone and non-histone proteins (Fig. 19A, lane 2 and 19B, lane 2). Figure 19A, lane 3 shows that the nuclease-digest (soluble fraction) included mostly non-histone proteins. By contrast, the nuclease-digested nuclei had a similar protein profile as the intact nuclei. Chromatin proteins were extracted with low and high ionic strength buffers. The Coomassie blue-stained profile of proteins showed that histones were present in the fractions containing chromatin (see Fig. 19A lane 5 and Fig. 19B lane 3). By contrast, the fraction that corresponds to nuclear matrix II (nuclear matrix/nuclear envelope) (Fig. 19B lane 4) did not contain histone proteins. This confirmed that chromatin was extracted with this treatment. Afterwards, the nuclear envelope was separated from the nuclear matrix with a 1% Triton X-100 wash. The nuclear envelope contained several proteins of high molecular weight that included the lamins (Fig. 19B, lane 5). As shown on Fig. 19B, lane 7, high molecular weight proteins were the main components of nuclear matrix III. In summary, all subnuclear domains analyzed for protein composition contained the components previously reported by Berezney, *et al.*, (1995).

Fig. 17. Experimental design used to identify PARG activiy in functional subdomains of the nucleus. **1,** isolation of nuclei from rat liver; **2,** Identification of PARG in the cell nucleus; **3,** fractionation of nuclei into chromatin, nuclear matrix and nuclear envelope; **4,** biochemical and structural studies of each functional domain; **6,** measurement of PARG activity in each domain.

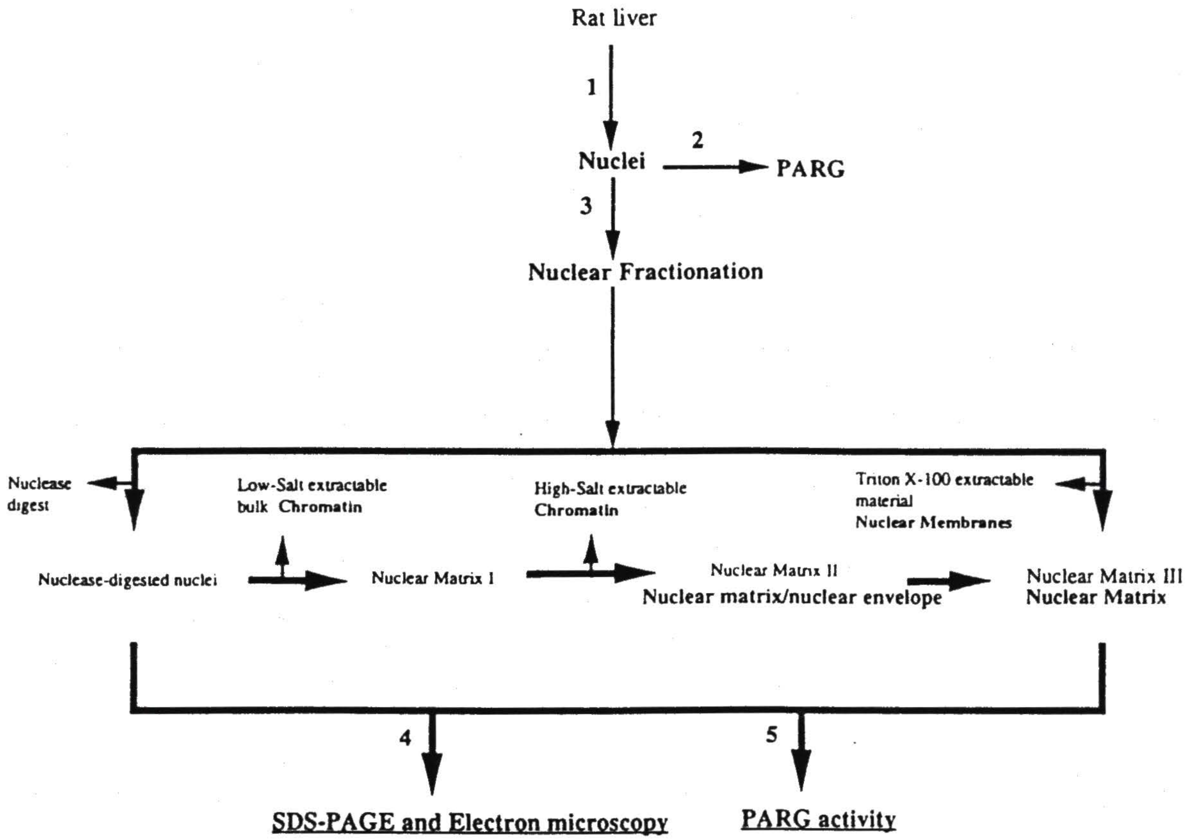
Rat liver
1
Nuclei
2
PARG
3
Nuclear Fractionation
Nuclease digest
Low-Salt extractable bulk Chromatin
High-Salt extractable Chromatin
Triton X-100 extractable material Nuclear Membranes
Nuclease-digested nuclei
Nuclear Matrix I
Nuclear Matrix II
Nuclear matrix/nuclear envelope
Nuclear Matrix III
Nuclear Matrix
4
5
SDS-PAGE and Electron microscopy
PARG activity

Fig. 18. Experimental protocol for the isolation of nuclear functional domains. The isolation of chromatin, nuclear matrix, and nuclear envelope was carried out as described by Berezney and Coffey (1975). The method is described in detail in the section of materials and methods.

Scheme for Preparation of Nuclear Domains

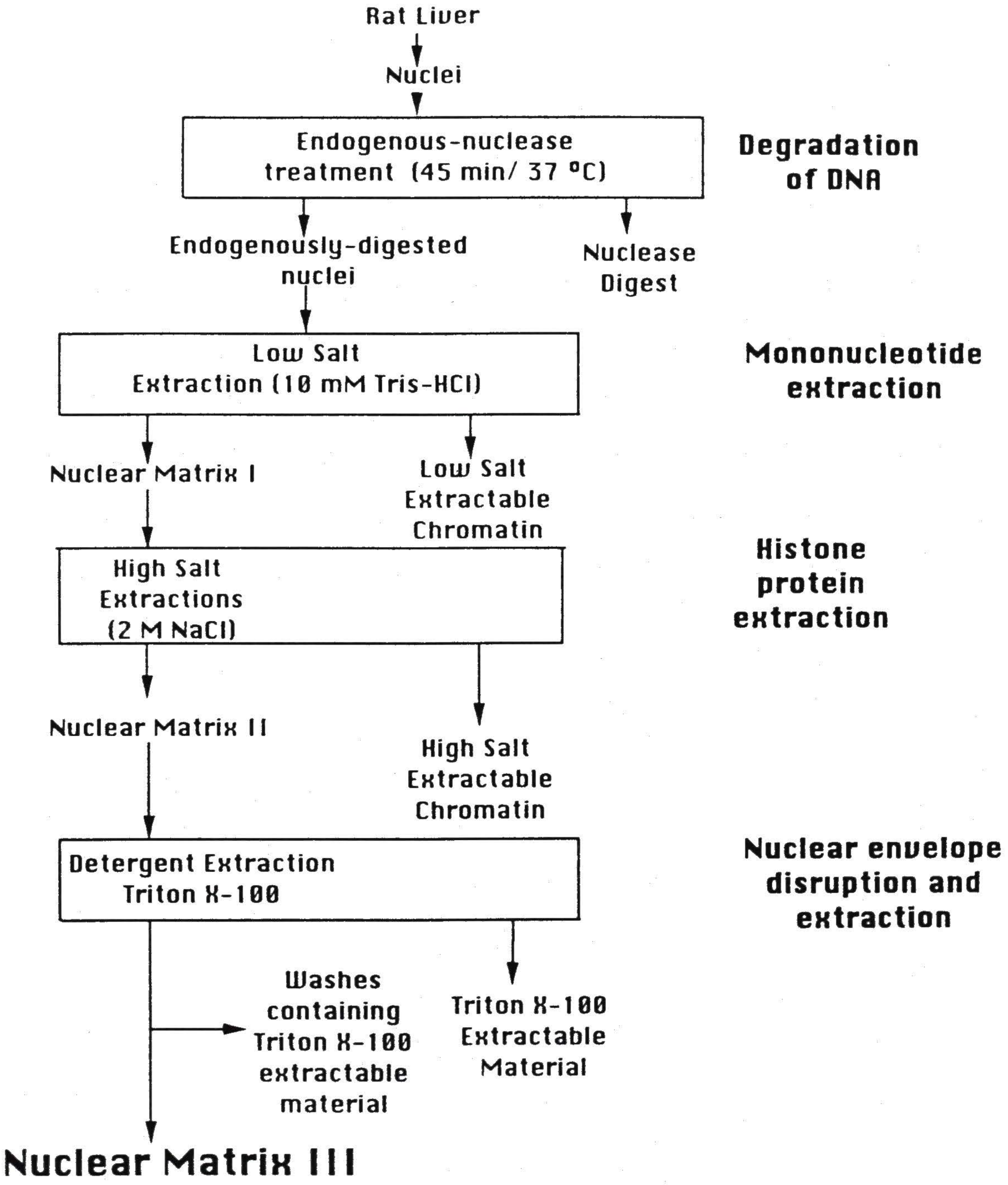
Rat Liver
Nuclei
Endogenous-nuclease treatment (45 min/ 37 °C)
Degradation of DNA
Endogenously-digested nuclei
Nuclease Digest
Low Salt Extraction (10 mM Tris-HCl)
Mononucleotide extraction
Nuclear Matrix I
Low Salt Extractable Chromatin
High Salt Extractions (2 M NaCl)
Histone protein extraction
Nuclear Matrix II
High Salt Extractable Chromatin
Detergent Extraction Triton X-100
Nuclear envelope disruption and extraction
Washes containing Triton X-100 extractable material
Triton X-100 Extractable Material
Nuclear Matrix III

Fig. 19. Protein composition of nuclei, nuclear matrix and nuclear envelope (Triton X-100 extract) as determined by the Coomassie blue staining following SDS-PAGE. Electrophoresis was carried out as described under "materials and methods". Lane 1 (M) of panels A and B correspond to pre-stained molecular weight markers (BIO-RAD). The apparent molecular weight of these standards is shown to the left of each panel. The sample applied to each lane is indicated above each lane. Equal amount of protein (9 μg) was applied per lane.

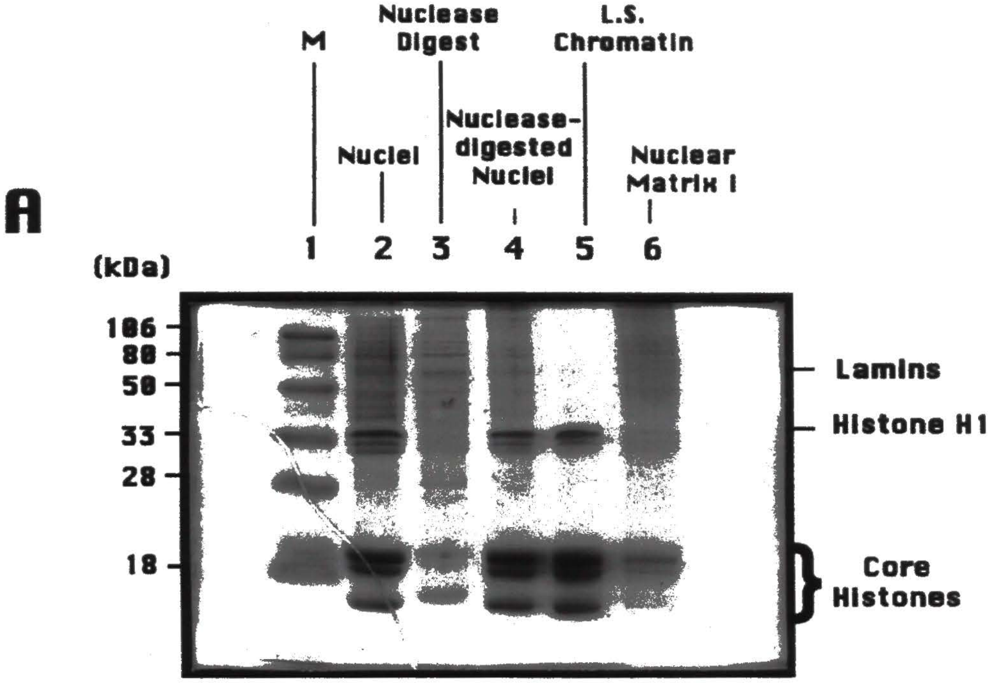
A
M
Nuclease Digest
L.S. Chromatin
Nuclei
Nuclease-digested Nuclei
Nuclear Matrix I
1
2
3
4
5
6
(kDa)
106
80
50
33
28
18
Lamins
Histone H1
Core Histones

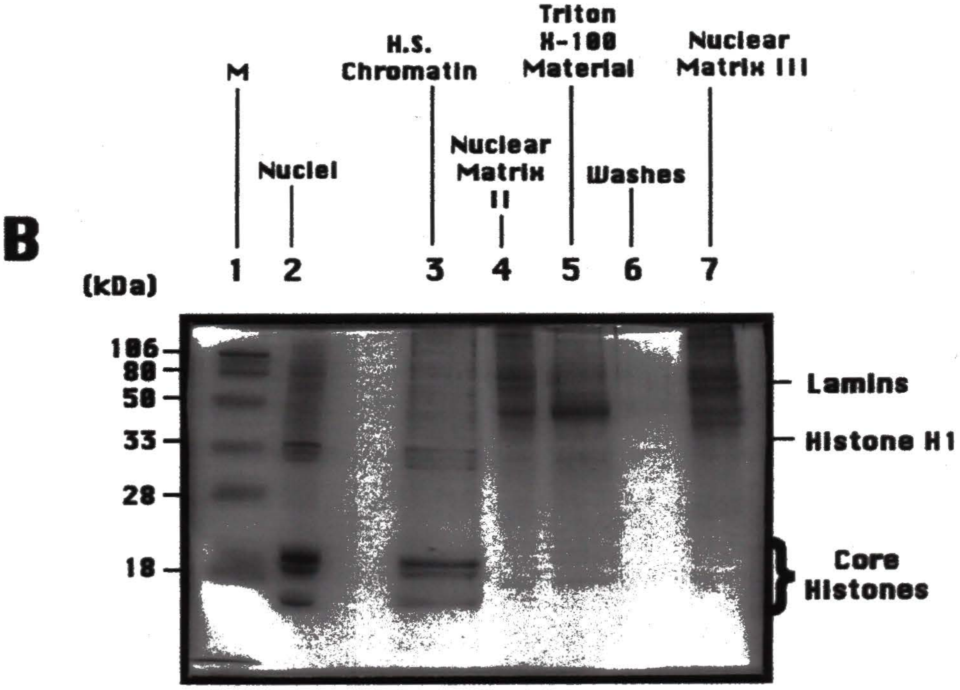
B
M
H.S. Chromatin
Triton X-100 Material
Nuclear Matrix III
Nuclei
Nuclear Matrix II
Washes
1
2
3
4
5
6
7
(kDa)
106
80
50
33
28
18
Lamins
Histone H1
Core Histones

Electron microscopy of each subnuclear domain. To further demonstrate the identity of each subnuclear domain, electron micrographic analysis was carried out. Figure 20 panels A, B, C, and D show the electron micrographs of the cell nucleus, nuclease-digested nuclei, nuclear matrix II and nuclear matrix III, respectively. Fig. 20, panel A clearly shows the nuclear envelope, disperse chromatin and nucleolus in isolated nuclei. These structures were also present in the endogenously digested nuclear preparation (Fig. 20 panel B). By contrast, nuclear matrix II was characterized for the nuclear envelope and a fibrogranular protein network or nuclear matrix (Fig. 20 panel C). As it has been described elsewhere (Aaronson and Blobel, 1974). Triton X-100 allowed for the separation of the nuclear envelope from the nuclear matrix. Fig. 20, panel D shows the microscopic structure of nuclear matrix III.

Identification of PARG activity in different subnuclear domains. PARG activity was detected in chromatin, nuclear envelope and nuclear matrix. This was demonstrated by the identification of monomeric ADP-ribose following incubations of each subnuclear fractions with protein-free $[^{32}P](ADP\text{-ribose})_{2\text{-}70}$. The results observed in this experiment are shown on Fig. 21. The strongest signal of PARG activity observed was associated with the nuclease digest which showed a specific enzyme activity of 9.0 nmoles of monomeric ADP-ribose/mg of protein (Fig. 22, lane 3). PARG activity was also detected in the nuclear matrix II (nuclear matrix/nuclear envelope) preparation (Fig. 21, lane 8). Interestingly, the Triton X-100 extractable material (nuclear envelope) contained a significant amount of PARG activity (Fig. 21, lane 9). Finally, enzyme activity was also observed in incubations with pure nuclear matrix (Fig. 21, lane 11).

Fig. 20. Electron micrographs of intact rat liver nuclei (panel A), nuclease digested nuclei (panel B), nuclear matrix II (with nuclear envelope) (panel C) and nuclear matrix III (without nuclear envelope) (panel D). Nuclei (**A**) were first incubated at 37 °C for endogenous nuclease treatment. The remaining nuclear structure (**B**) was extracted three times with a low salt buffer to obtain (**C**). Proteins form this structure were further extracted with 2 M NaCl. The residual structure was subsequently treated with 1% Triton X-100 to obtain the nuclear matrix III (**D**). Samples were subsequently processed for electron microscopy as follows: pellets corresponding to each fraction were fixed in 2% glutaraldehyde, dehydrated, embedded, sectioned and viewed under the electron microscope as described in materials and methods. Abbreviations, Nu, nucleolus; NE, nuclear envelope; C, chromatin; FGN, fibrogranular network; and NM, nuclear matrix. Bar=0.97 µm.

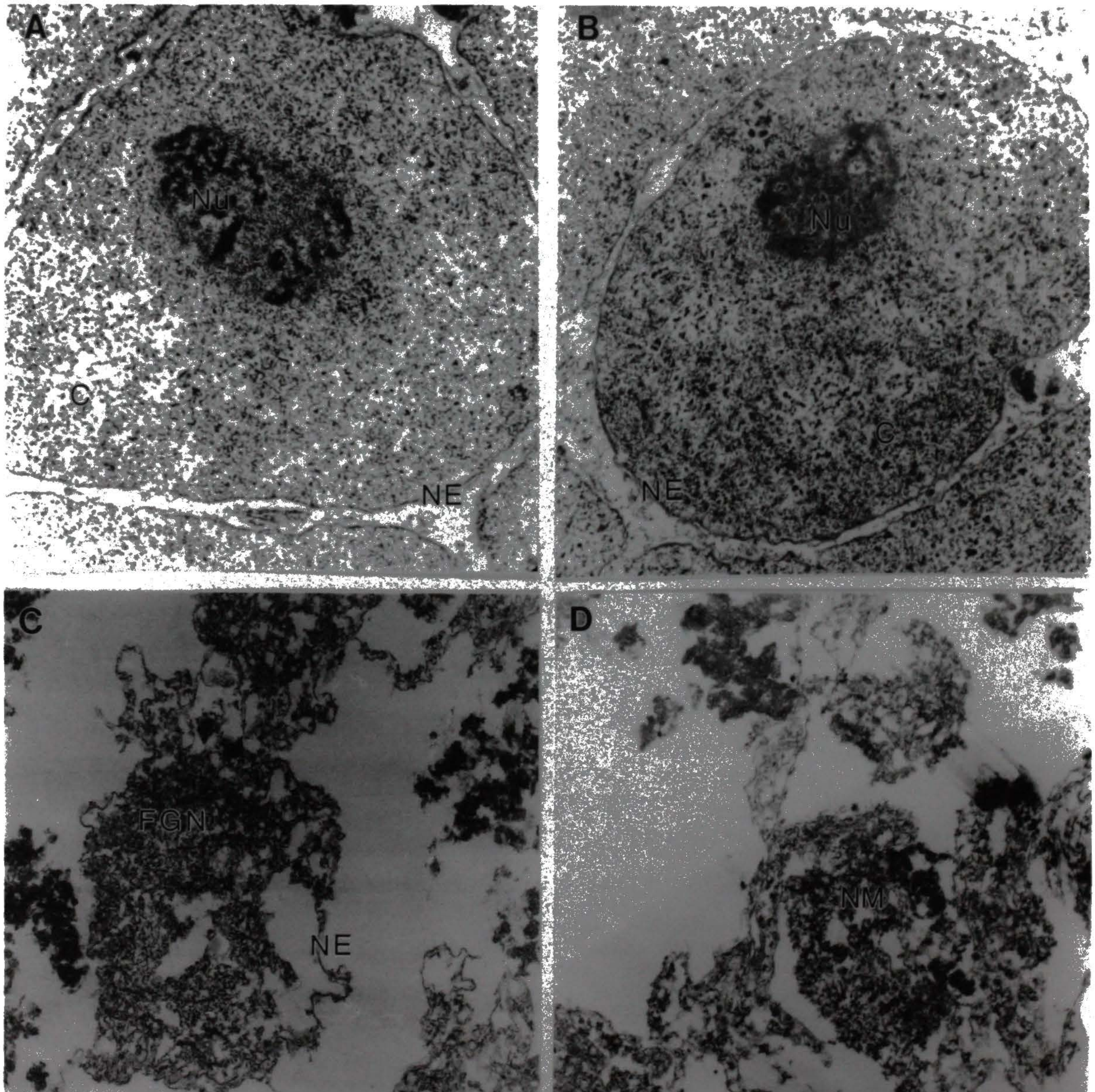
A
Nu
C
NE
B
Nu
C
NE
C
FGN
NE
D
NM

Fig. 21. Poly(ADP-ribose)glycohydrolase activity is associated with intact nuclei, chromatin, nuclear matrix III and the nuclear envelope. The assays were carried out as described under materials and methods. Each incubation (25 µl) contained 330 µg of protein/ml and 30 nM [^{32}P]poly(ADP-ribose). Lane 1 shows the substrate, protein-free [^{32}P]poly(ADP-ribose). Lanes 2-11 correspond to the products of incubation of the substrate with whole nuclei (2), nuclease soluble fraction (3), nuclease digested-nuclei (4), low-salt extractable chromatin (5), nuclear matrix I (6), high-salt extractable chromatin (7), nuclear matrix II (8), Triton X-100 soluble material (9), washes (10) and nuclear matrix III (11). The electrophoretic mobilities of [^{32}P]ADP-ribose (12), [^{32}P]AMP and [^{32}P]NAD$^+$ (13) are shown on the right side of the autoradiograph.

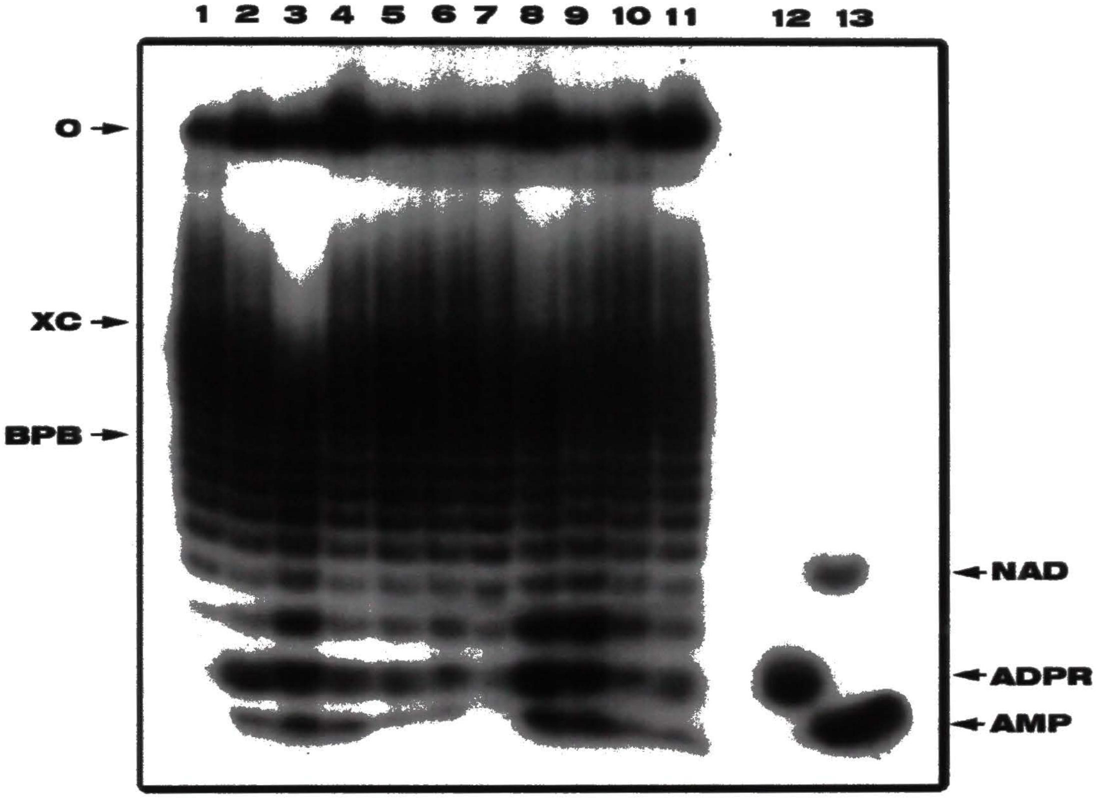
1
2
3
4
5
6
7
8
9
10
11
12
13
O
XC
BPB
NAD
ADPR
AMP

Fig. 22. Specific activity of PARG associated with chromatin, nuclear matrix and nuclear envelope. The percent of monomeric ADP-ribose generated was determined by densitometry following enzyme incubation (Fig. 21).

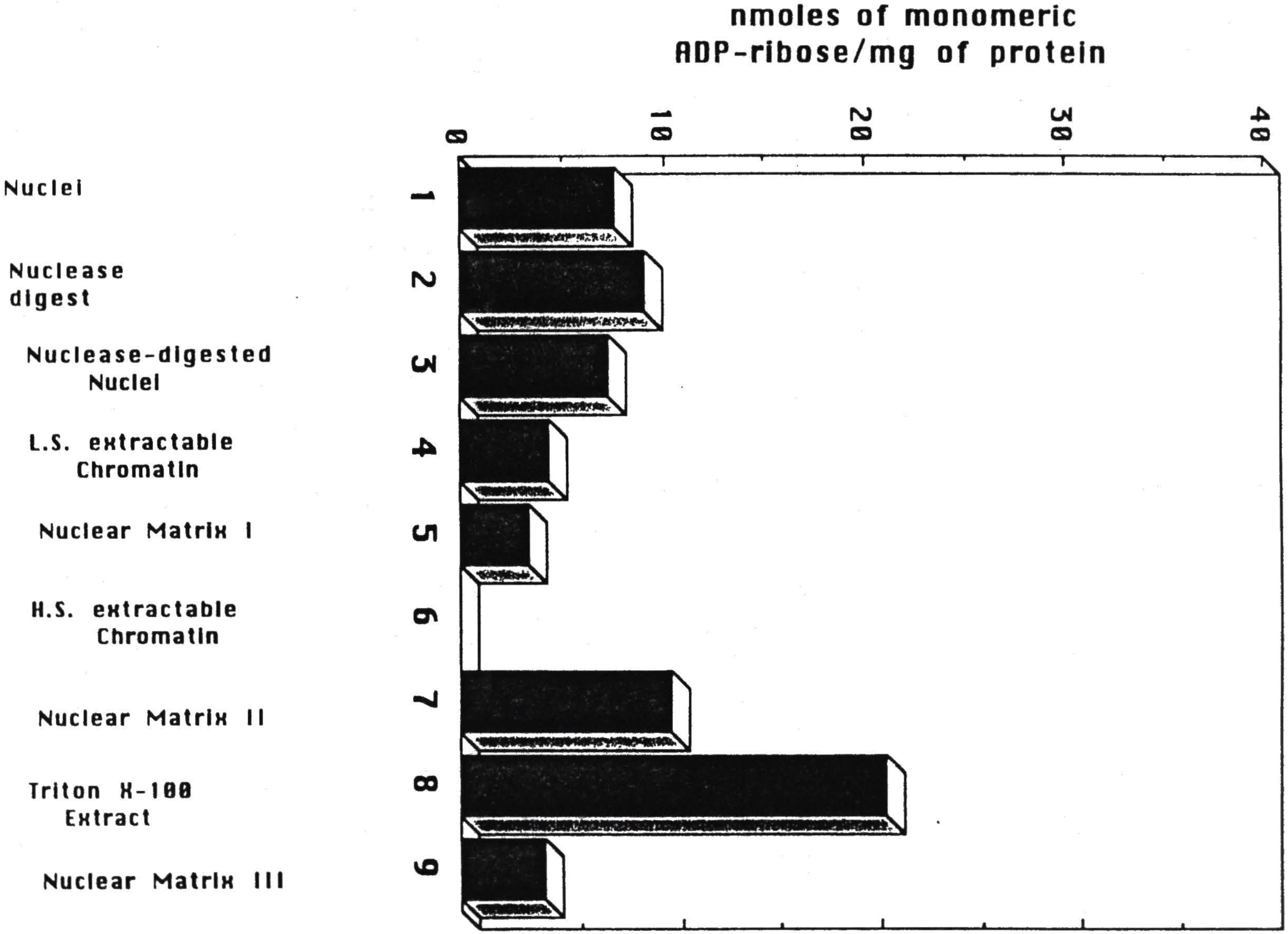
nmoles of monomeric ADP-ribose/mg of protein
0
10
20
30
40
1
2
3
4
5
6
7
8
9
Nuclei
Nuclease digest
Nuclease-digested Nuclei
L.S. extractable Chromatin
Nuclear Matrix I
H.S. extractable Chromatin
Nuclear Matrix II
Triton X-100 Extract
Nuclear Matrix III

The enzyme specific activity determined in each preparation is presented on Fig. 22. Surprisingly, a thirteen-fold increase in the specific activity of PARG is detected with nuclear envelopes. However, the overall amount of protein in this fraction is very low. By contrast, the ADP-ribose generated with the nuclear matrix fraction corresponds to about 50% of the control. This preparation had a specific activity of 10.4 which is a two fold increase compared to the incubation with nuclear extract. Thus, these findings demonstrate that PARG activity is associated with chromatin, the nuclear matrix, and the nuclear envelope.

The finding that poly(ADP-ribose) (Cardenas-Corona, *et al.,* 1987), PARP (Alvarez-Gonzalez and Ringer, 1988), and now the nuclear matrix-associated PARG activity prompted us to further study this activity.

Kinetic characterization of nuclear matrix-associated PARG activity. PARG activity associated with the nuclear matrix degraded poly(ADP-ribose) in a time-dependent manner (Fig. 23). Interestingly, a macromolecular complex forming at the origin of the gel was also detected. As expected, the generation of monomeric ADP-ribose increases with increasing amounts of nuclear matrix protein (Fig. 24).

Fig. 23. Formation of monomeric ADP-ribose by the nuclear matrix III extract. Time-dependent formation of monomeric ADP-ribose with nuclear matrix-associated PARG activity. 25 µl reaction mixtures containing 100 mM Tris-HCl, 10 mM DTT, and 30 nM [^{32}P]poly(ADP-ribose) were pre-incubated for 5 minutes at 37 °C. Reactions were triggered by the addition of 330 µg of nuclear matrix protein/ml. The reactions were carried out at 37 °C for the indicated times and were stopped by the addition of electrophoresis loading buffer.

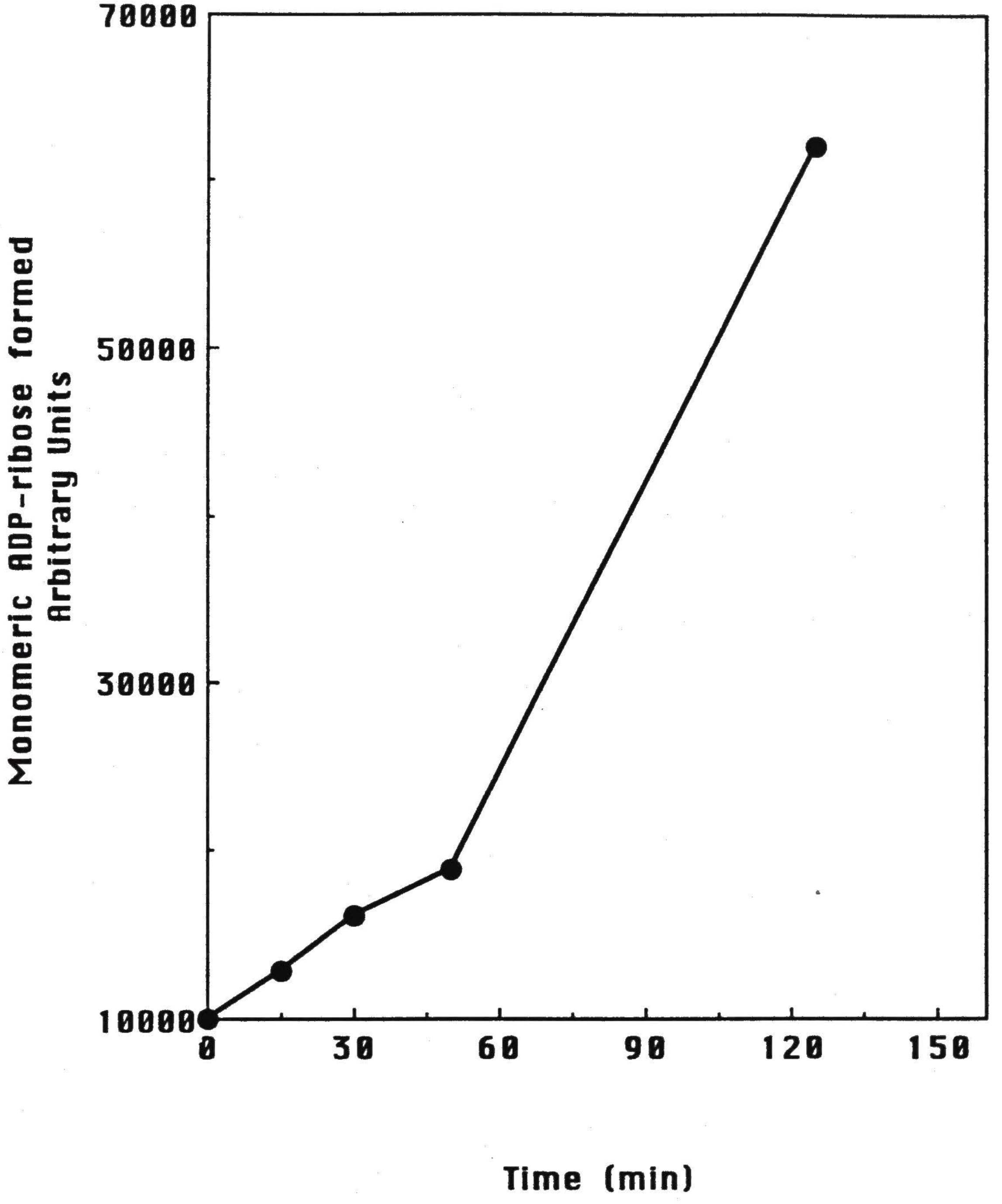
70000
50000
30000
10000
Monomeric ADP-ribose formed
Arbitrary Units
0
30
60
90
120
150
Time (min)

Fig. 24. Formation of free ADP-ribose with increasing amounts of nuclear matrix protein. These incubations were carried out as those described for figure 23. The degradation of poly(ADP-ribose) was initiated by the addition of increasing amounts of protein from the nuclear matrix (168, 336, 672, 1344 μg of protein/ml). The percent of poly(ADP-ribose) forming a protein:poly(ADP-ribose) complex is indicated by empty squares and the formation of monomeric ADP-ribose by the filled circles.

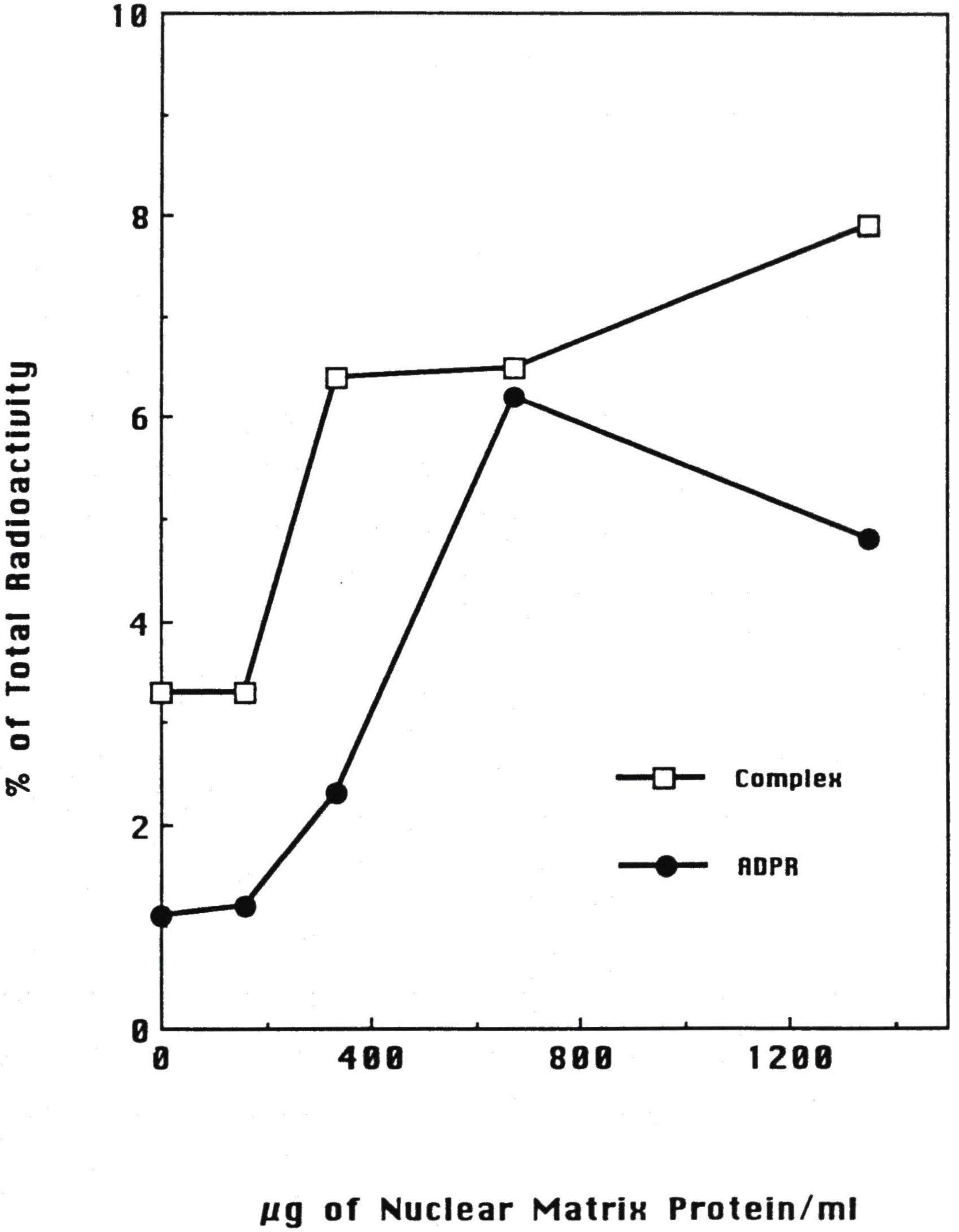
10
8
6
4
2
0
0
400
800
1200
% of Total Radioactivity
μg of Nuclear Matrix Protein/ml
Complex
ADPR

The distribution of PARG in different functional domains of the nucleus generated additional questions about the role of the protein-poly(ADP-ribosyl)tion pathway in nuclear processes. While the physiological function of this metabolic pathway remains elusive, it has recently been shown that non-covalent interactions of ADP-ribose polymers with nuclear components are important. Therefore, the next step in this project was to examine non-covalent interactions of free ADP-ribose polymers with chromatin and nuclear matrix proteins.

While carrying out the characterization of PARG activity associated with rat liver nuclei, a radiolabeled macromolecular complex at the origin of the gel was detected (Fig. 12, lane 3). This observation suggested that catalytically-important non-covalent interactions of the ADP-ribose polymers with nuclear proteins were occurring.

Non-covalent interactions of poly(ADP-ribose) with nuclear proteins. The same assay described above was used to monitor non-covalent interactions between [^{32}P]poly(ADP-ribose) and nuclear proteins. In order to substantiate this aspect, the ADP-ribose polymers utilized as substrate for PARG activity were prepared to contain negligible amounts of branched polymers as determined by the low amount of radioactivity at the origin of the gel. Therefore, non-covalent interactions of free polymers with nuclear proteins were monitored by the shift in the electrophoretic mobility of poly(ADP-ribose) molecules to the origin of the gel.

As explained in the introduction, the main components of eukaryotic nuclei are the histone proteins which contain a large number of positively charge amino acids. PARP and DNAase 1 bind to DNA, thus we evaluated whether non-covalent interactions of poly(ADP-ribose) with proteins is a property of DNA binding proteins. Furthermore, proteinase K, a basic protein, was evaluated to show that the poly(ADP-ribose) shift was not a result of trapping by a high molecular weight protein. Consistently with Panzeter *et al.* (1992), histone proteins interacted with poly(ADP-ribose) (Fig. 25, lanes 2-6). This was confirmed by the shift of the ADP-ribose polymers to the origin. By contrast, DNAase 1, proteinase K, and BSA did not shift poly(ADP-ribose) molecules at the same protein concentration as histone proteins (Fig. 25, lanes 8, 9 and 10). These proteins belong to the DNA binding, basic, high molecular weight proteins. Interactions of PARP with poly(ADP-ribose) were not detected (figure 25, lane 7) when poly(ADP-ribose):PARP dilutions were prepared at molar ratios of 1:2.

Inhibition of PARG activity by histone and nuclear matrix proteins. To investigate the role of histone and the nuclear matrix proteins in the PARG activity, PARG assays were carried out in the presence of either nuclear matrix or individual histone proteins. These experiments demonstrated that both the nuclear matrix and histone proteins inhibit PARG activity (Fig. 26A and 26B). Histone H1, H2A, H3 and H4 inhibited 50% of PARG activity in a molar ratio of poly(ADP-ribose):histone protein of 1:1 (Fig. 26A). Interestingly, histone H1 and H3 showed to be the strongest inhibitors of PARG. By contrast, histone H2B at this molar ratio was not very effective as an inhibitor. It is noteworthy that the poly(ADP-ribose):histone complex was not detected under these conditions.

In incubations with nuclear matrix proteins, 50% inhibition of PARG activity was obtained with 1344 μg of protein/ml. Because the protein composition of the nuclear matrix is complex, it is difficult to attribute the inhibition to a particular protein. Furthermore, it was interesting that poly(ADP-ribose) interacts non-covalently with nuclear matrix proteins as detected by the shift of poly(ADP-ribose) molecules to the origin (Fig. 27, lane 2). These non-covalent interactions may block the access of PARG for the substrate. Indeed, nuclear matrix protein include basic proteins (Berezney, *et al.*,

Fig. 25. Non-covalent interactions of protein-free [^{32}P]poly(ADP-ribose) with histone and non-histone proteins. Each protein indicated at the top of the autoradiograph was pre-incubated for 5 minutes at 37 °C with [^{32}P]poly(ADP-ribose). Afterwards, poly(ADP-ribose) (60 nM) was added and the mixture was further incubated for 5 minutes. The [protein][poly(ADP-ribose] complexes were detected at the origin of the gel following high resolution PAGE. The concentration of histone H1, H2A, H2B, H3, H4, P K (proteinase K), DNAase 1, and BSA (bovine serum albumin) was 100 µg/ml. PARP concentration was 100 nM. C, control, [^{32}P](ADP-ribose)$_{2-70}$; O, origin; XC (xylene cyanol) and BPB (bromophenol blue) co-migrate with ADP-ribose chains of 20 and 8 residues, respectively.

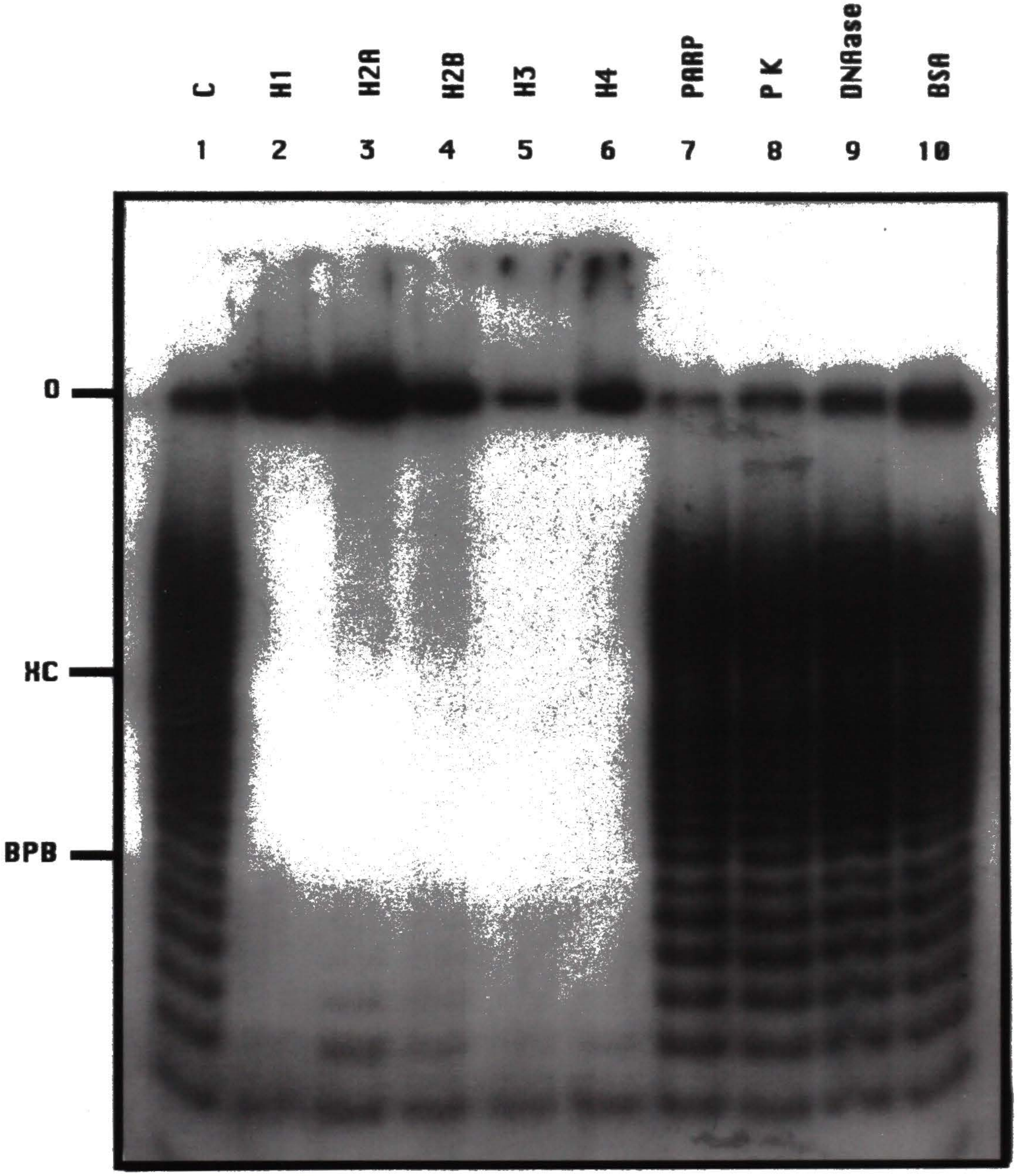
C
H1
H2A
H2B
H3
H4
PARP
P K
DNAse1
BSA
1
2
3
4
5
6
7
8
9
10
O
XC
BPB

Fig. 26. Inhibition of purified PARG activity by histone proteins and nuclear matrix proteins. Panel **A** shows the inhibition of PARG activity by histone proteins. Incubations of 50 µl each contained 1.5 nmoles of poly(ADP-ribose) and an equal molar amount of the indicated histone. The enzyme assays were carried out as described under materials and methods. Bar 1 shows the positive enzyme control (amount of monomeric ADP-ribose formed in the absence of histone proteins). Bars 2 to 6 show the percent of monomeric ADP-ribose produced in the presence of different histone proteins. Panel **B** shows the inhibition of PARG activity by nuclear matrix proteins. A 25 µl reaction mixture contained 30 nM [^{32}P]poly(ADP-ribose) and increasing amounts of nuclear matrix protein. The mixture was pre-incubated for 5 minutes at 37 °C. The reaction was initiated by the addition of PARG (6 µg/ml) and the mixture was incubated at 37 °C for 5 min. The radiolabeled products generated were resolved by 20% PAGE. Bar 1, control (monomeric ADP-ribose formed in the absence of nuclear matrix); Bars 2 to 5 show the percent of monomeric ADP-ribose produced in the presence of nuclear matrix III 168, 336, 672, 1344 µg of protein/ml, respectively.

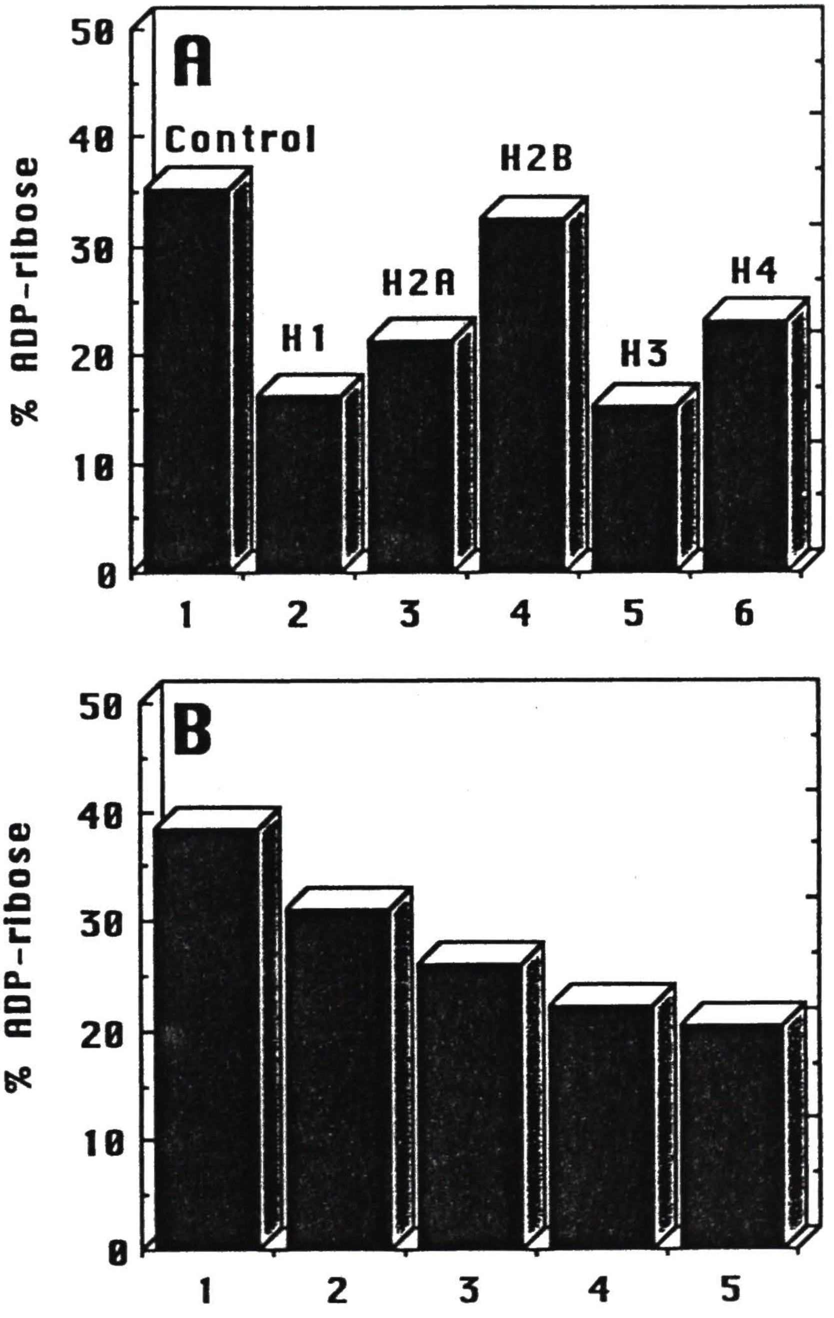
A
% ADP-ribose
50
40
30
20
10
0
Control
H1
H2A
H2B
H3
H4
1
2
3
4
5
6
B
% ADP-ribose
50
40
30
20
10
0
1
2
3
4
5

Fig. 27 Size distribution of ADP-ribose polymers following incubation of poly(ADP-ribose) with 150 ng of PARG in the presence of increasing amounts of nuclear matrix proteins. Reaction conditions are described on legend to figure 24. The hydrolytic products were resolved by PAGE on 20% gels. Lane 1 shows the control, [^{32}P](ADP-ribose)$_{2-70}$; lane 2 shows the product of incubation of the substrate with nuclear matrix (336 μg of protein/ml) in the absence of PARG; lane 3 shows the products of incubation of (ADP-ribose)$_{2-70}$ with PARG only; lanes 4-7 correspond to incubations of [^{32}P]poly(ADP-ribose) with PARG in the presence of 168, 336, 672, 1344 μg of protein/ml nuclear matrix, respectively; lane 8, [^{32}P]ADP-ribose; lane 9, [^{32}P]NAD$^+$ and [^{32}P]AMP. Bromophenol blue (BPB) and xylene cyanol (XC) co-migrated with (ADP-ribose)$_8$ and (ADP-ribose)$_{20}$, respectively.

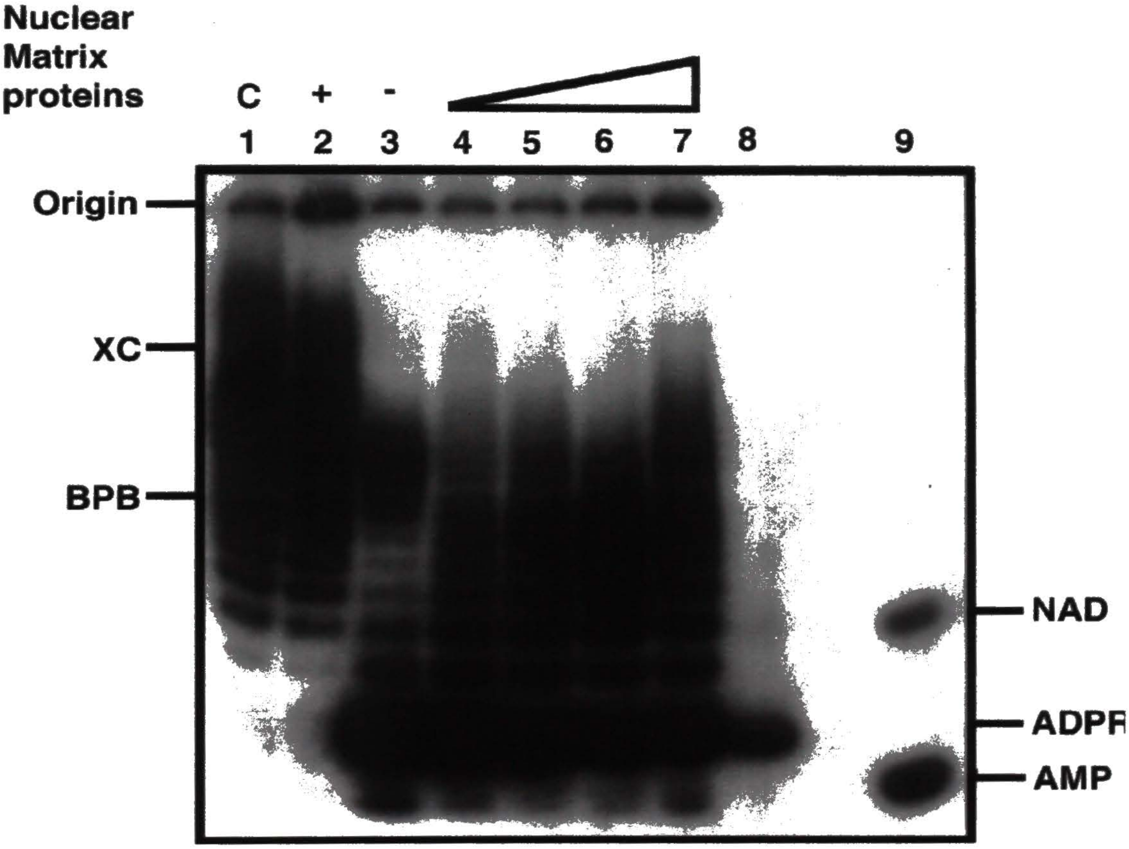
Nuclear Matrix proteins
C
+
-
1
2
3
4
5
6
7
8
9
Origin
XC
BPB
NAD
ADPR
AMP

1995), which are likely candidates for poly(ADP-ribose) protein interactions. This effect is similar to the one shown by histones. Additionally, these non-covalent interactions seem to be responsible for the low activity of PARG in the nuclear matrix. Therefore, histone and nuclear matrix proteins inhibit PARG in the absence of DNA.

While studies *in vitro* have shown that poly(ADP-ribose) interacts non-covalently with histone proteins (Panzeter, *et al.,* 1992; Wesierska-Gadek and Sauermann, 1988), the role of these interactions under physiological conditions have not been reported. For that purpose, poly(ADP-ribose) was further studied to determine whether these interactions affect endogenous PARG activity.

Non-covalent interactions of free poly(ADP-ribose) with nuclear proteins. To determine whether non-covalent interactions of poly(ADP-ribose) with nuclear proteins occur in the nuclear environment, poly(ADP-ribose) was incubated with crude nuclear extracts. Following a time-dependent incubation, non-covalent interactions were monitored by the shift of ADP-ribose polymers larger than a 20mer to the origin of the gel. Fig. 28, lane 2 shows that $(ADP\text{-ribose})_{20}$ interacts non-covalently with nuclear proteins as determined by the formation of a macromolecular complex at the origin of the gel. These experiments showed that either one or more nuclear proteins interact non-ionically with poly(ADP-ribose) even in the presence of chromosomal DNA (Fig 28, lane 2).

Protease treatment of isolated nuclei. To determine the nature of the macromolecule forming the complex at the origin of the gel, nuclei were incubated with proteinase K prior to incubation with the substrate . Proteolysis of nuclei was confirmed by SDS-PAGE (not shown). Then, poly(ADP-ribose) was allowed to interact with

Fig. 28 Non-covalent interactions of poly(ADP-ribose) with nuclear proteins. Lane 1 shows the distribution of poly(ADP-ribose) molecules (control). Lanes 2 and 3 were incubations of poly(ADP-ribose) with nuclei and proteinase K, respectively. In lane 4, disrupted nuclei were incubated with proteinase K (1 mg/ml) for 60 minutes at 37 °C. Proteolysis was stopped with 1 mM PMSF. Finally, poly(ADP-ribose) was added to the mixture and incubation was carried out for 10 minutes at 37 °C. Lane 5, poly(ADP-ribose) was incubated for 110 minutes at 37 °C. In lane 6, proteolysis of nuclei was carried out for 60 minutes in the presence of poly(ADP-ribose). Origin (O), xylene cyanol (XC), bromophenol blue (BPB).

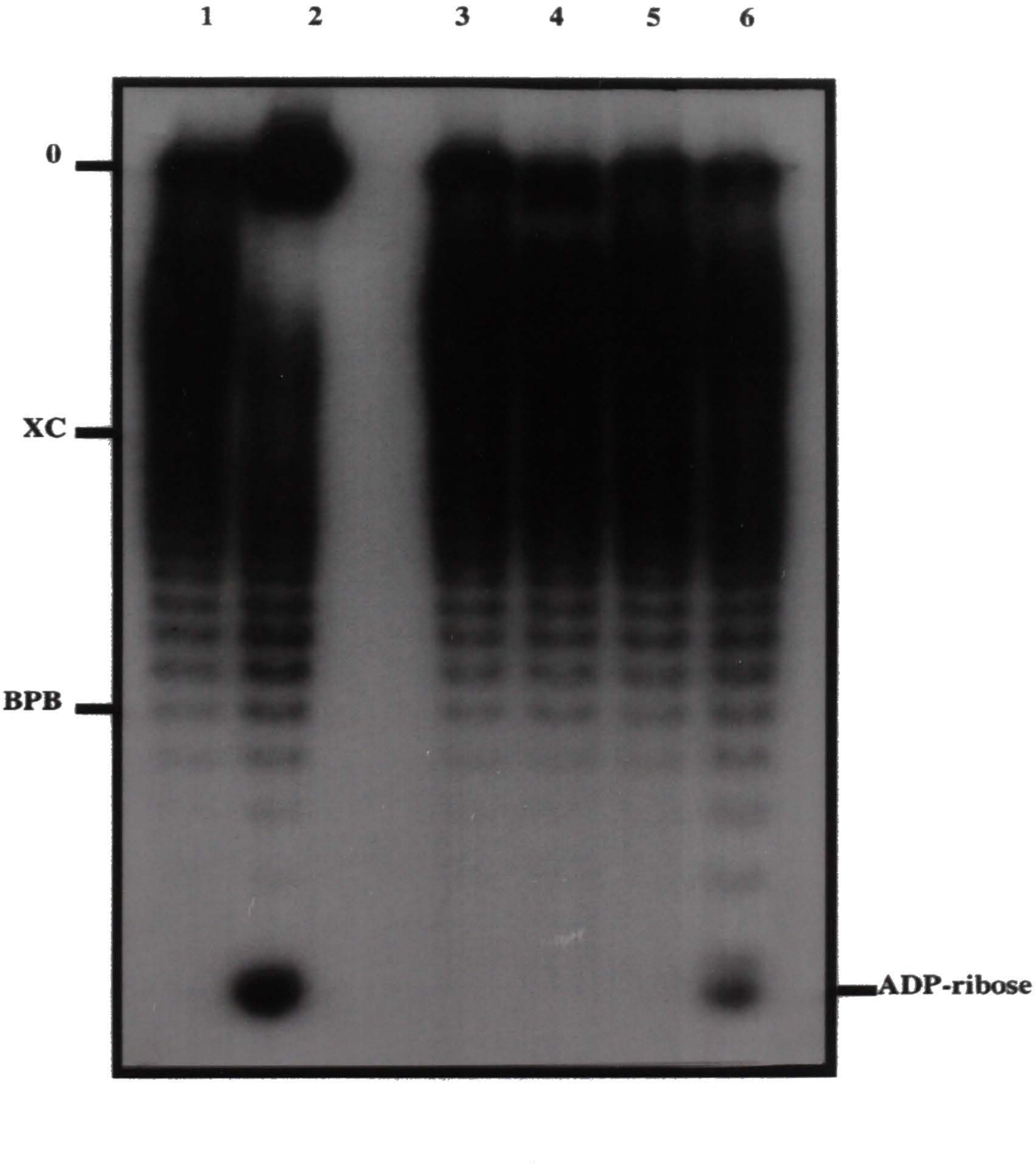
1
2
3
4
5
6
0
XC
BPB
ADP-ribose

proteolytic fragments. The formation of the macromolecular complex was not detected in proteinase K treated nuclei (Fig. 28, lane 4). Interestingly, PARG activity was not completely eliminated as determined by the formation of monomeric ADP-ribose. Thus, the macromolecular aggregate is formed by either PARG or a different protein. The formation of a ternary complex can not be discarded however.

To discard the possibility of the formation of an enzyme substrate complex, nuclei were incubated with poly(ADP-ribose) in the presence of 10 mM ADP-ribose, which is a potent competitive inhibitor of PARG activity (Maruta, *et al.*, 1991). In this case, PARG was quantitatively inhibited in long incubations of up to 180 minutes (figure 29). Interestingly, the formation of the [protein][poly(ADP-ribose)] complex was not blocked. In fact, the complex is stable up to three hours of incubation. It should also be noted that the macromolecular complex is not detected in incubations of purified PARG with poly(ADP-ribose). Therefore, our observations support the hypothesis that the formation of the [protein][polymer] complex involves a nuclear protein different than PARG.

An alternative explanation to the formation of the complex is the utilization of protein-free poly(ADP-ribose) as an acceptor molecule for ADP-ribose elongation by endogenous PARP. Several experiments were performed to discard this possibility. First, PARP was incubated with protein-free [^{32}P]poly(ADP-ribose) in the presence or absence of micromolar concentrations of NAD^{+}. In these experiments, we were unable to detect changes in the electrophoretic mobility of [^{32}P]poly(ADP-ribose). Second, the auto-poly(ADP-ribosyl)ation of PARP was carried out in the absence or presence of poly(ADP-ribose). In these experiments, the activity of PARP was not affected. Therefore, PARP was not utilizing the protein-free poly(ADP-ribose) molecules as substrates. Third, incubations of pure PARP with NAD^{+}, poly(ADP-ribose) and

Fig. 29. Inhibition of endogenous PARG activity with 10 mM ADP-ribose. 50 µl reaction mixtures contained 69.5 nM [^{32}P]poly(ADP-ribose) and 500 µg of protein/ml. The mixtures were incubated at 37 °C for the indicated times in the presence of 10 mM ADP-ribose. Lane 1, substrate control. Lane 2, shows the substrate control incubated 180 minutes in the absence of nuclear extract. Lanes 3-7 show the products generated after 15, 30, 60, 120, and 180 minutes of incubation, respectively. Lane 8, [^{32}P]PRAMP; lane 9, [^{32}P]ADP-ribose; lane 10, [^{32}P]NAD$^+$.

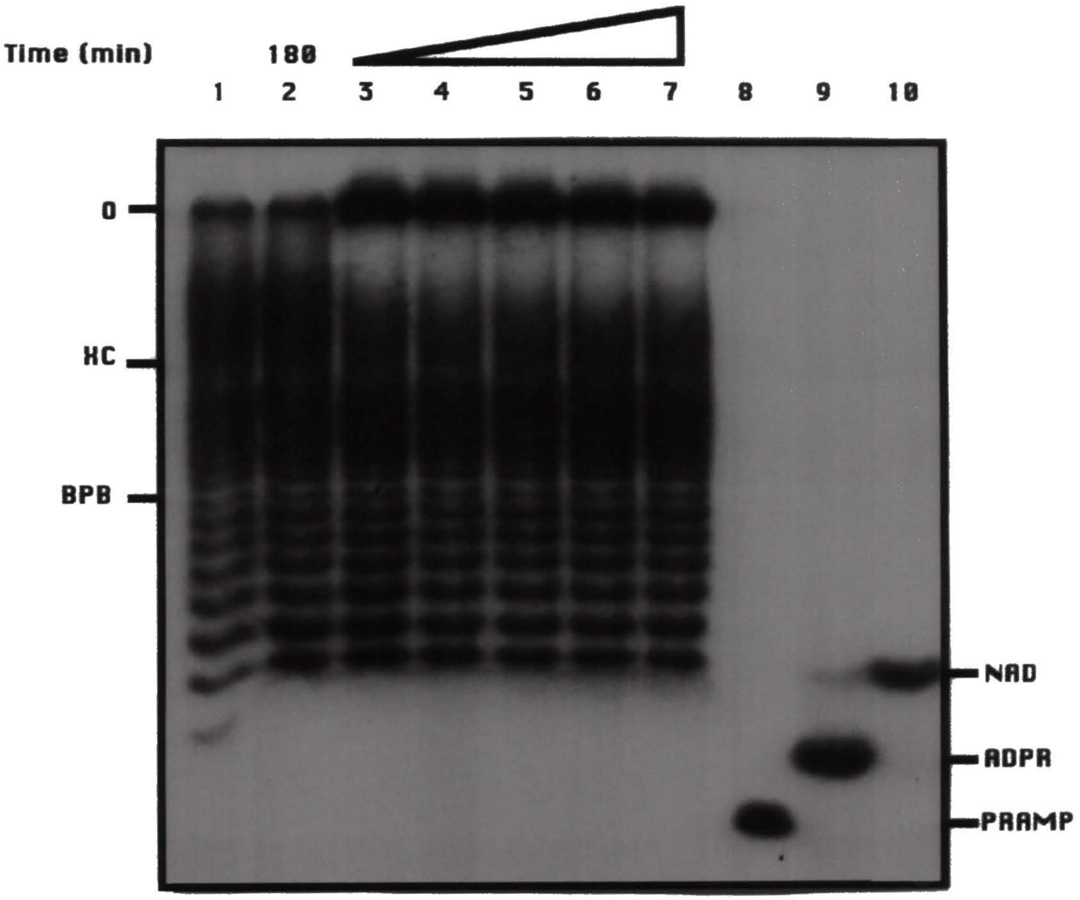
Time (min)
180
1
2
3
4
5
6
7
8
9
10
O
XC
BPB
NAD
ADPR
PRAMP

formation of the macromolecular complex resulted from the interaction of nuclear protein(s) with free polymers, and the complex was not formed by ADP-ribose elongation catalyzed by endogenous PARP.

Because the polymers of ADP-ribose that more efficiently formed this complex corresponded to molecules of 20 ADP-ribose residues or more, we decided to determine the nuclear protein binding specificity for ADP-ribose chains. For that purpose, protein-free poly(ADP-ribose) was synthesized, purified and fractionated according to Alvarez-Gonzalez and Jacobson (1987) (Fig. 30). In this process, total protein-free poly(ADP-ribose) was separated using a gel permeation column with molecular exclusion limit of 125 kDa. This procedure allowed collection of populations of ADP-ribose chains devoid of highly branched polymers of ADP-ribose. As shown on Fig. 31, each population contains a mixture of different sizes of poly(ADP-ribose) molecules. The size distribution of poly(ADP-ribose) molecules was analyzed by high resolution polyacrylamide gel electrophoresis (Fig. 31). Typically, fractions 12-15 contained ADP-ribose chains larger than 20 residues. Finally, to determine the specificity of nuclear proteins of a population of poly(ADP-ribose) molecules, different fractions were incubated with nuclear extracts.

The efficiency of ADP-ribose polymers to interact non-covalently with nuclear proteins is size-dependent. Incubations of fractionated poly(ADP-ribose) with nuclear extracts showed that the best population of free polymers to interact with proteins correspond to molecules larger that 20 ADP-ribose residues (Fig. 32). The formation of monomeric ADP-ribose was more evident with samples forming larger amounts of macromolecular complex (fraction 15). In order to correlate the formation of the macromolecular complex with the generation of free ADP-ribose, we analyzed the

Fig. 30. HPLC molecular sieving of protein-free [^{32}P]poly(ADP-ribose) on a BioSil TSK-125 column. The fractionation of protein-free poly(ADP-ribose) was carried out as described under materials and methods. Fractions were collected every 0.5 minutes and counted Cerenkov on a Scintillation counter.

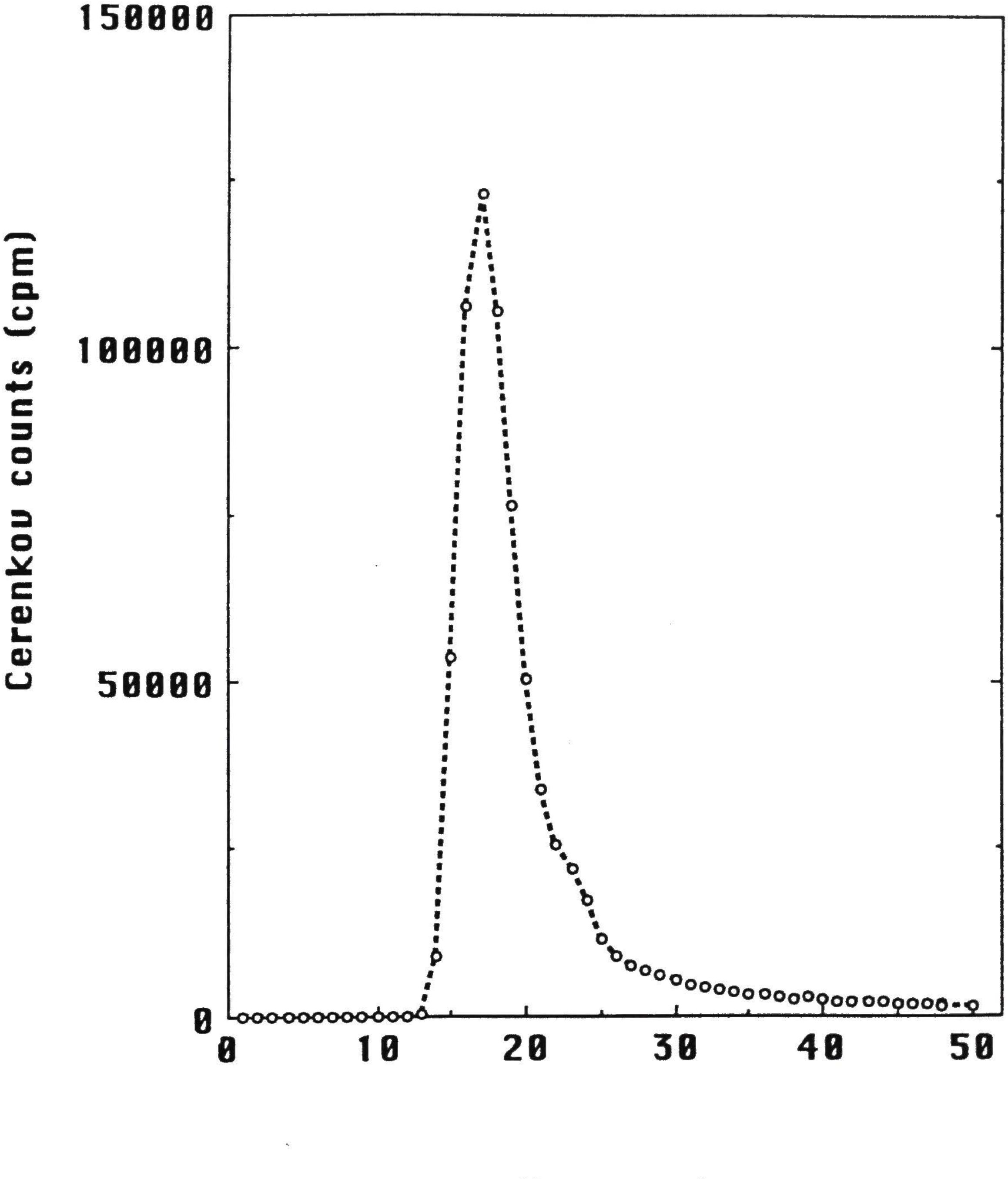
150000
100000
50000
0
Cerenkov counts (cpm)
0
10
20
30
40
50
Fraction number

Fig. 31. Size distribution of [^{32}P]poly(ADP-ribose) following molecular sieve chromatography on a TSK-125 column. 20 µl of each fraction were loaded on a 20% acrylamide gel as indicated. The samples were diluted 1:2 with the loading buffer. Electrophoresis was run as described under materials and methods.

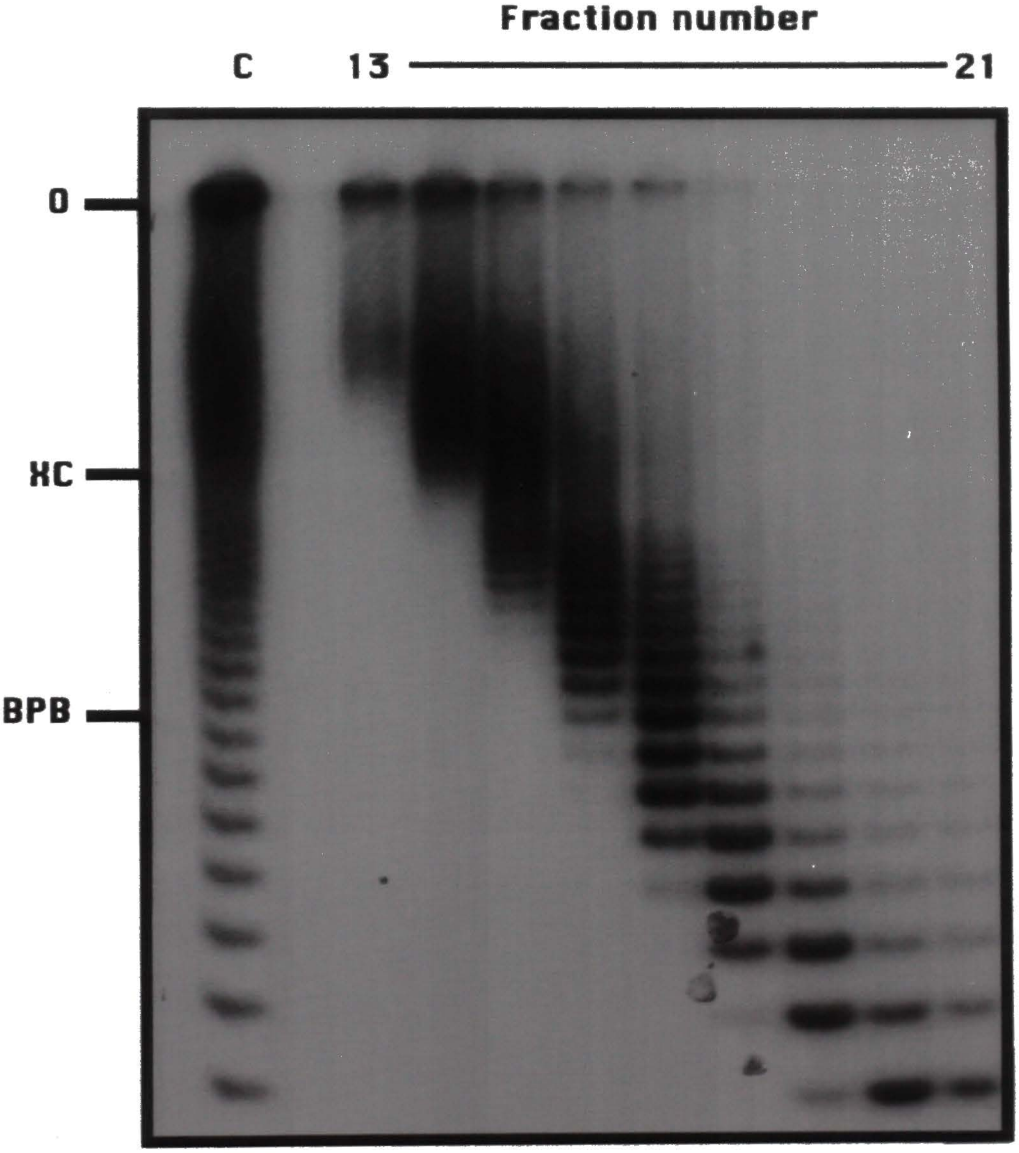
Fraction number
C
13
21
O
XC
BPB

Fig. 32. Non-covalent interactions of ADP-ribose polymers of various sizes with nuclear proteins. Incubations contained 20 µl of [^{32}P]poly(ADP-ribose) from each fraction collected from the TSK-125 column, 100 mM Tris-HCl, pH 8.0, 10 mM DTT and 500 µg of protein/ml from nuclear extract in a total volume of 50 µl. Samples were incubated 10 minutes at 37 °C. Next, samples were diluted by the addition of 50 µl of loading buffer. Lane 1, non-purified [^{32}P]poly(ADP-ribose); lane 2, fraction 15; lane 3, fraction 15 incubated with rat liver nuclei (RLN) in the absence of NAD$^+$; lane 4, ADP-ribose polymers synthesized with RLN; lane 5, purified [^{32}P]poly(ADP-ribose); lanes 6, 8, 10, 12 and 14 correspond to ADP-ribose polymers from fractions 15, 16, 17, 18, respectively. Lanes 7, 9, 11, 13, 15 show the complexes formed following incubation of fractions 15 to 19 with isolated RLN.

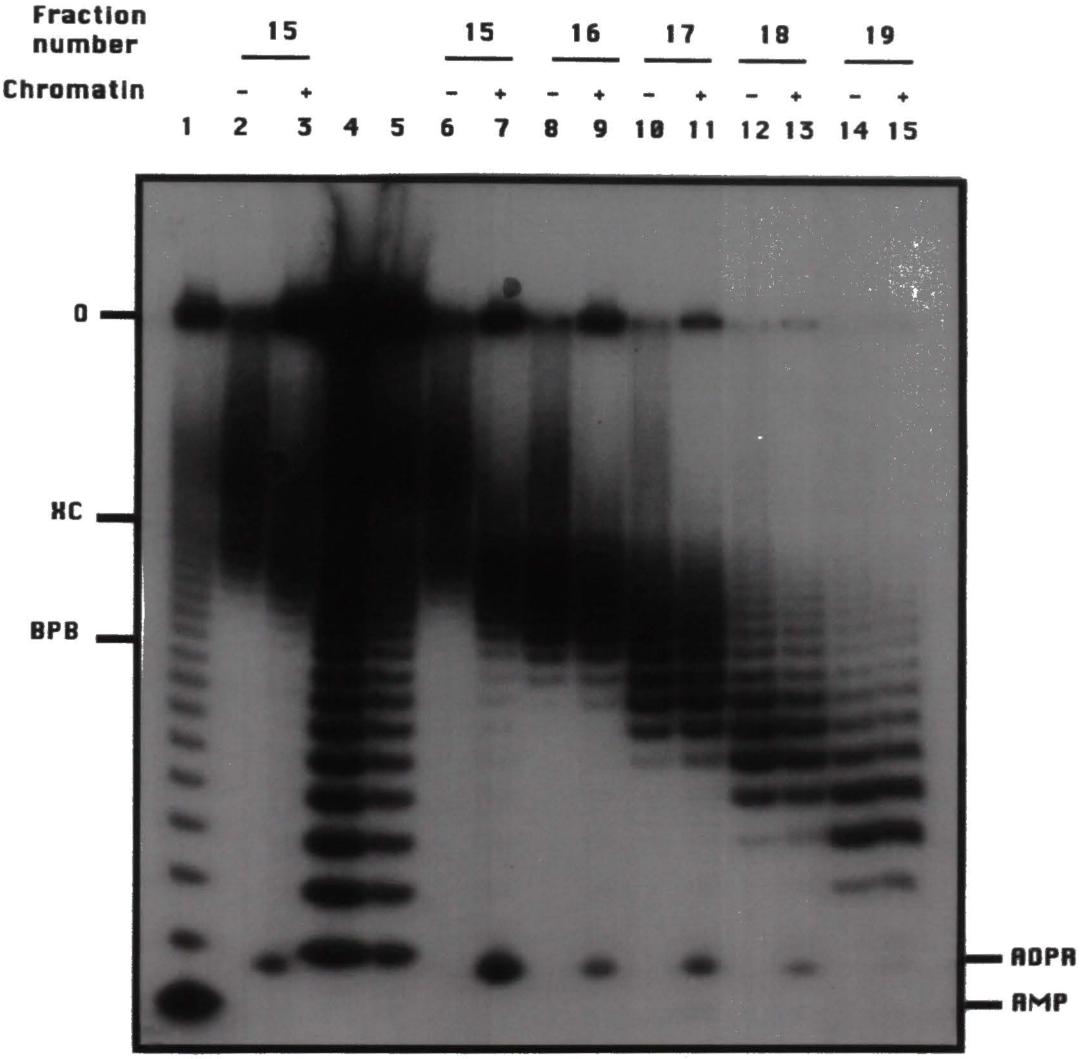
Fraction number
15
15
16
17
18
19
Chromatin
- +
- + - + - + - + - +
1 2 3 4 5 6 7 8 9 10 11 12 13 14 15
O
XC
BPB
ADPR
AMP

percent of monomeric ADP-ribose generated concomitantly with the amount of the macromolecular complex formed by densitometric analysis. Figure 33A shows that ADP-ribose polymers bigger than 20 ADP-ribose residues efficiently bind nuclear proteins as detected by the formation of the macromolecular complex. The average polymer size of these fractions was 22.88 and 12.72, respectively. In addition, figure 33B shows that in incubations of poly(ADP-ribose) with nuclear extracts, the formation of monomeric ADP-ribose detected as compared with control incubations in the absence of nuclear extract. The large amount of monomeric ADP-ribose formed correlates with the increase of [protein][poly(ADP-ribose] complex.

Next, we proceeded to determine the role of the complex formed in crude chromatin extracts in the activity of PARG.

The protein(s) integrating the complex show high affinity for ADP-ribose chains larger than 20 ADP-ribose residues (Fig. 32). Therefore, the formation and degradation of the [protein][poly(ADP-ribose)] complex could be studied concomitantly. Kinetically, the complex was formed prior to the degradation of poly(ADP-ribose) (Fig. 34). Therefore, PARG appears to use the [protein][poly(ADP-ribose)] complex as a substrate early in the incubation (Fig. 35)

Complex formation as function of temperature. Poly(ADP-ribose) was incubated with rat liver nuclei at 0, 37 and 60 °C. Figure 36 shows that the complex formation was avoided at the temperature of 0 and 60 °C. This demonstrates that the complex is formed during the incubation and it does not represent trapping of poly(ADP-ribose) at the site of sample application on the gel. Since the activity of PARG was not detected (Fig. 37) at 0 °C and 60 °C while the complex was still formed, the idea that poly(ADP-ribose) interacts non-covalently with nuclear proteins before PARG activation was further

Fig. 33. Formation of monomeric ADP-ribose and complex formation in interactions of RLN with different fractions of [^{32}P]poly(ADP-ribose). The percent indicated was obtained from figure 32.

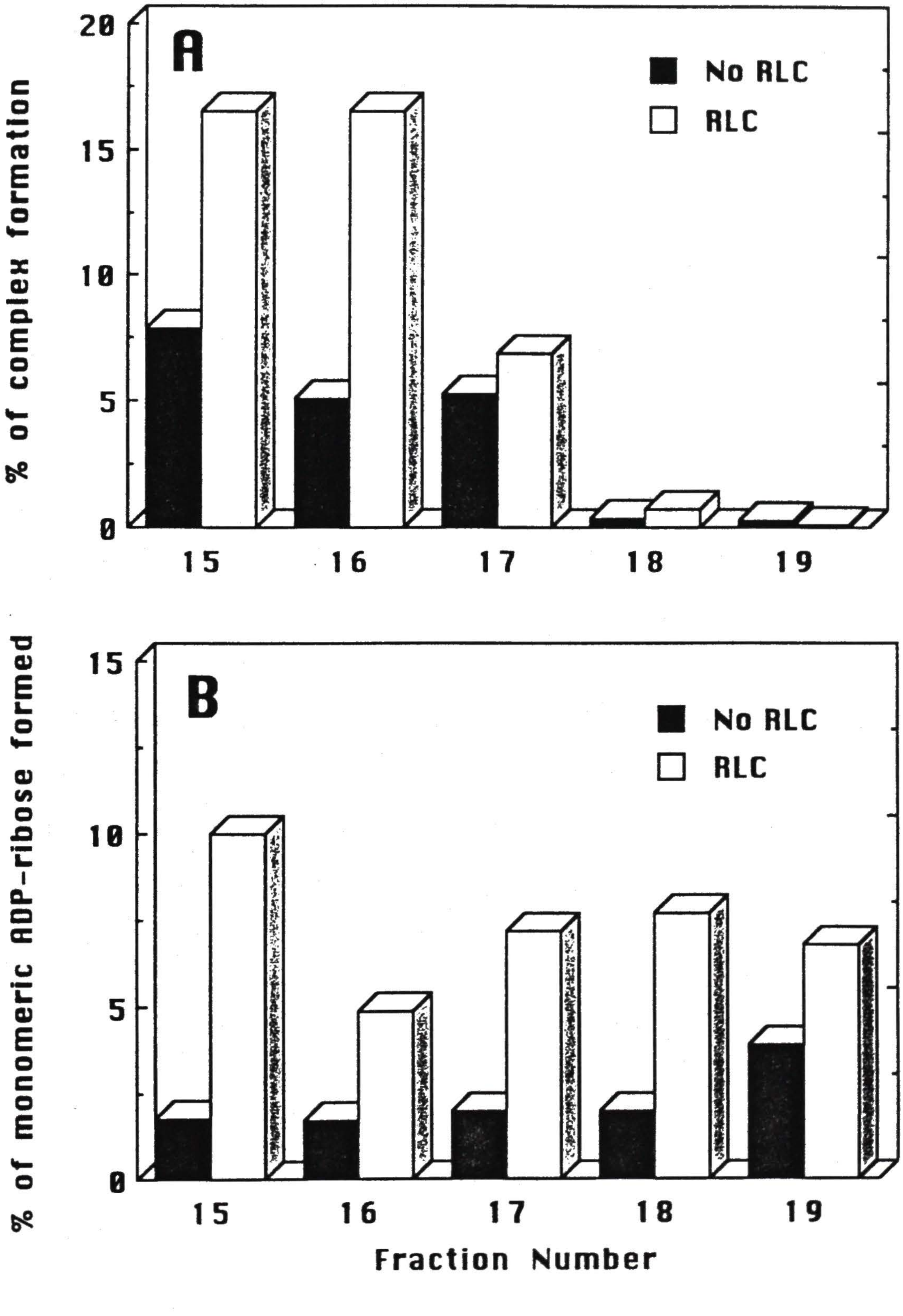
A
No RLC
RLC
% of complex formation
0
5
10
15
20
15
16
17
18
19
B
No RLC
RLC
% of monomeric ADP-ribose formed
0
5
10
15
15
16
17
18
19
Fraction Number

Fig. 34. Kinetics of complex formation and PARG activity with a crude nuclear extract. [^{32}P]poly(ADP-ribose) (56.9 nM) was pre-incubated in a 50 µl reaction mixture for 5 minutes. Then, 500 µg of protein/ml of crude rat liver nuclear extract was added. The reaction was stopped by the addition of 20% electrophoresis loading buffer. Lane 1, [^{32}P]poly(ADP-ribose), control; lane 2, [^{32}P]poly(ADP-ribose) incubated for 30 minutes in the absence of nuclear extract; lanes 3 to 10 correspond to incubations of 0.5, 1.0, 2.0, 5.0, 10.0, 20.0 and 30.0 min. The origin is indicated by O. The dyes XC and BPB co-migrated with (ADP-ribose)$_{20}$ and (ADP-ribose)$_{8}$, respectively.

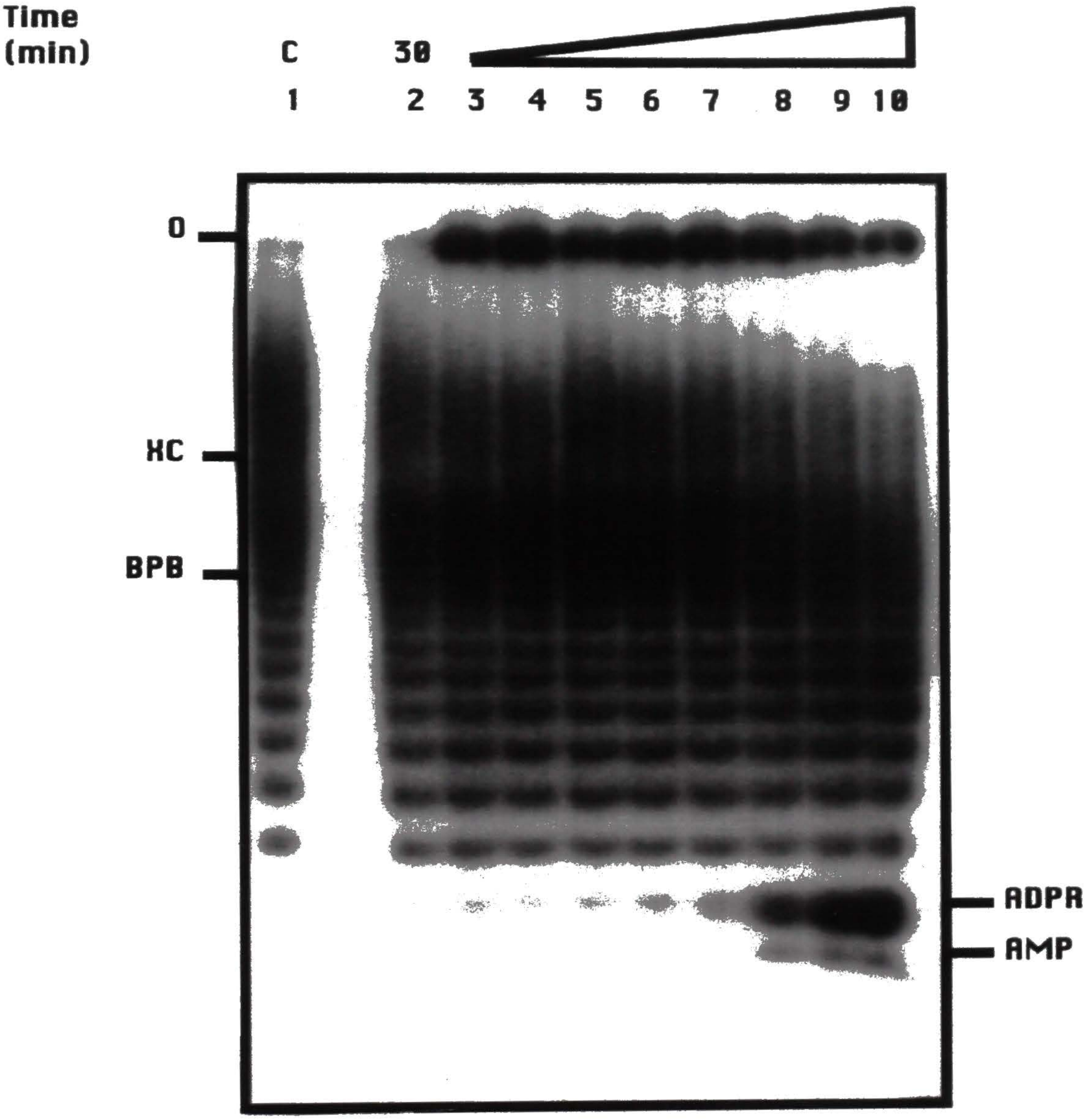
Time (min)
C
30
1
2
3
4
5
6
7
8
9
10
O
XC
BPB
ADPR
AMP

Fig. 35. Graphical representation of Fig. 34 following densitometric scanning of the complex and free monomeric ADP-ribose. The graph shows time-dependent degradation of the complex (open triangles) and monomeric ADP-ribose formation (filled triangles).

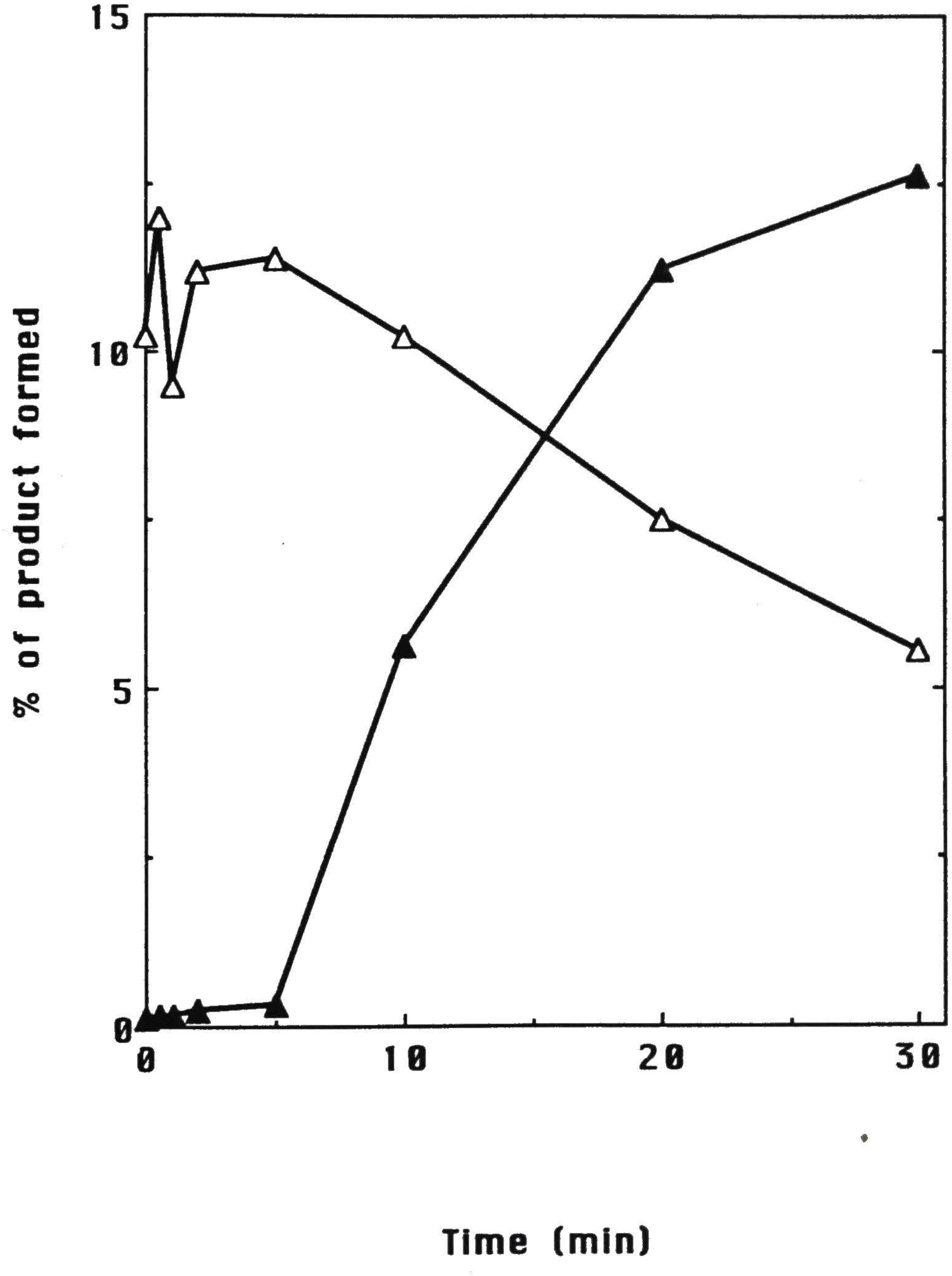

15
10
5
0
0
10
20
30
% of product formed
Time (min)

Fig. 36. Kinetics of nuclear associated poly(ADP-ribose) glycohydrolase at 0, 37 and 60 °C. Open triangles show incubations at 37 °C; filled circles show activity at 0 °C and open squares at 60 °C. Each point corresponds to the percent of monomeric ADP-ribose formed.

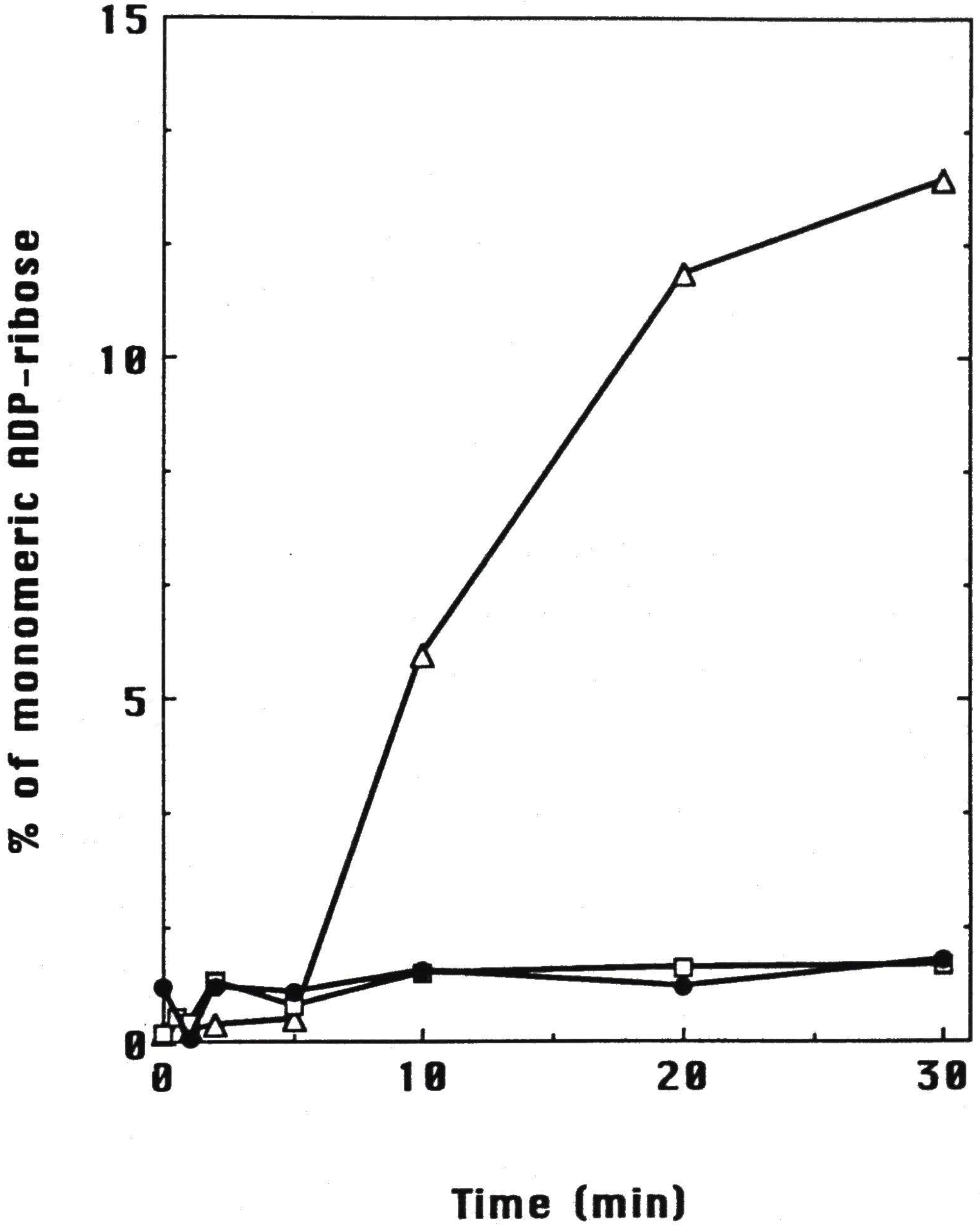
15
10
5
0
% of monomeric ADP-ribose
0
10
20
30
Time (min)

Fig. 37. Kinetics of [protein][poly(ADP-ribose)] degradation at 0, 37 and 60 °C. Open triangles show incubations at 37 °C; filled circles show activity at 0 °C and open squares at 60 °C. Each data point indicates the percent of ADP-ribose chains complexed.

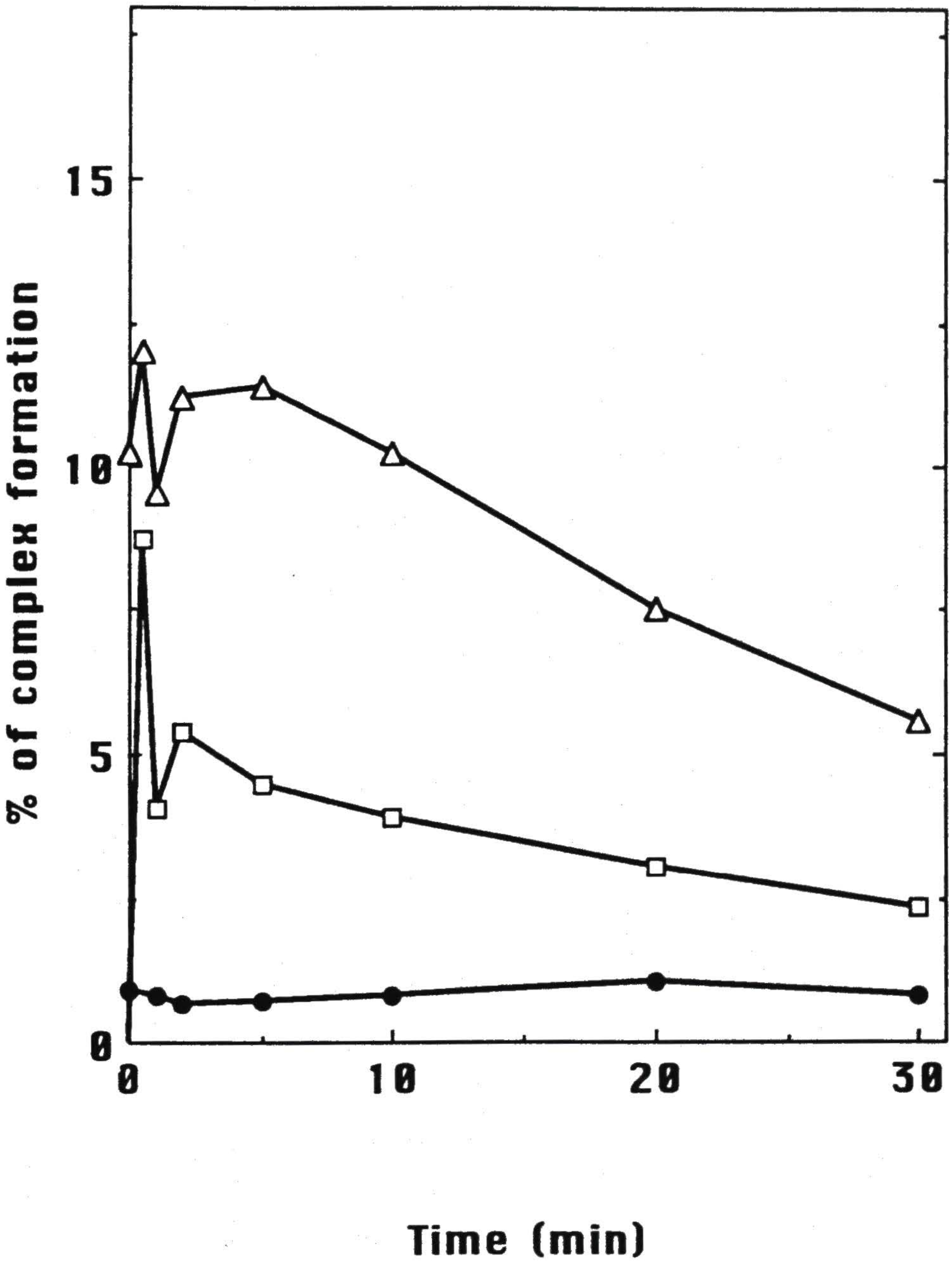
% of complex formation
15
10
5
0
0
10
20
30
Time (min)

substantiated.

The formation of the [protein][poly(ADP-ribose)] complex suggest that this is a physiological substrate for PARG. Thus, this lead us to identify the protein responsible for the formation of this catabolic intermediate.

Non-covalent interactions of nuclear proteins with protein-free poly(ADP-ribose) by SDS-PAGE. Due to the fact that histone proteins are the most abundant proteins in the cell nucleus, and that they are positively charged, they might interact with poly(ADP-ribose). Therefore, we decided to incubate free polymers with isolated nuclei and followed complex formation by SDS-PAGE. In this experiment, complex formation which suggests interactions of histone proteins with poly(ADP-ribose), was detected (Fig. 38). Non-covalent interactions with histone H1 appeared to be absent. Non-covalent interactions seemed stable in 0.1% SDS. Interestingly, no radioactivity co-migrated with the expected molecular mass of PARG. In conclusion, this experiment supports the idea that histone proteins interact non-covalently with poly(ADP-ribose) *in vivo.*

Ionic interactions of poly(ADP-ribose) with histone H1 were not observed in the experiments described above. This result was unexpected in light of the observation of Panzeter, *et al.*, (1992). Therefore, in order to further examine whether histone H1 is a component of the complex, histone H1-depleted chromatin was prepared.

Poly(ADP-ribose) ionic interactions with H1-depleted chromatin. Histone H1 binds to core and linker DNA in chromatin. Additionally, it also participates in the compaction of chromatin (Thoma, *et al.*, 1981). Displacement of this histone from native chromatin results in unfolding of the 30 nm fiber to oligonucleosomes (Thoma, *et al.*, 1979). Due to the fact that poly(ADP-ribosyl)ation plays a role in compaction-relaxation of chromatin (De Murcia, *et al.*, 1988), and that histone H1 is poly(ADP-

Fig. 38 Non-covalent interactions of poly(ADP-ribose) with total nuclear proteins. Poly(ADP-ribose) (78 nM) was incubated with a crude nuclear extract (2 mg of protein /ml) at 37 °C for 0, 5, 15, 30, 60 and 90 minutes. The reactions were quenched by adding SDS-PAGE loading buffer and samples were placed on ice. Panel **A**, Coomassie blue stain of nuclear proteins. Lane 1, pre-stained standards, lanes 2-7, samples incubated for 0, 5, 15, 30, 60 and 90 minutes; lane 8, nuclear proteins control [- poly(ADP-ribose)]; lane 9, protein standards. Panel **B**, autoradiograph of panel A.

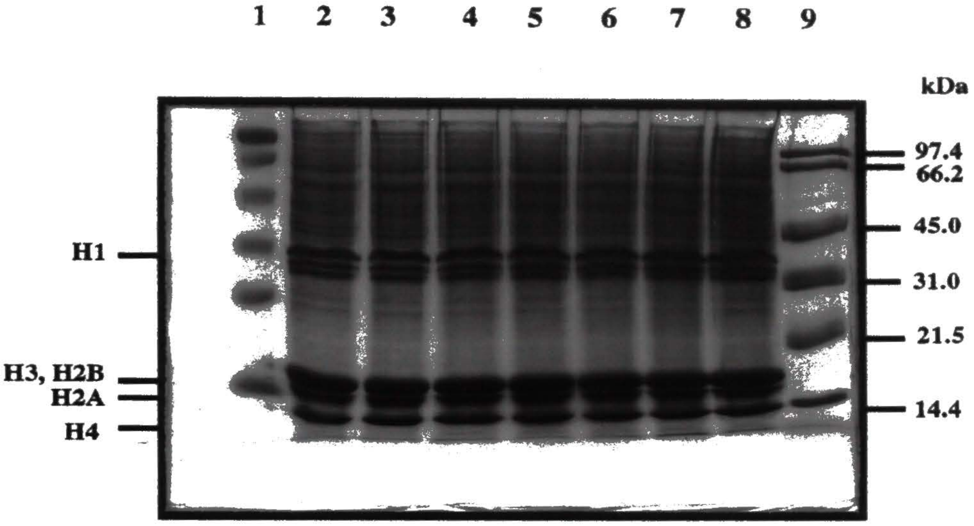
1 2 3 4 5 6 7 8 9
kDa
97.4
66.2
45.0
31.0
21.5
14.4
H1
H3, H2B
H2A
H4

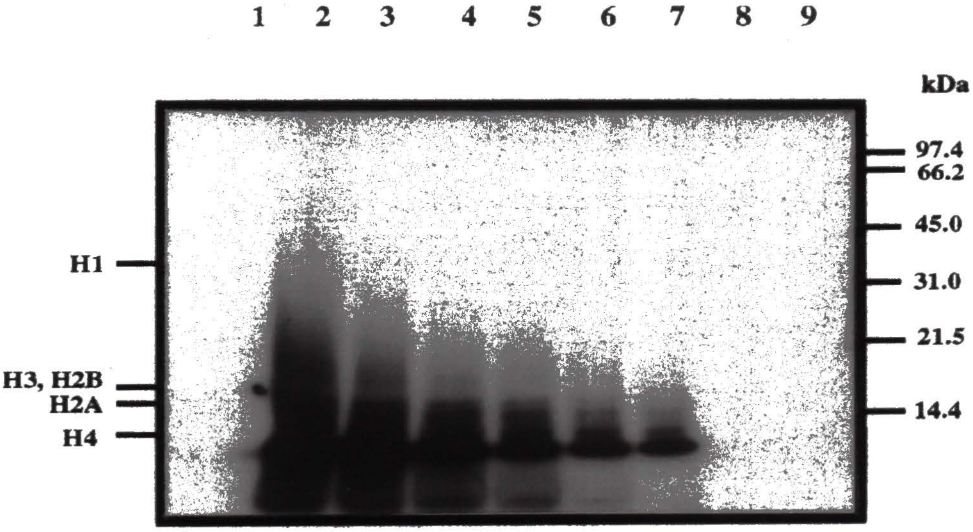
1 2 3 4 5 6 7 8 9
kDa
97.4
66.2
45.0
31.0
21.5
14.4
H1
H3, H2B
H2A
H4

ribosyl)ated in this process (Aubin, *et al.*, 1983), it was thought that this histone protein may be responsible for binding to poly(ADP-ribose). To examine this possibility chromatin was depleted of histone H1 (Fig. 39). Surprisingly, incubation of this extract in the absence of histone H1 with free polymers resulted in the formation of the [protein][poly(ADP-ribose)] complex. Furthermore, PARG activity was detected in H1-depleted chromatin (Fig. 40). Therefore, these experiments further suggested that histone H1 was not involved in the formation of the macromolecular complex.

The ability to detect the formation of the [protein][poly(ADP-ribose)] complex by electrophoresis prompted me to study the binding of histone proteins to poly(ADP-ribose). The idea arose from the concept that, among the nuclear proteins tested for binding to poly(ADP-ribose), histone proteins were the likely candidates (Panzeter, *et al.*, 1992). This is also supported by the fact that this proteins are the most abundant proteins of the cell nucleus.

Non-covalent interactions of histone proteins with poly(ADP-ribose). The experimental approach used consisted of incubations of poly(ADP-ribose) and individual histones at different molar ratios. Molar ratios [poly(ADP-ribose): histone] below 1:8 did not show complex formation. By contrast, molar ratios of poly(ADP-ribose):histone above 1:8 resulted in significant amounts of [histone][poly(ADP-ribose)] complex. Although, histone H1 showed the highest affinity for poly(ADP-ribose) (Fig. 41). This affinity was not equivalent to the observation with crude chromatin extracts. Seemly, at molar ratios of 1:16, histone H3 showed interaction with poly(ADP-ribose) (Fig. 41); however, this was non-specific. Interestingly, histone H4 displayed a strong affinity for the same population of ADP-ribose polymers as that observed with crude chromatin (Fig. 41, lanes 7,13).

Fig. 39. Coomassie blue staining of Histone H1-depleted chromatin. Chromatin was depleted of histone H1 as described under "material and methods". Lane 1, molecular weight markers; lane 2, chromatin;lane 3, H1-depleted chromatin; lane 4, histone H1; lane 5, pre-stained molecular weight markers (BIO-RAD).

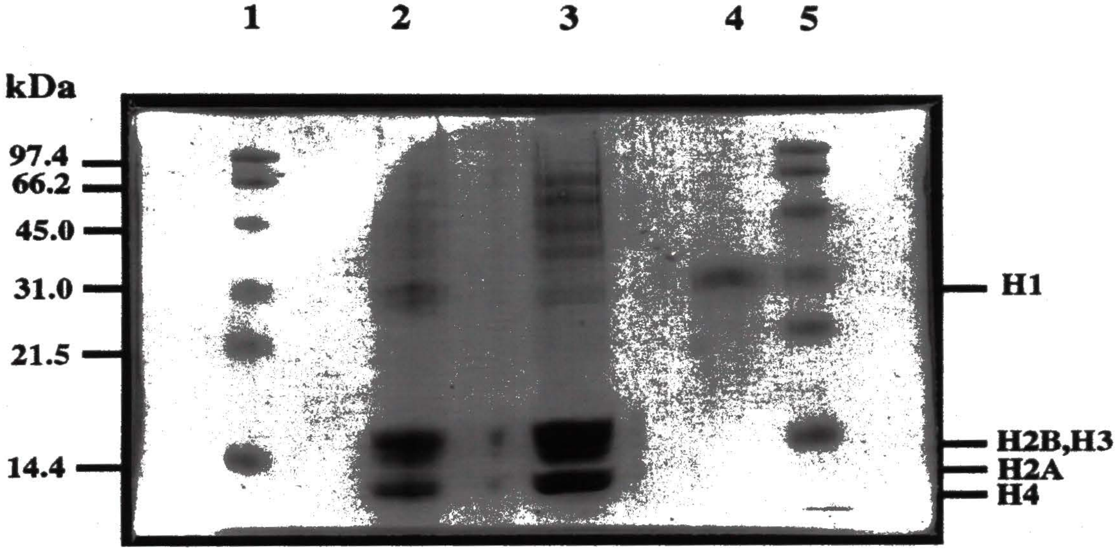
1
2
3
4
5
kDa
97.4
66.2
45.0
31.0
21.5
14.4
H1
H2B,H3
H2A
H4

Fig. 40. Non-covalent binding of poly(ADP-ribose) to H1-depleted chromatin. H1-depleted chromatin was obtained as described under "materials and methods". A 50 µl reaction mixture contained 120 nM [^{32}P]poly(ADP-ribose) and 500 µg of RLN protein/ml, the mixture was incubated for 5 and 30 minutes. Similar incubations were carried out with H1-depleted chromatin. Lane 1, control, size distribution of [^{32}P]poly(ADP-ribose). Lane 2, 3, and 4 samples incubated for 5 minutes. Lanes, 7, 8, and 9 were incubated 30 minutes. Lanes 2 and 5, RLN; lanes 3 and 6, H1-depleted chromatin; lanes 4 and 7 were H1 depleted chromatin with the addition of purified histone H1 (2.5 µg).

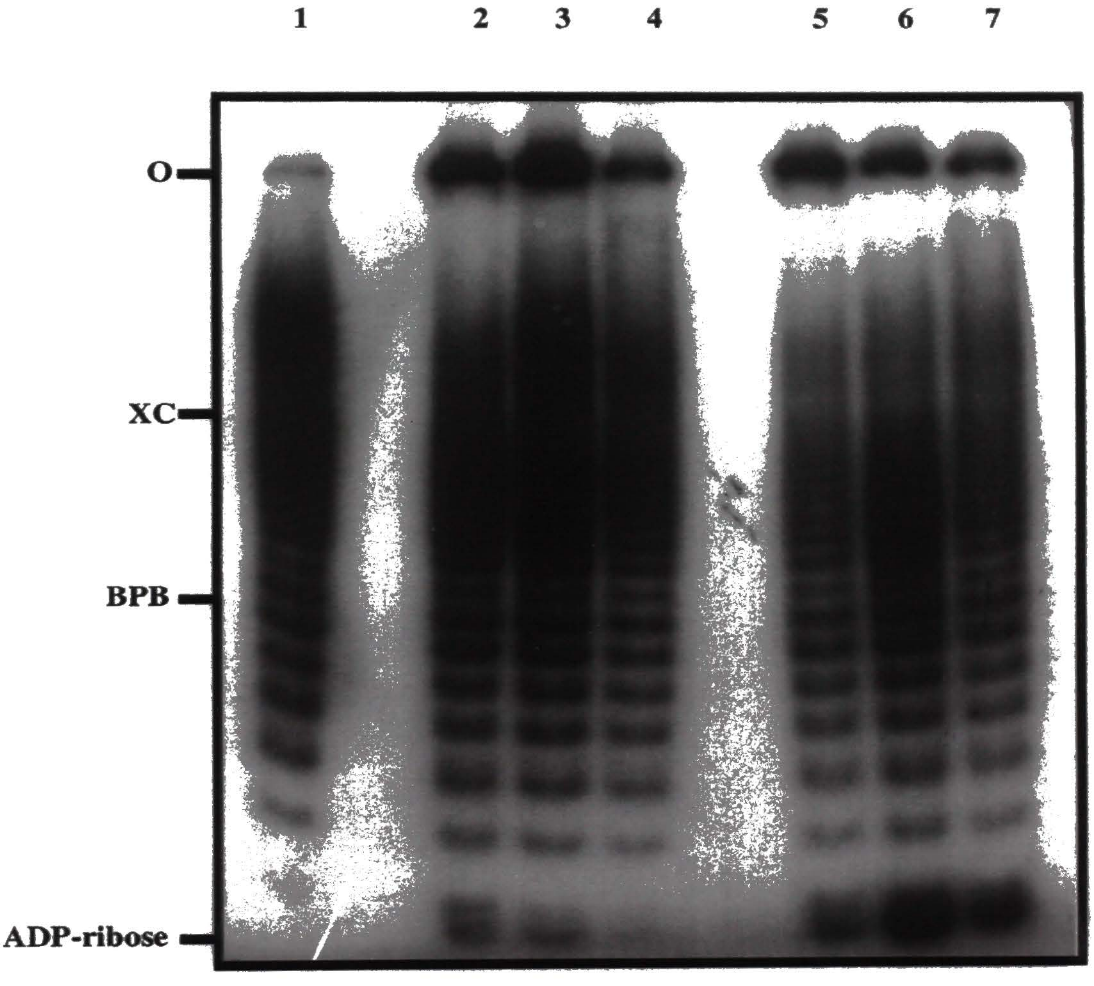
1
2
3
4
5
6
7
O
XC
BPB
ADP-ribose

Fig. 41. Binding of individual histone proteins to poly(ADP-ribose) at 1:8 and 1:16 molar ratios of poly(ADP-ribose):Histone. These incubations were carried out as described under materials and methods. The molar concentration of poly(ADP-ribose) was 60 nM. The histone tested is indicated above each lane.O, origin; XC and BPB co-migrated with ADP-ribose chains of 8 and 20 ADP-ribose residues. C, control; CI, control one, the poly(ADP-ribose) was incubated.

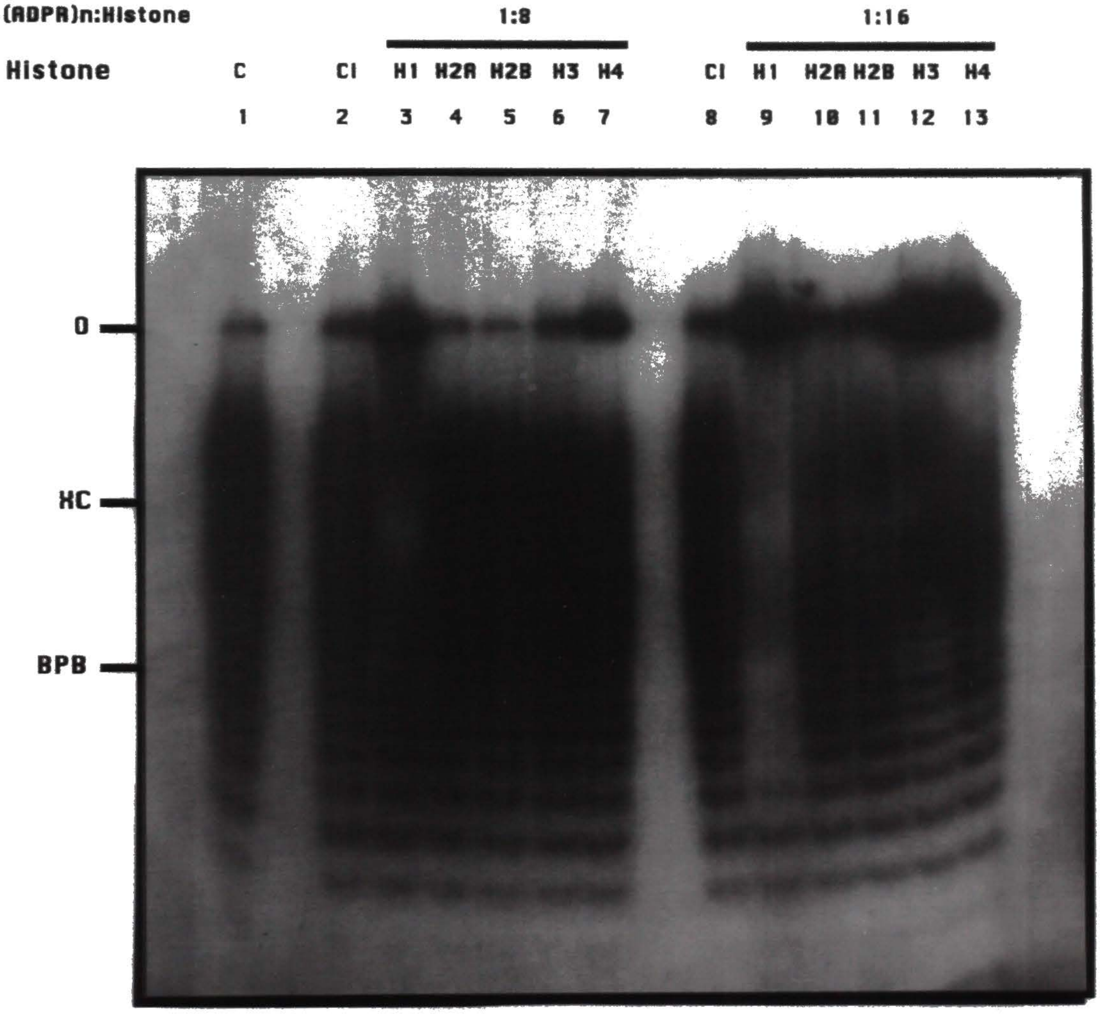
(ADPR)n:Histone
1:8
1:16
Histone
C
Cl
H1
H2A
H2B
H3
H4
Cl
H1
H2A
H2B
H3
H4
1
2
3
4
5
6
7
8
9
10
11
12
13
O
XC
BPB

The lowest molar ratios at which histone H4 showed affinity for long ADP-ribose chains was further evaluated. Thus, incubations of histone H4 at molar ratios of [poly(ADP-ribose):histone H4] 1:1, 1:2, 1:4, 1:8 (Fig. 42, lanes 2-5). These results demonstrated that at the molar ratio of 1:2 a considerable amount of poly(ADP-ribose) was shifted to the origin of the gel by histone H4.

Three possible scenarios may partially explain my results. First, PARG may be activated by a nuclear protein that binds non-covalently to free polymers and this serves as a signal of poly(ADP-ribose) catabolism by binding to free polymers. Second, poly(ADP-ribose) may interact non-covalently with nuclear protein to delay the catabolic step. Third, proteins interacting with free poly(ADP-ribose) may be required for PARG enzyme recognition. In order to distinguish between these possibilities, we decided to follow the degradation of poly(ADP-ribose) in the presence of histone H4.

PARG activity in the presence of histone H4. Figure 43 shows the time-dependent formation of monomeric ADP-ribose in the presence of histone H4. Comparison of the amount of monomeric ADP-ribose formed in the absence or presence of histone H4 indicates that histone H4 actually inhibits PARG activity. Notice, the percent of complex formed did not decrease during the incubation. Thus, histone H4 may serve as a presenting molecule of poly(ADP-ribose) to PARG.

It has been reported that covalent poly(ADP-ribosyl)ated acceptors are better substrates for PARG than protein-free poly(ADP-ribose) (Uchida, *et al.,* 1993b). Thus, I carried out experiments to determine the role of protein acceptors on PARG activity. Since PARP itself is the main polypeptide poly(ADP-ribosyl)ated, we also performed experiments in the presence or absence of PARP first.

Fig. 42. Non-covalent binding of histone H4 to free poly(ADP-ribose). Incubations were performed as described on legend to figure 35. Molar ratios of poly(ADP-ribose):histone H4 were 1:1 (lane 2), 1:2 (lane 3), 1:4 (lane 4) and 1:8 (lane 5).

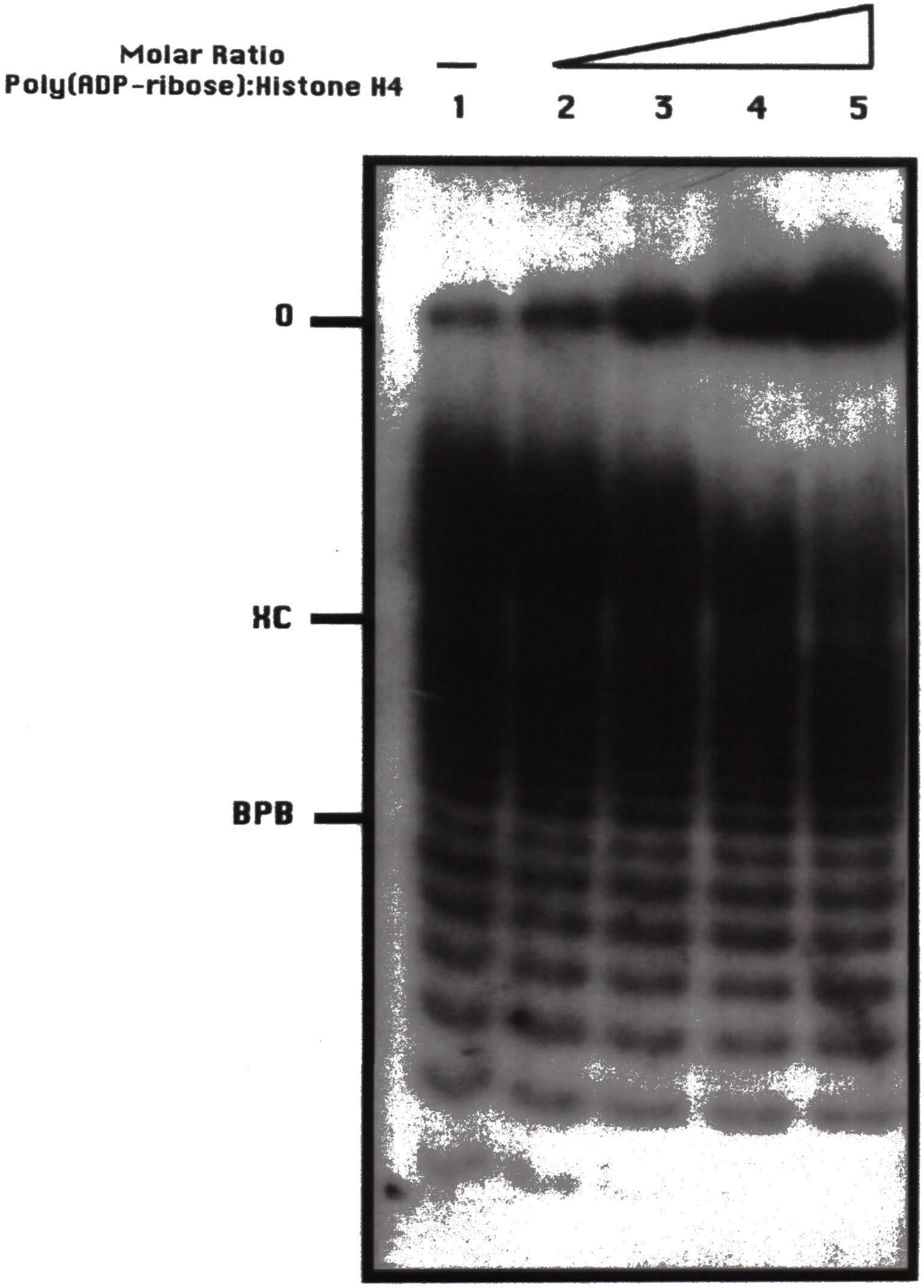
Molar Ratio
Poly(ADP-ribose):Histone H4
1
2
3
4
5
O
XC
BPB

Fig. 43. PARG activity in the presence of histone H4. The percent of monomeric ADP-ribose formed (open squares) and the percent of poly(ADP-ribose) complex (filled squares) was determined. Reaction mixtures of 25 µl containing 100 mM Tris-HCl, pH 8.0, 10 mM DTT, 30 nM [^{32}P]poly(ADP-ribose) and 6 µg/ml of PARG were incubated at 37 °C for the indicated times. The reactions were stopped with electrophoresis loading buffer. Following PAGE, the amount of poly(ADP-ribose) was quantified by densitometric scanning.

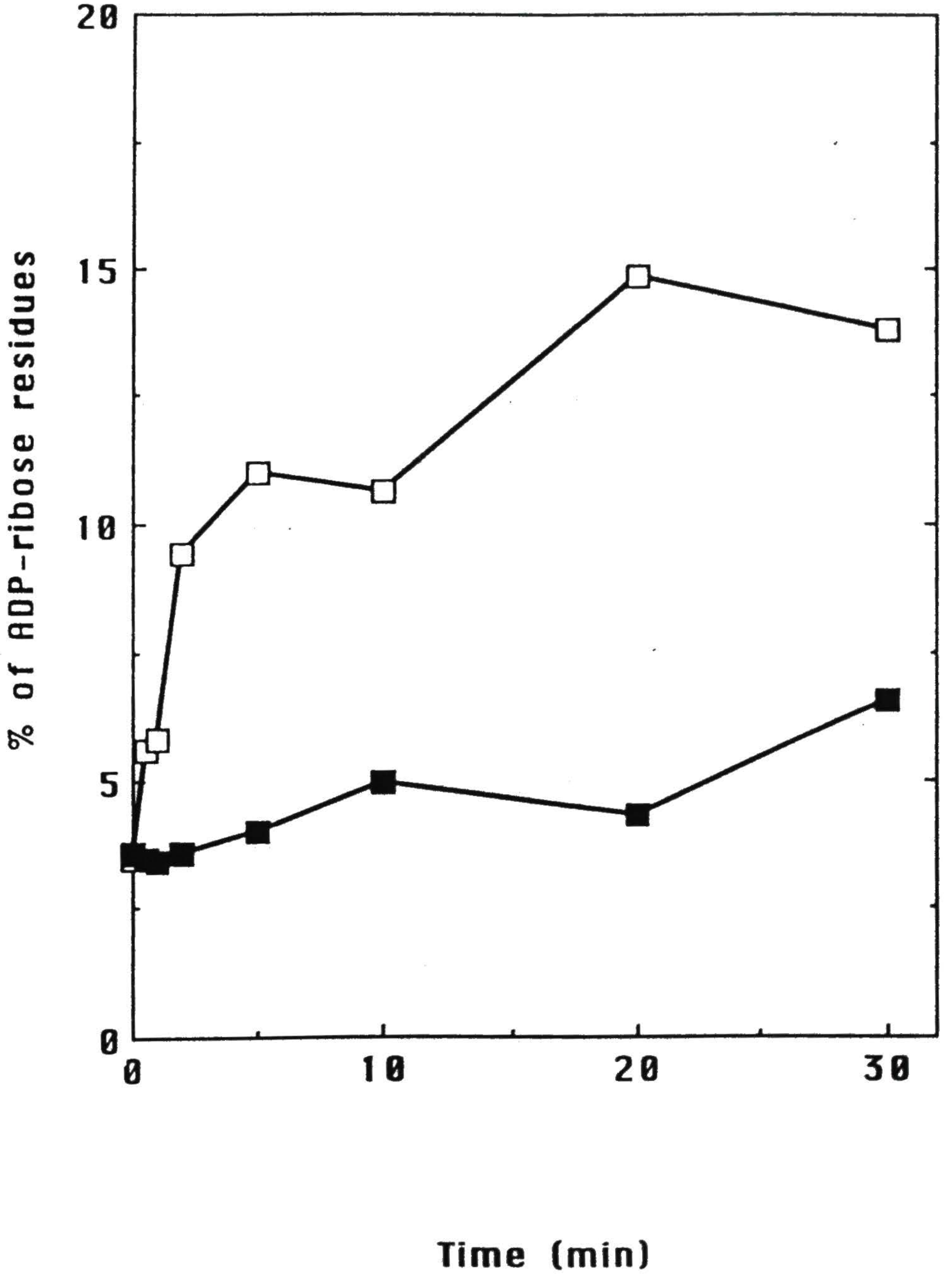
% of ADP-ribose residues
20
15
10
5
0
0
10
20
30
Time (min)

Role of PARP in the degradation of poly(ADP-ribose) by PARG activity. First, we observed that PARP interacts non-covalently with poly(ADP-ribose) at 1:4 and 1:8 molar ratios of poly(ADP-ribose):PARP. PARG assays were carried out in the presence of PARP and the results showed that the percent of monomeric ADP-ribose increased (Fig. 44) with time. It was noticed in these incubations that ADP-ribose chains larger than 20 residues were protected by PARP.

In summary, we have developed an assay that allows the simultaneous determination of PARG activity and non-covalent interactions of poly(ADP-ribose) with cationic proteins. Detection of non-covalent interactions is based on a "gel mobility shift" assay. This assay allowed us to detect non-covalent interactions of poly(ADP-ribose) with purified proteins or proteins in the nuclear environment. The catabolism of poly(ADP-ribose) seems to be mediated by the formation of a catabolite intermediate constituted of a protein(s) and poly(ADP-ribose). The formation of this complex appears to trigger the catabolism of poly(ADP-ribose). The identity of the protein has not been definitively confirmed; however, the affinity of the nuclear associated protein responsible for triggering of poly(ADP-ribose) degradation correlates with the affinity of histone H4 for the long ADP-ribose chains. we have also found evidence that PARG activity is associated with chromatin, the nuclear matrix and the nuclear envelope. We also determined that poly(ADP-ribose) interacts non-covalently with histone proteins and the nuclear matrix; inhibition of PARG activity by this protein components suggest that the catabolism of poly(ADP-ribose) is influenced by the subnuclear distribution of the enzyme activity. The finding that PARG activity is found in several nuclear subdomains strengthens the hypothesis that poly(ADP-ribosyl)ation is a multifunctional pathway.

Fig. 44. Poly(ADP-ribose) glycohydrolase activity in the presence of different amounts of PARP. Assays were carried out either in the absence or presence of the indicated concentration of PARP. Reaction mixtures of 25 µl containing 100 mM Tris-HCl, pH 8.0, 10 mM DTT, 30 nM [^{32}P]poly(ADP-ribose and 6 µg/ml of PARG were incubated at 37 °C for the indicated times.

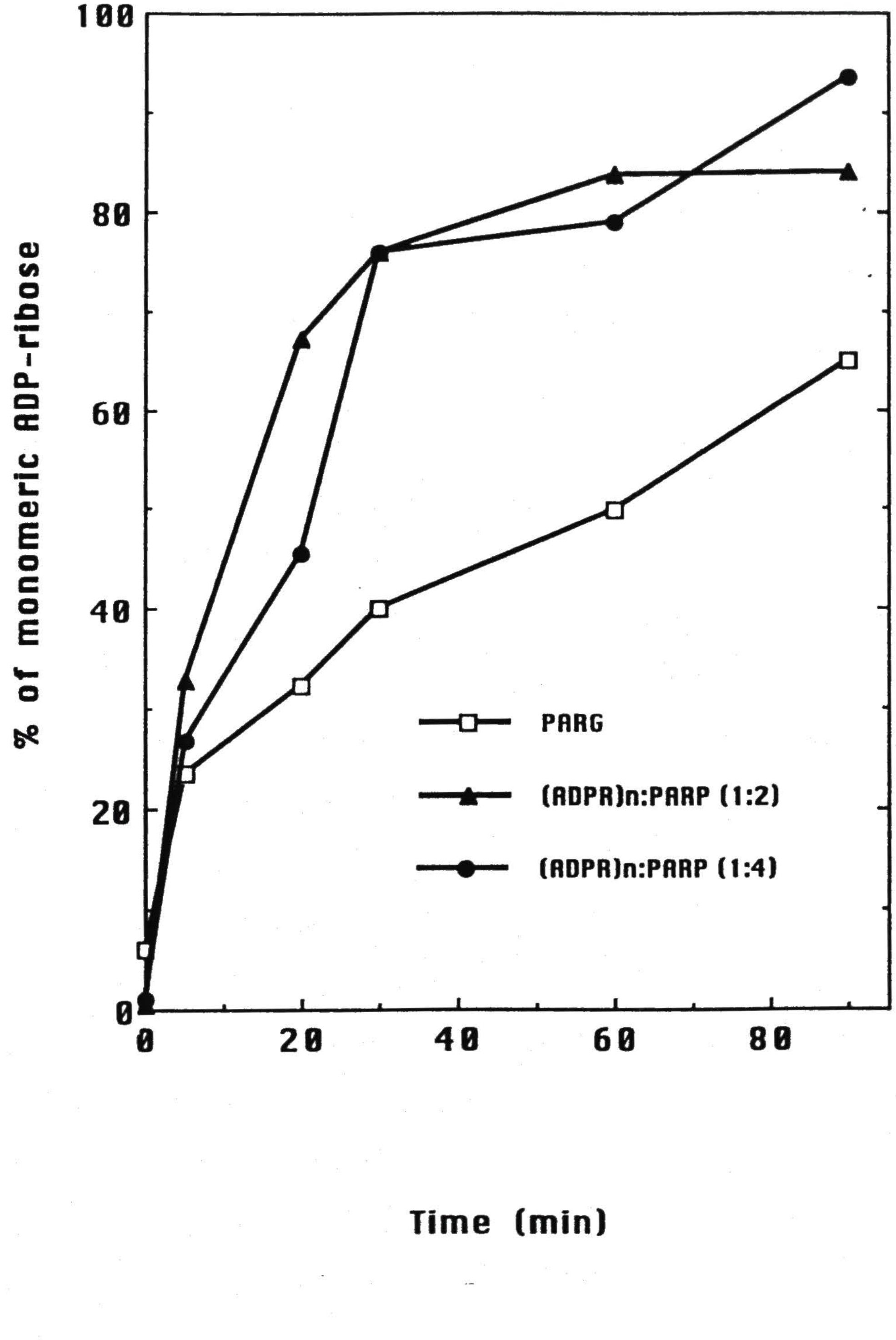
100
80
60
40
20
0
0
20
40
60
80
% of monomeric ADP-ribose
Time (min)
PARG
(ADPR)n:PARP (1:2)
(ADPR)n:PARP (1:4)

CHAPTER IV

DISCUSSION

The substrate for PARG activity in this project consisted of ADP-ribose chains from 2-70 residues (Fig. 11). This preparation of poly(ADP-ribose) did not contain significant amounts of branched polymers. This population of poly(ADP-ribose) molecules was obtained with pure PARP and low concentrations of NAD^+ (Alvarez-Gonzalez and Mendoza-Alvarez, 1995). Branched polymers are not synthesized under these conditions. Subsequent purification of these polymers on a boronate resin was highly selective for $(ADP\text{-}ribose)_{2\text{-}70}$. The substrate for PARG did not contain AMP, the alkaline product of monomeric ADP-ribose. Previous methods in the past to determine PARG activity involved acid precipitation of residual poly(ADP-ribose) (Miwa, *et al.,* 1975). That method is inconvenient because both monomeric ADP-ribose and ADP-ribose chains smaller than 20 ADP-ribose residues remain in the supernatant. A more recent method involves thin layer chromatography (TLC) (Menard and Poirier,1987) which appears to be a more accurate method; however, in this method, it is difficult to analyze the substrate remaining. HPLC methods have also been utilized (Brochu, *et al.,* 1994), however, they do not show the sequential aspects of poly(ADP-ribose) hydrolysis. An assay similar to the one presented here was recently used to examine whether endoglycosidic cleavage is catalyzed by PARG (Braun, *et al.*, 1994). In this assay, the polymer substrate utilized contained monomeric ADP-ribose and NAD$^+$. Therefore, the enzyme assay described in this dissertation is advantageous because it allows the monitoring of the formation of monomeric ADP-ribose as well as the different oligomeric structures remaining in the incubation.

The method developed in this project may also be equivalent to a gel mobility shift assay. These type of assays have been useful to determine specific interactions of proteins with DNA. Therefore, it was thought that poly(ADP-ribose), a polynucleotide similar to DNA, might also interact with nuclear proteins. Other assays that evaluate non-covalent interactions of poly(ADP-ribose) with proteins have been described by Panzeter, *et al.* (1992) and Nozaki , *et al.*, (1994). Nozaki *et al*. (1994) showed specific non-covalent interactions of HeLa cell crude extracts with ADP-ribose chains larger than 20 residues. This observation was consistent with the results presented here since long polymers of ADP-ribose (Fig. 28) interacted non-covalently with proteins of the nuclear extract. The gel mobility shift assay presented here also allowed to concomitantly determine the extent of non-covalent interactions of poly(ADP-ribose) with nuclear proteins and PARG. It these experiments, purified histones interacted non-covalently with free polymers (Fig. 25). This result is also in agreement with studies by the method of Panzeter *et al.*, (1992). Their phenol partitioning assay (Panzeter, *et al.*, 1992) was used to study the non-covalent interactions with several proteins such as proteinase K, DNAase 1, BSA and PARP. These proteins did not interact ionically with free polymers under those conditions. Similar results are shown with our polymer mobility shift assay (Fig. 25). It was interesting that the non-covalent interactions of poly(ADP-ribose) with histone proteins depend on the stoichiometry of poly(ADP-ribose) with histone proteins (Fig. 41). It appears that histone proteins possess a high binding affinity for ADP-ribose chains. This binding affinity depends on the histone tail length and the net charge of the histone protein. Congruently with previous results, histone H1 showed to be the protein with higher affinity for poly(ADP-ribose) molecules of any given size (Fig. 41). In addition, non-covalent interactions of poly(ADP-ribose) with purified PARP were detected at high molar ratios of PARP:poly(ADP-ribose) (1:16). These observations favor the suggestion that PARP possesses a binding site for ADP-ribose polymers which is different than the NAD^+ binding site.

In this study, we have also demonstrated that core histone proteins interact non-covalently with poly(ADP-ribose) (Fig. 25). This affinity was observed also in the presence of SDS (Fig. 38). Thus, these results provide evidence that poly(ADP-ribose) interacts specifically and non-covalently with regulating proteins in the chromatin environment.

In order to measure the degradation of poly(ADP-ribose) in a "native" chromatin environment, the following steps might be necessary. First, a slow step that allows for binding of poly(ADP-ribose) to histone proteins should be implemented. Second, a fast step that would allow the binding of PARG to the [histone][poly(ADP-ribose]complex with consequent degradation of poly(ADP-ribose). Thus, it is expected that the formation of the [histone][poly(ADP-ribose)] complex precedes the degradation of poly(ADP-ribose). The formation of this complex should be independent of PARG. Our results show that in fact, the formation of monomeric ADP-ribose is detected after 10 minutes of incubation (Fig. 34 and Fig. 35), and that degradation of poly(ADP-ribose) is biphasic. The protein(s) interacting with poly(ADP-ribose) have also been studied by SDS-PAGE. In these experiments, it was found that the stronger signals correspond to core histones (Fig. 38). It is believed that histone proteins block the binding of PARG with poly(ADP-ribose) to allow for proper processing of the damaged DNA.

The formation of protein-polymer complex may result from trapping poly(ADP-ribose) at the site of sample application. However, if this were the case, changes during the incubation would not affect the formation of the complex. It was shown that incubations at different temperatures affected the formation of this complex (Fig. 36 and

37). Thus, the interactions of poly(ADP-ribose) with nuclear proteins was not the result of poly(ADP-ribose) trapping.

In this project, we also observed that a crude nuclear matrix extract inhibited PARG activity, presumably via the ionic protection of ADP-ribose chains (Fig. 27). In support of this conclusion, the studies of Nozaki, *et al.*, (1994) showed that proteins from HeLa cells that specifically interacted with free-poly(ADP-ribose) corresponded to the same molecular weight of the nuclear matrix proteins. One should not forget that poly(ADP-ribose) is tightly bound to the nuclear matrix (Cardenas-Corona, *et al.*, 1987). Therefore, the observation that the nuclear matrix inhibits PARG activity might explain the low levels of PARG activity detected in this fraction.

Histone proteins have been shown to block the access of PARG for the non-reducing-end of poly(ADP-ribose) molecules (Panzeter, *et al.*, 1993). Since histone proteins are the most abundant proteins in the nucleus, they may play an important role in the catabolism of poly(ADP-ribose). However, the degradation of poly(ADP-ribose) *in vitro* in the presence of 1:1 ratios of DNA with histone proteins was not inhibited (Tanuma, *et al.*, 1986b). Thus, the inhibition of PARG by histone proteins in the native environment appears to depend on the large amounts of DNA-free histone proteins. Thus, it is proposed that histone proteins bind non-covalently to poly(ADP-ribose) by competing with DNA. Not surprisingly, poly(ADP-ribose) has been proven to effectively compete for purified histones with DNA (Sauerman and Wesierska-Gadek, 1985).

Based on the affinity shown by the protein interacting with free poly(ADP-ribose) and the studies of ionic interactions of purified histones with poly(ADP-ribose), it may be suggested that histone H4 is a negative modulator of poly(ADP-ribose) catabolism. Indeed, Wesierska-Gadek and Sauerman (1988) have also showed that poly(ADP-ribose) competes with DNA for binding to histone H4. Since the poly(ADP-ribosyl)ation of polynucleosomes results in changes of native chromatin, it has been proposed that the covalent modification of histone H1 is responsible for the unfolding of this unit (Aubin, *et al.*, 1983; De Murcia, *et al.*, 1988). While these results seem contradictory at first, histone H4-tails not only participate in nucleosome formation but also in higher order chromatin structure (Garcia-Ramirez, *et al.*, 1992). Therefore, it is possible that the poly(ADP-ribosyl)ation of histone H1 and PARP are required as a prerequisite for the non-covalent interactions of poly(ADP-ribose) with histone H4. In support of this notion, Mathis and Althaus (1987) have shown the that poly(ADP-ribosyl)ation of polynucleosomes result in the displacement of the DNA from the histone nucleosome core. This report showed that it was likely that histone H4 interacted specifically and with high affinity with poly(ADP-ribose) in the native chromatin environment. In our assays, the histone protein with lower molar ratios as compared with poly(ADP-ribose) was histone H4. This also suggested that non-covalent interactions of poly(ADP-ribose) with histone H4 may in fact participate in the disruption of the nucleosome. The finding that PARG activity is preceded by formation of a [protein][poly(ADP-ribose)] complex also suggests that histone H4 may work as a modulator of ADP-ribose chain degradation.

The finding that histone H1 interacts non-covalently with different sizes of poly(ADP-ribose) (Fig. 41) could be explained by its participation in the unfolding of the 30 nm fiber. In fact, partial release of histone proteins appear to disrupt this structure (Thoma, *et al.*, 1981). However, affinity of H4 for specific size of ADP-ribose chains may cause (a) nucleosome displacement and unfolding of the 30 nm fiber.

PARP is the main acceptor of poly(ADP-ribosyl)ation (Ogata, *et al.*, 1981). Therefore, we also performed catabolism studies in the presence of exogenous PARP. Poly(ADP-ribosyl)ated-PARP had previously been shown to be the better substrate for PARG than protein-free poly(ADP-ribose) (Uchida, *et al.*, 1993b). Thus, it was suggested that protein-protein interactions between PARG and PARP are important for the proper catabolism of poly(ADP-ribose). We addressed this issue by incubating protein-free poly(ADP-ribose) with PARG in the presence of purified PARP. In these experiments, it was observed that the activity of PARG increased when PARP was added(Fig. 44). Thus, it appears that PARP may also serve as an activator of PARG activity via protein-protein interactions.

Previous investigators have also shown that PARG is tightly bound to chromatin in isolated nuclei (Miwa and Sugimura, 1971; Tanuma, *et al.*, 1986b; Uchida, *et al.*, 1993b). However, the distribution of PARG in functionally distinct subnuclear domains has not been directly addressed. Here, we searched for the distribution of PARG in the cell nucleus. The results show that different amounts of PARG activity are associated with chromatin, the nuclear matrix, and nuclear envelope. In these experiments, it was found that the bulk of PARG activity is extracted in the chromatin fraction (Fig.21 and 22). The efficient extraction of chromatin-associated PARG was confirmed by the very low level of activity of PARG in the high salt extractable fraction of chromatin. The presence of PARG activity in the nuclear envelope (Triton X-100 extract) was surprising. Indeed, electron micrographic analysis of the nuclear matrix shows this fraction devoid of the nuclear envelope. Recently, immunoelectron microscopy studies have shown that PARP is localized in close proximity to the nuclear envelope (Mosgoeller, *et al.*, 1996).

The finding that PARG is associated with the nuclear matrix correlates with the presence of poly(ADP-ribose) in this fraction (Cardenas-Corona, *et al.*, 1987), and the poly(ADP-ribosyl)ation of nuclear matrix proteins (Wesierska-Gadek, and Sauermann, 1985). Furthermore, PARP has also been found to co-purify with the nuclear matrix as demonstrated *in vivo* (Alvarez-Gonzalez and Ringer, 1988). The association of PARG with the nuclear matrix contrast with the observation that incubations of nuclear matrix do not release large amounts of nuclear matrix associated ADP-ribose polymers (Cardenas-Corona, *et al.*, 1988). Both findings can be reconciled by the observation that the nuclear matrix proteins inhibited PARG (Fig. 26). It was also observed that the nuclear matrix interact non-covalently with poly(ADP-ribose) (Fig. 27). Thus, poly(ADP-ribose) may interact with nuclear matrix proteins and sterically block binding of PARG with poly(ADP-ribose). In summary, these observations suggest that the protein poly(ADP-ribosyl)ation pathway is enzymatically as well as topologically regulated. These findings should prove useful in the understanding of the diverse nuclear processes in which protein poly(ADP-ribosyl)ation is implicated.

In conclusion, poly(ADP-ribose) is catabolized by PARG *in vivo*. This enzyme appears to be associated with chromatin, the nuclear matrix and the nuclear envelope. It also seems that the degradation of this homopolymer is dependent on its non-covalent interactions with nuclear cationic proteins.

CHAPTER V

REFERENCES

Aaronson, R.P., and Blobel, G. (1974) *J. Cell. Biol.* **62**, 746-754

Adamietz, P., and Rudolph, A. (1984) *J. Biol. Chem.* **259**, 6841-6846

Adamietz, P. (1987) *Eur. J. Biochem.* **169**, 365-372

Adolph, K.W., and Song, M-K.H. (1985) *Biochem. Biophys. Res. Commun.* **126**, 840-847

Aebi, U., Cohn, J., Buhle, L., and Gerace, L. (1986) *Nature* **323**, 560-564

Althaus, F. R. and Richter, C. (1987) *ADP-ribosylation of proteins.* Springer-Verlag, Berlin, Heidelberg, New York

Althaus, F.R. (1992) *J. Cell Sci* **102**, 663-670

Althaus, F.R., Bachmann, S., Hofferer, L., Kleczkowska, H.E., Malanga, M., Panzeter, P.L., Realini, C. and Zweifel, B. (1995) *Biochimie* **77**, 423-432

Alvarez-Gonzalez, R., Juarez-Salinas, H., Jacobson, E.L., and Jacobson, M.K. (1983) *Anal. Biochem.* **135**, 69-77

Alvarez-Gonzalez, R. and Jacobson, M.K. (1987) *Biochemistry* **26**, 3218-3224

Alvarez-Gonzalez, R., and Ringer, D.P. (1988) *FEBS lett.* **236**, 362-366

Alvarez-Gonzalez, R., and Althaus, F.R. (1989) *Mut. Res.* **218**, 67-74

Alvarez-Gonzalez, R., and Mendoza-Alvarez, H. (1995) *Biochimie* **77**, 403-407

Amar-Costesex, A., Beuatay, H., Wibo, M., Thines-Sempoux, D., Feytmans, E., Robbi, M., and Berthet, J. (1974) *J. Cell. Biol.* **61**, 201-212

Arents, G., Burlingame, R.W., Wang, B-C, Love, W.E. and Moudrianakis, E.N. (1991) *Proc. Natl. Acad. Sci. USA* **88**, 10148-10152

Arents, G., and Moudrianakis, E.N. (1995) *Proc. Natl. Acad. Sci. USA* **92**, 11170-11174

Aubin, R.J. Frechette, A., De Murcia, G., Mandel, P., Lord, A. Grondin, G., and Poirier, G.G. (1983) *EMBO J.* **2**, 1685-1693

Auer, B., Nagl, U., Herzog, H., Schneider, R., and Schweiger, M. (1989) *DNA* **8**, 575-580

Benjamin, R.C., and Gill, D.M. (1980) *J. Biol. Chem.* **255**, 10493-10501

Berezney, R and Coffey, D.S. (1974) *Biochem. Biophys. Res. Commun.* **60**, 1410-1417

Berezney, R., and Coffey, D.S. (1975) *Science* **189**, 291-293

Berezney, R., and Coffey, D.S. (1977) *J. Cell. Biol.* **73**, 616-637

Berezney, R., and Bucholtz, L.A. (1981) *Exp. Cell Res.* **132**, 1-13

Berezney, R. (1984) In *Chromosomal nonhistone proteins* (L. S.Hnilica, ed.), Volume IV pp. 120-180, CRC press, Inc. Boca Raton Florida

Berezney, R., Mortillaro, M.J., Ma, H., Wei, X., and Samarabandu, J. (1995) *Int. Rev. Cytol.* **162A**, 1-65

Blenkowe, B., Nickerson, J. A. Issner, R., Penman, S., and Sharp, P. A. (1994) *J. Cell. Biol.* **127**, 593-607

Blobel, G., and Potter, V.R. (1966) *Science* **154**, 1662-1665

Blow, J.J., and Laskey, R.A. (1988) *Nature* **332**, 546-548

Boulikas, T. (1993) *Tox. Lett.* **67**, 129-150

Bolund, L.A, and Johns, E.W. (1973) *Eur. J. Biochem.* **35**, 546-553

Bourgeois, C.A., and Hubert, J. (1988) *Int. Rev. Cytol.* **111**, 1-52

Bradbury, E.M. (1992) *Bioessays* **14**, 9-16

Braun, S.A., Panzeter, P.L., Collinge, M. A. and Althaus, F.R. (1994) *Eur. J. Biochem.* **220**, 369-375

Brochu, G., Duchaine, C., Thibeault, L., Lagueux, J., Shah, G.M. and Poirier, G.G. (1994) *Biochem. Biophys. Acta* **1219**, 342-350

Buki, K.G. Bauer, P.I., Hakam, A., and Kun, E. (1995) *J. Biol. Chem.* **270**, 3370-3377

Cardenas-Corona, M.E., Jacobson, E.L. and Jacobson, M.K. (1987) *J. Biol. Chem.* **262**, 14863-14866

Cardenas-Corona, M. E., Jacobson, E. L. and Jacobson, M. K. (1988) In *ADP-ribose Transfer Reactions* (M.K. Jacobson and E.L. Jacobson, eds), pp. 173-178, Springer Verlag, New York

Cherney, B.W., McBride, O.W., Chen, D., Alkhatib, H., Bhatia, K., Hensley, P., and Smulson, M.E. (1987) *Proc. Natl. Acad. Sci. USA* **84**, 8370-8374

Coghlan, V.M., Langeberg, L.K., Fernandez, A., Lamb, N.J.C., and Scott, J.D. (1994) *J. Biol. Chem.* **269**, 7658-7665

Cook, P.R. (1991) *Cell* **66**, 627-637

De Murcia, G., Huletsky, A., Lamarre, D., Gaudreu, A., Pouyet, J., Daune, M., and Poirier, G.G. (1986) *J. Biol. Chem.* **261**, 7011-7017

De Murcia, G.M., Huletsky, A. and Poirier, G.G. (1988) *Biochem. Cell. Biol.* 66, 626-635

Eickbush, T.H. and Moudrianakis. E.N. (1978) *Biochemistry.* **17**, 4955-4964

Fernandez, D.J., and Catapano, C.V. (1991) *Cancer cells* **3**, 134-140

Ferro, A.M. and Olivera, B.M. (1984) *J. Biol. Chem.* **259**, 547-554

Fey, E., and Penman, S. (1988) *Proc. Natl. Acad. Sci. USA* **85**, 121-125

Fisher, D.Z., Chaudhary, N., and Blobel, G. (1986) *Proc. Natl. Acad. Sci. USA* **83**, 6450-6454

Foisner, R., and Gerace, L. (1993) *Cell* **73**, 1267-1279

Garcia-Ramirez, M., Dong, F., and Ausio, J. (1992) *J. Biol. Chem.* **267**, 19587-19595.

Gasser, S.M., and Laemmli, U.K. (1987) *Trends Genet.* **3**, 16-22

Gerace, L., and Burke, B. (1988) *Annu. Rev. Cell Biol.* **4**, 335-374

Gerace, L., and Foisner, L. (1994) *Trends Cell Biol.* **4**, 127-131

Gradwohl, G., Menissier-de Murcia, J., Molinete, M., Simonin, F., Koken, M., Hoeijmakers, J.H.J., and deMurcia, G. (1990) *Proc. Natl. Acad. Sci. USA* **87**, 2990-2994

Hakes, D.J., and Berezney, R. (1991) *J. Biol. Chem.* **266**, 11131-11140

Hansen, J.C. and Wolffe, A.P. (1994) *Proc. Natl. Acad. Sci. USA* **91**, 2339-2343

Harris, J. R. (1978) *Biochem. Biophys. Acta* **551**, 55-104

Hatakeyama, K., Nemoto, Y., Ueda, K., and Hayaishi, O. Hayaishi. (1986) *J. Biol. Chem.* **261**, 14902-14911

Holtz, D., Tanaka, R.A., Hartwig, J., and McKeon, F. (1989) *Cell* **59**, 969-977.

Hyde, J.E., Igo-Kemenes, T., and Zachau, H.G. (1979) *Nucleic Acids Res.* **7**, 31-48

Ikejima, M. and Gill, D.M. (1988) *J. Biol. Chem.* **263**, 11037-11040.

Ikejima, M., Noguchi, S., Yamashita, R., Ogura, T., Sugimura, T., Gill, D.M., and Miwa, M. (1990) *J. Biol. Chem.* **265**, 21907-21913

Jackson, D.A., and Cook, P.R. (1985) *EMBO J.* **5**, 919-925

Jackson, D.A., Balajee, A.,S., Mullenders, L., and Cook, P.R. (1994a) *J. Cell. Sci.* **107**, 1745-1752

Jackson, D.A., Hassen, A.B., Errington, R.J. and Cook, P.R. (1994b) *J. Cell. Sci.* **107**, 1753-1760

Jonsson, G.G., Menard, L., Jacobson, E.L., Poirier, G.G. and Jacobson, M.K. (1988a) *Cancer Res.* **48**, 4240-4243

Jonsson, G.G., Jacobson, E.L., and Jacobson, M.K. (1988b) *Cancer Res.* **48**, 4233-

4239

Kameshita, I., Matsuda, M., Nishikimi, M., Ushiro, H., and Shizuta, Y. (1986) *J. Biol. Chem.* **261**, 3863-3868

Kasid, U.N., Halligan, B., Liu, L. F., Dritschilo, A. and Smulson, M. (1989) *J. Biol. Chem.* **264**, 18687-18692

Kornberg, R. (1974) *Science* **184**, 868-871

Kurosaki, T., Ushiro, H., Mitsuuchi, Y., Suzuki, S., Matsuda, M., Matsuda, Y., Katunuma, N., Kangawa, K., Matsuo, H., Hirose, T., Inayama, S., and Shizuta, Y. (1987) *J. Biol. Chem.* **262**, 15990-15997

Laemmli, U.K. (1970) *Nature* **227**, 680-685

Lewis, C.D., Lebkowski, J.S., Daly, A.K., and Laemmli, U.K. (1984) *J. Cell. Sci* **1**(suppl), 103-122

Marsischky, G.T., Wilson, B.A., and Collier, R.J. (1995) *J. Biol. Chem.* **270**, 3247-3254

Maruta, H., Inageda, K., Aoki, T., Nishina, H., and Tanuma, S. (1991) *Biochemistry* **30**, 5907-5912

Mathis, G., and Althaus, F.R. (1987) *Biochem. Biophys. Res. Commun.* **143**, 1049-1054

McKeon, F., Kirschner, M., and Caput, D. (1986) *Nature* **319**, 439-468

Menard, L. and Poirier, G.G. (1987) *Biochem. Cell. Biol.* **65**, 668-673

Mendoza-Alvarez, H., and Alvarez-Gonzalez, R. (1993) *J. Biol Chem.* **268**, 22575-22580

Miwa, M., and Sugimura, T. (1971) *J. Biol. Chem.* **146**, 6362-6364

Miwa, M., Tanaka, M., Matsushima, T., and Sugimura, T. (1974) *J. Biol. Chem.* **249**, 3475-3482

Miwa, M., Nakatsugawa, K., Hara, K., Matsushima, T., and Sugimura, T. (1975) *Arch. Biochem. Biophys.* **167**, 54-60

Miwa, M., and Sugimura, T. (1982) in *ADP-ribosylation Reactions, Biology and Medicine* (Hayaishi, O., and Ueda, K., eds.), pp 43-62, Academic, New York

Miyakawa, N., Veda, K., and Hayaishi, O. (1972) *Biochem. Biophys. Res. Commun.* **49**, 239-245

Mosgoeller, W., Steiner, M., Hozak, P., Penner, E., and Wesierska-Gadek, J. (1996) *J. Cell Sci.* **109**, 409-418

Nakayasu, H., and Berezney, R. (1991) *Proc. Natl. Acad. Sci. USA* **88**, 10312-10316

Nozaki, T., Masutani, M., Akagawa, T., Sugimura, T., and Esumi, H. (1994) *Biochem. Biophys. Res. Commun.* **198**, 45-51

Ogata, N., Ueda, K., Kawaichi, M., and Hayaishi, O. (1981) *J. Biol. Chem.* **256**, 4135-4137

Ohaviano, Y., and Gerace, L. (1985) *J. Biol. Chem.* **260**, 624-632

Okayama, H., Honda, M., and Hayaishi, O. (1978) *Proc. Natl. Acad. Sci. USA* **75**, 2254-2257

Padan, R., Nainudel-Epszteyn, S., Goitein, R., Foinsod, A., and Gruenbaum, Y. (1990) *J. Biol. Chem.* **265**, 7808-7813

Pante, N., and Aebi, U. (1995) *Int. Rev. Cytol.* **162B**, 225-255

Pante, N., and Aebi, U. (1996) *Curr. Opin. Cell Biol.* **8**, 397-406

Panzeter, P.L., Realini, C.A., and Althaus, F.R. (1992) *Biochemistry*, **31**, 1379-1385

Panzeter, P.L.,Zweifel, B., Malanga, M., Waser, S.H., Richard, M.C., and Althaus, F.R. (1993) *J. Biol. Chem.* **268**, 17662-17664

Panzeter, P.L. and Althaus, F.R. (1994) *Biochemistry* **33**, 9600-9605

Pardoll, D.M., Vogelstein, B., and Coffey, D.S. (1980) *Cell* **19**, 527-536

Pathak, R.K., Luskey, K.L., and Anderson, R.G.W. (1986) *J. Cell. Biol.* **102**, 2158-2168

Poirier, G.G., de Murcia, G., Jongstra-Bilen, J., Niedergang, C. and Mandel, P. (1982)

Proc. Natl. Acad. Sci. USA **79**, 3423-3427

Raben, D.M., Jarpe, M.B. and Leach, K.L. (1994) *J. Membrane Biol.* **142**, 1-7

Rawling, J. M. and Alvarez-Gonzalez, R. (1996) *FASEB J.* **10**, A1119

Razin, S.V., Kelkelidze, M.G., Lukanidin, E.M., Scherrer, K., and Georgiev, G.P. (1986) *Nucleic Acids Res.* **14**, 8189-8207

Realini, C. A., and Althaus, F.R. (1992) *J. Biol. Chem.* **267**, 18858-18865

Reichelt, R., Holzenburg, A., Buhle, E.L., Jarnik, M., Engel, A. and Aebi, U. (1990) *J. Cell. Biol.* **110**, 883-894

Romanowski, P., and Madine, M.A. (1996) *Trends Cell Biol.* **6**, 184-188

Sato, T (1968) *J. Elec. Micros.* **17**, 158-159

Sauermann, G., and Wesierska-Gadek, J. (1986) *Biochem. Biophys. Res. Commun.* **139**, 523-529

Schreiber, V., Molinete, M., Boeuf, H., De Murcia, G., and Menissier-de Murcia, J. (1992) *EMBO J.* **11**, 3263-3269

Schroder, H.C., Steffen, R., Wenger, R., Ugarkovic, D. and Muller, W.E. G. (1989) *Mut. Res.* **219**, 283-294

Slama, J.T., Aboul-Ela, N., Goli, D. M., Cheesman, B.V. Simmons, A.M., and Jacobson, M.K. (1995) *J. Med. Chem.* **38**, 389-393

Smith, P.K., Krohn, R.I., Hermanson, G.T., Mallia, A.K., Gartner, F.H., Provenzano, M.D., Fujimoto, E.K., Goeke, N.M., Olson, B.J., and Klenk, D.C. (1985) *Anal. Biochem.* **150**,76-85

Taniura, H., Glass, C., and Gerace, L. (1995) *J. Cell. Biol.* **131**, 33-44.

Tanuma, S., Arita, T., Kawashima, K., and Endo, H. (1982a) *Biochem. Biophys. Res. Commun.* **104**, 483-490

Tanuma, S. and Kanai, Y. (1982b) *J. Biol. Chem.* **257**, 6565-6570

Tanuma, S., and Johnson, G.S. (1983a) *J. Biol. Chem.* **258**, 4067-4070

Tanuma, S., Kawashima, K., and Endo, H. (1986a) *J. Biochem.* **99**, 915-922

Tanuma, S., Kawashima, K. and Endo, H. (1986b) *J. Biol. Chem.* **261**, 965-969.

Tanuma, S., Kawashima, K., and Endo, H. (1986c) *Biochem. Biophys. Res. Commun.* **135**, 979-986

Tanuma, S., Tsai, Y.-J., Sakagami, H., Konno, K., and Endo, H. (1989) *Biochem.. Int.* **19**, 1395-1402

Tanuma, S., and Endo, H. (1990) *Eur. J. Biochem.* **191**, 57-63

Tavassoli, M., Tavassoli, M.H., and Shall, S. (1983) *Eur. J. Biochem.* **135**, 449-455.

Tavassoli, M., Tavassoli, M. H., and Shall, S. (1985) *Biochem. Biophys. Acta* **827**, 228-234.

Thibeault, L., Hengartner, M., Lagueux, J., Poirier, G.G. and Muller, S. (1992) *Biochem. Biophys. Acta* **1121**, 317-324

Thoma, F., Koller, T.H., and Klug, A. (1979) *J. Cell. Biol.* **83**, 407-427

Thoma, F.,and Koller, T.H. (1981) *J. Mol. Biol.* **103**, 709-733

Thomassin, H., Jacobson, M.K., Guay, J., Verreault, A., Aboul-ela, N., Menard, L. and Poirier, G.G. (1990) *Nucleic Acids Res.* **18**, 4691-4694

Tsai, Y., Aoki, T., Maruta, H., Abe, H., Sakagami, H., Hatano, T., Okuda, T., and Tanuma, S. (1992) *J. Biol. Chem.* **267**, 14436-14442

Tubo, R. A., and Berezney, R. (1987) *J. Biol. Chem.* **263,** 5857-5865

Uchida, K., Hanai, S., Ishikawa, K-I., Ozawa, Y-I., Uchida, M., Sugimura, T., and Miwa, M. (1993a) *Proc. Natl. Acad. Sci. USA* **90**, 3481-3485

Uchida, K., Suzuki, H., Maruta, H., Abe, H., Aoki, K., Miwa, M., and Tanuma, S. (1993b) *J. Biol. Chem.* **268**, 3194-3200

Ueda, K., Oka., J., Narumiya, S., Miyakawa, N., Hayaishi, O. (1972) *Biochem. Biophys. Res. Commun.* **46**, 516-523

Ueda, K., Omachi, A., Kawaichi, M., Hayaishi, O. (1975) *Proc. Natl. Acad. Sci. USA* **72,** 205-209 van Holde, K.E. (1988) *Chromatin*, Springer-Verlag, New York

van Wijnen, A.J., Bidwell, J.P., Fey, E.G., Penman, S., Lian, J.B., Stein, J.L., and Stein, G. S. (1993) *Bichemistry* **32,** 8397-8402

Wesierska-Gadek, J., and Sauermann, G. (1985) *Eur. J. Biochem.* **153**, 421-428

Wesierska-Gadek, J., and Sauermann, G. (1988) *Eur. J. Biochem.* **173**, 675-679

Yoshihara, K., Itaya, A., Tanaka, Y., Ohashi, Y., Ito, K., Teraoka, H., Tsukada, K., Matsukage, A., Kamiya, T. (1985) *Biochem. Biophys. Res. Commun.* **128**, 61-67.

Zahradka, P., and Ebisuzaki, K. (1984) *Eur. J. Biochem.* **142**, 503-509

Zeng, C., He, D., and Brinkley, B.R. (1994) *Cell. Motil. Cytoskel.* **29,** 167-176

MAN
INC.
EC 96
N. MANCHESTER,
INDIANA 46962